A GENERALIZED PROCEDURE TO DEVELOP TRANSFER FUNCTION BASED MODELS OF ELECTRICAL POWER SYSTEMS

Sembukuttige Lahiru Darshana De Silva

(178506K)

Thesis submitted in partial fulfillment of the requirements for the degree Master of Science in Electrical Engineering

Department of Electrical Engineering

University of Moratuwa

Sri Lanka

February 2022

Declaration of the candidate and supervisor

I declare that this is my own work and this thesis does not incorporate without acknowledgement any material previously submitted for a Degree or Diploma in any other University or institute of higher learning and to the best of my knowledge and belief it does not contain any material previously published or written by another person except where the acknowledgement is made in the text.

Also, I hereby grant to University of Moratuwa the non-exclusive right to reproduce and distribute my thesis/dissertation, in whole or in part in print, electronic or other medium. I retain the right to use this content in whole or part in future works (such as articles or books).

Signature: Date:

The above candidate has carried out research for the Masters thesis under my supervision.

Name of the supervisor: Dr. W.D Prasad

Signature of the supervisor: Date :

Abstract

More and more renewable electricity generating sources such as wind and solar power plants are being integrated into electrical power systems, which in turn complicates processes such as power system stability studies due to the complex nature of controls in these power plants. Since most such studies are done using simulations, it is necessary to have accurate dynamic models of those power plants which describe the behaviour of the power plant during a disturbance to the network or to an internal control or the power plant. Nevertheless, it might be difficult to obtain these detailed models from manufacturers due to proprietary concerns and even if the detailed model is available, modelling complicated power electronic components in the simulation environment might be a difficult without knowing how each component operates. Moreover, when parameters change over time, physical parameters of these models need to be updated and it cannot be done without standard practical measurements. These standard tests require the generating sources to be taken out of the system for testing purposes.

Therefore, instead of a detailed model, a dynamic equivalent model could be used for achieving the same requirement. This research presents a generalized procedure that can be used to accurately estimate black-box dynamic equivalent models of synchronous generators, wind and solar power plants by utilizing measurements and estimating parameters of the dynamic equivalent model. Simulations have been conducted to estimate and verify the accuracy of the proposed methodology by comparing the accuracy of the actual model and the estimated models.

Keywords: Dynamic equivalent, power system stability, black-box, parameter estimation

Acknowledgement

First, I offer my sincere gratitude to my supervisor, Dr W.D Prasad of Department of Electrical Engineering, University of Moratuwa for his unwavering and continuous support in many ways throughout the course of this whole research. From the research idea to formulation of the methodology, he provided immense support and guidance which enabled me to conduct this research.

Likewise, I am extremely grateful to all the academic and non-academic staff of University of Moratuwa who have provided me assistance and guidance throughout this whole period.

Furthermore, I would like to thank Dr Dharshana Muthumuni, Managing Director of Manitoba HVDC Research centre, Prof. Udaya Annakkage of University of Manitoba and Dr Narendra De Silva, General Manager of Lanka Electricity Company (Pvt) Ltd for their valuable insights for making this research a success.

Moreover, I would extend my sincere gratitude to the management of Ante LECO Metering Company (Pvt) Ltd where I was employed when I started the research and the course work of my Masters degree and Lanka Electricity Company (Pvt) Ltd, where I am employed now for the support and guidance provided for the completion of this degree and the research work.

Ultimately, a special thank goes to my parents, family and friends who as always have provided me encouragement and support to complete the studies.

Table of Contents

List of Figures

List of Tables

List of Abbreviations

Abbreviation	Description
AC	Alternating Current
AIC	Akaike’s Information Criterion
ANN	Artificial Neural Networks
ARMAX	Autoregressive Moving Average eXogenous
ARX	Autoregressive with Extra Input
AVR	Automatic Voltage Regulator
BIC	Bayesian Information Criterion
BJ	Box-Jenkins
CSP	Concentrated Solar Power
CVA	Canonical Value Analysis
DC	Direct Current
DE	Differential Evolution
DEM	Dynamic Equivalent Model
GA	Genetic Algorithm
HPP	Hydro Power Plant
LFO	Low Frequency Oscillations
MIMO	Multiple Input Multiple Output
MOESP	Multi-variable Output-Error State Space
N4SID	Numerical algorithm for Subspace State Space System Identification
NREL	National Renewable Energy Laboratory
OE	Output Error
PBSID	Predictor Based Subspace Identification
PCIe	Peripheral Component Interface Express
PEM	Predictive Error Method
PMU	Phasor Measurement Unit
POI	Point of Interconnection

PSO	Particle Swarm Optimization
PSS	Power System Stabilizer
PV	Photovoltaic
RAM	Random Access Memory
REEC	Renewable Energy Electrical Controller
REGC	Renewable Energy Generator Controller
REPC	Renewable Energy Plant Controller
RLS	Recursive Lest Squares
SIMO	Single Input Multiple Output
SISO	Single Input Single Output
SPP	Solar Power Plant
SSD	Solid State Drive
SSSA	Small Signal Stability Analysis
WECC	Western Electricity Coordinating Council
WLS	Weighted Least Squares
WPP	Wind Power Plant

1 INTRODUCTION

1.1 Background for research

Electrical power systems, consisting of many types of components, perform the core tasks of generating, transmitting and finally distributing electricity throughout vast geographically spread regions. These systems are highly nonlinear and experience both small and large magnitude disturbances. Small magnitude or norm-type disturbances such as load perturbations occur frequently, whereas large magnitude disturbances or event type disturbances such as three-phase faults are also inevitable [1]. Instability in power systems subsequent to these different types of disturbances can be observed in three main variables: rotor angle, frequency and/or voltage. Furthermore, the time spans of interest for stability studies under different types of disturbances also vary with the aforementioned variables. Thus, the power system stability studies are complex even though they are essential for secure operation. On the other hand, the low inertia associated with increased penetration of power electronic converter-based electricity generation in modern power systems demands real-time dynamic security assessment to maintain operational security.

The power system is represented for dynamic analyses using a set of first order differential and algebraic equations in the form of $\dot{X} = f(X, U, V)$ and $I = g(X, U, V)$ where, X, U, V, I are vectors of state variables, inputs, bus voltages and current injections. $\dot{X}$ is the time derivative while f and g are nonlinear functions. These equations are solved using numerical techniques and the resulting time domain trajectories are analysed further to derive the stability conclusions of post-fault power systems subsequent to large magnitude disturbances. Nevertheless, the previously mentioned equations are linearized about a steady-state operating point and the small signal stability is determined based on the eigenvalues of the state matrix. It is clearly evident that the conclusions derived based these dynamic security analyses are largely dependent of the accuracies of the dynamic models as well as the dynamic data.

Traditionally, the power systems were energized by large synchronous generators where their dynamic models are well established. Furthermore, the dynamic data of these generators are either provided by the manufacturers or there exist standard test procedures to determine those. However, these dynamic model parameters might change when synchronous generators are subjected to ageing. Furthermore, the standard tests available to estimate dynamic data need large disturbances such as short circuits at the generator terminals. Therefore, releasing generators for such tests may not be allowed by the system operators. On the other hand, the accuracy of dynamic models and data of power electronic converter-based generation is of utmost importance in dynamic security analyses of modern power systems. There are generic models to represent the dynamic behaviour of the said power generation sources such as wind plants. However, these power electronic converter-based sources accompany different control logics where their data are hardly provided by the manufacturers. This limitation is overcome by the power system planners in system studies by setting values for the controller data in trial-and-error approach to match the system response. One way to overcome these limitations is the system identification where a model that can accurately reflects the dynamics of the generating source under a disturbance is developed using terminal measurements.

Real-time measurements in power systems are facilitated by Phasor Measurement Units (PMU). They provide time synchronized voltage and current measurements with respect to a common reference facilitating many applications such as real-time monitoring, control and protection. These measurements can also be used in system identification in order to develop accurate dynamic models for power system studies.

This research presents a generalized procedure that can be used to accurately estimate the dynamic models of synchronous generators, wind and solar power plants. The proposed technique overcomes the limitations of not having proper dynamic data. Further it can also be used as a systematic approach replacing the conventional trial-and-error approach in which the dynamic data are tuned to match the system response.

1.2 Objectives of the research

The main goal of this research is to devise a generalized methodology to estimate a Dynamic Equivalent Model (DEM) of a power plant which can be used to perform power system stability related studies. The key objectives of the research are as follows:

a) Devise a procedure to develop a DEM of a synchronous generator, wind power plant and a solar power plant using terminal measurements
b) Implement the developed procedure in MATLAB for estimating a transfer function-based model using measurement parameters of a power plant.
c) Validate the performance of the developed DEM comparing the output responses against that of a detailed model simulated using a non-linear simulation platform (such as PSCAD/EMTDC).

1.3 Organization of the thesis

The rest of this thesis is organized as mentioned to achieve the aforementioned objectives.

- Chapter 2 – A detailed literature review has been presented which explores the existing types of detailed dynamic models of synchronous generators, wind and solar power plants, research done on estimation of dynamic equivalent models of power plant using parameter estimation and research gaps.
- Chapter 3 – The estimation methodology proposed to derive the dynamic equivalent models using parameter estimation has been explained in detail.
- Chapter 4 – The proposed mythology has been verified by estimating transfer function-based power plant models in PSCAD by using measurements obtained by simulating power systems with already available detailed power plant models. First, the estimation method has been verified by back-estimating generator transfer function using simulated data in MATLAB. Next, an IEEE 12-bus power system has been modelled in PSCAD which has been verified by comparing

measurements of the steady state load flow simulation with that of a PSS®E simulation. Afterwards, detailed models of synchronous generator, wind and solar power plant have been simulated to obtain measurement data from which DEMs have been estimated. Finally, detailed models have been replaced by DEMs and the measurements have been compared with that of detailed model.

- Chapter 5 – Conclusion of the research and the practical applications of the proposed methodology have been presented.

2 LITERATURE REVIEW

Nowadays with an increasing integration of various types of non-conventional renewable power plants such as wind, solar, hydro, Concentrated Solar Power (CSP), Geothermal and Ocean wave, the power systems are required to handle both synchronous and asynchronous generators, which can be either controllable or intermittent. It has been predicted that global renewable capacity additions in 2021, which amounts to 218 GW worldwide, would be a record 10% expansion compared to 2020. Between 2020 and 2025, it is expected that total wind and solar capacity expands by 1,123 GW which would make their total installed capacity exceed that of natural gas in 2023 and coal in 2024. By 2025, this significant growth is expected to make renewables become the largest electricity generation source by overtaking coal. Therefore, studying the behaviour of power systems when large wind power plants (WPP) or Solar Power Plants (SPP) are integrated is just as important as studying conventional thermal or hydro power plants [2].

Power system stability analyses are mainly categorized as: rotor angle stability, frequency stability and voltage stability. Rotor angle stability is further sub-divided into small signal stability and transient stability, while voltage stability is sub-divided into small-signal and large signal stability. Therefore, small signal stability analysis (SSSA) is a key stability analysis method that is used in power system stability studies, to analyse the ability of the system to maintain synchronism when subjected to small-magnitude disturbances. For performing SSSA, dynamic models of power system components are used. These models, derived using differential equations, are used to describe the dynamic behaviour of the component under observation [3].

For small disturbances, the differential equations that represent the system state can be linearized about an operating point when performing Eigenvalue analysis. Eigenvalue analysis can be used to calculate the dominant oscillation mode of a power system. Any small signal stability problem can be categorized as either local or interarea. Local mode is referred to rotor oscillations that occur in a single generator against all the others in a power system. An interarea mode is where group of generators oscillate against another set of geographically separated generators.

The frequency for local mode usually is in the range of 2-3 Hz. For the inter-area mode, the frequency is usually less than 1 Hz. These oscillations are known as low frequency oscillations (LFO) in literature and these oscillations continue for a relatively long period of time, threatening the stability of the system.

When a small disturbance occurs in the power system, two types of instabilities could occur. Those are oscillatory instability and non-oscillatory instability. Non-oscillatory instability means increase in rotor angle due to insufficient synchronizing torque. Oscillatory instability means amplitude increase of rotor oscillations due to insufficient damping torque. Dynamic models are hence utilized in power system simulations to model and observe how power system parameters change during disturbances that could happen in power systems. These models are used to identify disturbances or components that can threaten the stability of the power system, plan future projects and augmentations required and develop system improvements by tweaking parameters of dynamic models [4], [5].

2.1 Dynamic models of power plants

2.1.1 Dynamic models of thermal and hydro power plants with synchronous generators

For conventional power plants such as thermal and hydro power plants, which consists of synchronous machines, well established dynamic models have been defined in literature. The classical model, also known as the constant voltage behind the transient reactance, is considered the simplest of all those. [6] This classical model has been further modelled in detail by the addition of the field circuit, Automatic Voltage Regulator (AVR) and Power System Stabilizer (PSS) as a sixth order state space model. For machine parameters such as: $H,\ K_D,\ A_{sat},\ B_{sat},\ \psi_{T1}$, $X_l,\ X_d,\ X_q,\ X'_d,\ X''_d,\ X'_q,\ X''_q,\ T'_{q0},\ T''_{q0},\ T'_{d0},\ T''_{d0}$ typical values are obtained experimentally and through calculations too are specified in literature which can be readily used to simulate such a machine easily [7].

For synchronous machine modelling, a standard has been published by IEEE which includes variations of the synchronous generator model that can be used. In the latest IEEE Guide for Synchronous Generator Modelling [8] , three direct-axis and four quadrature-axis models, have been introduced along with the basic transient reactance model. Direct-axis models described are: model with only armature winding and field winding, model with field winding and one damper circuit and model with field winding and two equivalent damper circuits. Quadrature-axis models described in this document are: model with only armature winding, model with one equivalent damper circuit, model with two equivalent damper circuits and model with three equivalent damper circuits.

Similarly, for excitation systems and power systems stabilizers [9] and turbine-governors [10] too standards which include several model variants have been published by IEEE for developing detailed synchronous generator models.

2.1.2 Dynamic models of wind power plants

Unlike synchronous machines, WPPs have varying controls which are manufacturer specific. Therefore, the dynamic models of these plants are also manufacturer specific making it difficult to use these models for generic studies. Nevertheless, in a report compiled by National Renewable Energy Laboratory (NREL), four types of Wind Power plant models, having four different operational technologies as per Western Electricity Coordinating Council (WECC) classifications, have been introduced as generic models. Each model consists of components such as: aerodynamic model (including parameters such as C_p, λ, β), mechanical drivetrain model, induction generator, control block (including PI controller parameters) and electrical model. The advantages of these generic models are they can be used for dynamic studies as manufacturer-independent models, can be modelled for fast and slow transients and allow scalability. Moreover, these models have been implemented in PSCAD/EMTDC software for model verification. However, these generic models will always be approximate and can be used for obtaining estimates rather than precise outputs. They do have the advantage of not requiring large datasets for validation [11], [12].

2.1.3 Dynamic models of Solar power plants

For SPPs too, generic dynamic models have been modelled by NREL for both current source as well as voltage source inverters, which have control architectures based on the model developed by the Renewable Energy Modelling Task Force of the WECC [13]. Two types of generic SPP dynamic models have been developed by WECC: central station model which represent large scale (greater than 10 MW) SPPs connected to transmission system through a central point of interconnection and distributed PV system model which represents a combination of smaller PV generators connected to distribution system.

The central station model is based on 3 submodules namely: Renewable Energy Plant Controller (REPC), Renewable Energy Electrical Controller (REEC) and Renewable Energy Generator Controller (REGC). REPC module controls real power (governor response) and reactive power (voltage regulation) using inputs such as reference voltage, reference reactive power, reference real power. REEC module limits currents to suit limits of power electric switches and other components. REGC provides non-linear control at grid interface for protection in cases such as over/under voltage situations.

For distributed PV systems a model named PVD1 which consists of active power control, reactive power control and protective measures has been defined. For newer plants, a model named DER_A has been introduced recently which is based on large scale central station model [14].

2.2 Dynamic equivalent models for power plants

Even though above mentioned detailed dynamic models are required for performing accurate dynamic behavioural studies of a power system, sometimes utilizing these detailed representative internal controls would require significant computational times when simulating. Moreover, the more detailed the model is, the more parameter details will be required when mapping the model to an actual scenario which is usually difficult to obtain practically. When WPP models defined by NREL is considered, there are several PI controllers whose correct PI values could vary from generator to generator. Even the general power electronic converters mentioned may be different in actual implementation and their switching signalling algorithms, switching frequencies, filter parameters could vary vastly from manufacturer to manufacturer.

Additionally, for a power plant like a WPP, when many wind turbines are added to a single aggregated model, it would create a very high-order model, making it computationally intensive and difficult to predict the operational state of each wind turbine. Therefore, dynamic equivalent models (DEMs) are preferred usually in performing power system stability analyses where a detailed model is represented by an equivalent and simpler model which exhibits characteristics similar to the detailed model. Determining DEM could be done either by theoretical aggregation which requires detailed parameters of internal components or measurement-based parameter estimation techniques which requires recorded dynamic response data. These parameter estimations of nonlinear models are usually based on optimization algorithms which minimizes the square error between the measured output the calculated dynamic response output [15]. It has been shown that DEMs provide dynamic responses similar to that of detailed models. Moreover, an added advantage highlighted is the significant improvement of computational times. In [16], for verifying the accuracy of dynamic responses for DEM and detailed model, active power, reactive power and output voltage at the generator have been used which are easily measurable parameters.

There are 3 types of DEMs described in literature: white-box in which the complete information about model structure and parameters is available and verified, black-box where model structure is completely invisible and grey-box where there is some physical insight into the model structure which makes it a hybrid model of black and white box models. Black-box models can only be estimated through measurement data [17].

2.3 Parameter estimation for modelling black box models

Estimating of black-box models by mapping measured input and output data of the system and fitting a mathematical model to that data set is known as system identification which consists of several steps. The first step is collection of input-output data. Second step is choosing a set of candidate models of different model orders that would be suitable to represent this system and using an estimation technique to obtain those respective models using input output data. The third step is to choose the most suited model among the candidates based on a certain ranking criterion such as Akaike’s Information Criterion (AIC) and Bayesian Information Criterion (BIC). Both these types of criteria provide a penalizing score for both model complexity as well as model fit to estimate so that an overly complicated model would not be considered the best model even if the fit to estimate is high [18]. The fourth step is model validation in order to decide whether the selected model is appropriate for its intended use. This can be done by comparing measured and simulated outputs for estimated models when same inputs are given, performing residual analysis or even by performing spectral analysis on the estimated models and comparing bode plots [19].

There are many parameter estimation techniques discussed in literature. For linear time-invariant systems several types of such models have been described such as autoregressive with extra input (ARX), transfer function, state-space, output error (OE) and Box-Jenkins (BJ) models [20], [21].

In [22] ARMAX (Autoregressive Moving Average eXogenous) model has been used to fit a DEM using solar irradiation as input and DC link voltage as output. The model parameters have been optimized using several recursive algorithms and the results of actual and estimated outputs have been compared.

Parameter estimation fundamentally requires finding the best parameters through optimization algorithms. Several optimization techniques have been compared in literature One such method is Metaheuristic methods which includes Genetic Algorithm (GA), Particles Swarm Optimization (PSO) and Differential Evolution (DE). Moreover, there are methods such as Least Squares Method (Non-Linear and

Linear least square), Kalman Filter, Prediction Error Method (PEM) and Maximum Likelihood method. Furthermore, there are a set of methods called subspace methods which are categorized as: Numerical algorithm for Subspace State Space System Identification (N4SID), Multi-variable Output-Error State Space (MOESP) and Canonical Variate Analysis (CVA) [23].

For estimating dynamic models of synchronous generators, many studies have been conducted using several techniques. Recursive Least Square (RLS), Recursive Instrumental Variable (RIV) and PEM have been used in [24] to estimate inertia constant and damping constant parameters of Heffron-Phillips generator model. In [25] usage of Weighted Least Squares (WLS) method for estimating physical parameter values of synchronous generator has been demonstrated. In [26] N4SID methodology has been demonstrated to estimate the states of a 2 generator 2 area as well as a 4 generator 2 areas system. Further, in [27] three subspace methods: MOESP, N4SID and CVA have been used to estimate parameters in a power system comprising of synchronous generators and their effectiveness have been demonstrated. Methods such as Artificial Neural Networks (ANN) [28] and GA [29] too have been utilized for estimation of synchronous generator physical parameters by using measurements.

Several research have been conducted in developing DEMs for WPPs using parameter estimation. A WPP can be represented as a single machine equivalent model if all turbines in the plant are identical or as a multi machine model where wind turbines can be clustered by the wind speed or other parameters [30].

In developing such DEMs it is first required to determine the points at which measurements are obtained for inputs and outputs. It has been shown that measurements obtained at the point of interconnection (POI) of the WPP to the power system accurately estimates the black-box model irrespective of the actual internal structure. In most research, the parameters that have been measured at POI are voltage, current, active power and reactive power. Additionally, wind speed too has been considered as an input to estimate the model behaviour due to changes in wind speed [31].

In [32] RLS method has been utilized to estimate DEMs for a wind power plant and for slow dynamics the method had significantly reduced the model order without sacrificing accuracy. PSO has been utilized in [33] for estimating a state space-based DEM of a WPP. A different flavour of subspace identification techniques named Predictor Based Subspace Identification (PBSID) has been demonstrated in [34].

For SPPs, considerably less research has been conducted in estimating DEMs for grid connected power plants than for WPPs. Most dynamic model related research for SPPs have been done for white-box or grey-box models by independently modelling internal controls using standard WECC models. For SPPs with many converters, aggregation techniques have been used to reduce the number of units considered [35], [36]. Most studies done for system identification and parameter estimation are for modelling of solar PV cells or modules and not for the whole generator with controls and power electronic converters [37], [38].

One such research has been conducted to estimate gain parameters of a standard WECC generic (REGC_A and REEC_B) dynamic model using a hybrid parameter estimation method named ZN-PSO, which utilizes PSO along with Zeigler Nichols method [39].

In [40], a matrix of variables based white-box modelling method has been used for a SPP with a distributed photovoltaic grid-connected system with many panel-level DC optimizers.

As evident from above mentioned sources, for different types of generators in power systems, parameter estimation using measurement-based approaches have been done mainly for synchronous generators as well as WPPs. Out of those methods, Metaheuristic methods such as PSO and least square methods have been predominantly researched upon. Moreover, subspace methods such as N4SID and MOESP too have been demonstrated in several research especially for synchronous generators which are supposed to provide faster estimates than other methods.

When using a least square method, first an equivalent model must be initialized with estimate parameter values and then parameter values shall be iteratively optimized until the cost function reaches a defined minimum [41]. To obtain faster initial estimates of parameters during system identification, it has been shown that subspace estimation methods would be the most suitable. Out of those, N4SID method has been predominantly discussed in studies done for power system related parameter estimations [42], [43].

2.4 Chapter Summary

In the literature survey it was evident that modelling of black-box DEM using parameter estimation has been done using several methods for synchronous generators and WPP. However, for SPP the research that have been conducted for estimation of DEM is scarce which presents a research gap that can be bridged by finding a methodology to estimate DEM of such a power plant which is one of the most rapidly integrated renewable power plants nowadays. In order to compare the performance, it is therefore important to apply such a methodology to synchronous generators as well as for WPPs for assessing the generic nature.

When selecting a suitable methodology for parameter estimation, it was evident that least squares method has been used in several research successfully but for deriving a satisfactory estimate a good initial estimate needs to be available. Such a least squares optimization method can be used if a fast and accurate parameter initialization method such as N4SID can be utilized. N4SID is a method which has been used for parameter estimation in the domain of power systems and therefore, could be suitable for this use case too.

3 PROPOSED METHODOLOGY

3.1 Overview of proposed estimation methodology

In this study, a method to estimate a generalized transfer function based dynamic equivalent model for 3 types of generators: synchronous, wind and solar, using practically measurable parameters has been proposed.

The transfer function-based model estimated using measured data can be implemented in simulation platform for power system dynamic simulations in place of actual detailed models.

Two separate DEMs have been proposed to be used to model the behaviour of all 3 types of power plants for both network disturbances (external disturbance) as well as input disturbances (internal disturbances). All models are interpreted as transfer function models where ΔY(s) represents the change in output and ΔU(s) represents the change in input subjected to the condition number of poles is greater than number of zeros (m>n).

$$\frac{\Delta Y(s)}{\Delta U(s)} = \frac{a_0 s^n + a_1 s^{n-1} + a_2 s^{n-2} + \cdots + a_n}{b_0 s^m + b_1 s^{m-1} + b_2 s^{m-2} + \cdots + b_m} \tag{3.1}$$

The goal of the estimation methodology is to estimate the model orders m and n that fits the given input and output data while estimating each of the coefficients of denominator [b_0-b_m] and numerator [a_0-a_n]. Input measurements used for estimating the models are phase angle (Ph) and Root Mean Square (RMS) voltage magnitude (V) of the bus voltage which are easily measurable using the existing measuring instruments. Moreover, since the actual validation is done using PSCAD/EMTDC, these 2 measurements are directly used to control phase angle (Ph) and voltage magnitude (V) of a three-phase controlled voltage source block which is used to interface the estimated transfer function-based model to the electrical network of the simulation.

For estimation of parameters, it is proposed to use N4SID for initializing the parameters quickly and optimize the initial estimate by using non-linear least squares (NLS) method which have been discussed in the literature review.

3.2 Model for representing behaviour of power plant for internal disturbances

The proposed DEM for internal disturbances is a Single Input Multiple Output (SIMO) model. Inputs selected for modelling internal disturbances (U_{int}) for each type of power plant are as follows:

- Hydro Power Plant with Synchronous generator - Active Power reference
- Wind power plant - wind speed (ms^{-1})
- Solar power plant - Solar irradiance (Wm^{-2})

Transfer functions $H_1(S)$ and $H_2(S)$ need to be estimated using the change in measured input ΔU and change in measured outputs ΔPh (in degrees with respect to the reference of swing bus. Bus 10 is the swing bus) and ΔV (p.u).

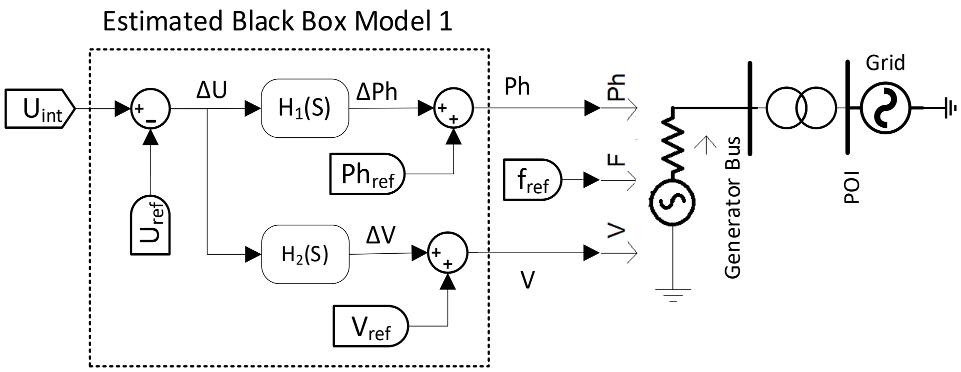

Figure 3.1: Blackbox model structure for simulating behaviour due to internal disturbances

Reference parameters for steady state operation: Input reference (U_{ref}), Phase angle reference (Ph_{ref}), Generator bus voltage reference (V_{ref}) and Frequency reference (f_{ref}) shall be set manually before running the simulation. These steady state values can be obtained from the pre-fault steady state measurements obtained from the simulation or actual power system.

3.3 Model for representing behaviour of power plant for external disturbances

For modelling external disturbances that happen in the network, the proposed model is a Multiple Input Multiple Output (MIMO) model. The inputs used are active power (MW) and reactive power (MVAr) measured at generator bus which are easily measurable parameters. Transfer functions $H_3(S)$ and $H_4(S)$ need to be estimated using the change in measured inputs ΔP, ΔQ and change in measured outputs ΔPh, ΔV.

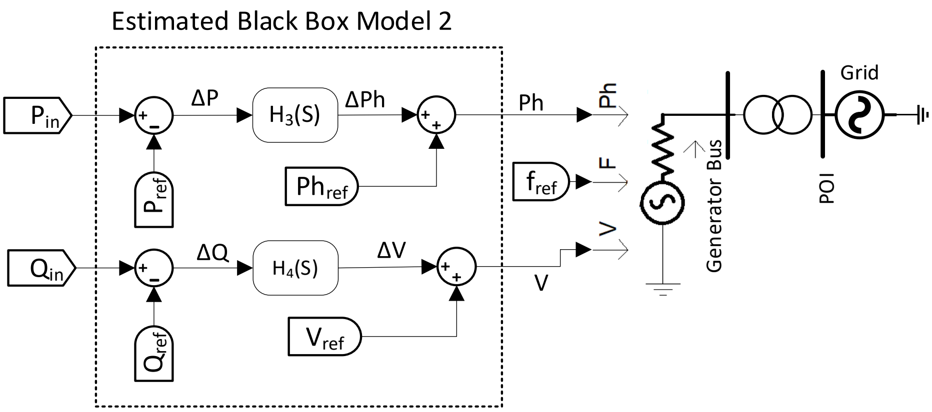

Figure 3.2: Blackbox model structure for simulating behaviour due to external disturbances

Reference parameters for steady state operation: Active Power reference (P_{ref}), Reactive Power reference (Q_{ref}), Phase angle reference (Ph_{ref}), Generator bus voltage reference (V_{ref}) and Frequency reference (f_{ref}) shall be set manually before running the simulation. These steady state values too can be obtained from the pre-fault steady state measurements obtained from the simulation or actual power system as for the internal disturbance model.

3.4 Estimation of the transfer function

For estimation, input-output data during an internal or external disturbance shall be obtained either through real measurements or through a PSCAD/EMTDC simulation. Based on the observations of this study it was evident that both input and output data should be sampled at same rate and at least 50 samples sampled at 100 ms are required for an accurate transfer function estimation in MATLAB. Moreover, it was apparent that for obtaining measurement data a first order filter with a smoothing time constant of about 20 ms is required for filtering noise.

Next, a possible range of values for number of poles (m) and number of zeros (n) shall be specified depending on the type of generator used. For a hydro synchronous generator an actual white box transfer function model would not be greater than 10 poles. Therefore, selecting a range of 4-10 poles would be sufficient for a synchronous generator.

Similarly for wind and solar power plants too, fitting models having poles of orders greater than 10 would not give any special benefit as it would unnecessarily increase model estimation time. Further, the model evaluation criteria will anyhow limit the model to the lowest possible best fit by evaluating fit to estimate as well as complexity. After selection of the number of poles, a set of all possible combinations of poles and zeros shall be generated, subjected to the condition that the number of poles shall always to greater than number zeros.

Next step is to loop through all the pole-zero combinations to estimate the most optimum transfer function by using recorded input-output data. For each iteration, the first step is to use N4SID method to initialize coefficients and derive an estimate transfer function. Then, by using NLS method iteratively the loss function as given below is minimized by optimizing coefficients. Here, $\mathrm{y}_{\mathrm{measured}}(\mathrm{t})$ and $\mathrm{y}_{\mathrm{estimated}}(\mathrm{t})$ are the outputs obtained from measurement and output obtained from the estimated transfer function respectively while $e(t)$ is the one step prediction error.

$$e(\mathrm{t}) = \mathrm{y}_{\mathrm{measured}}(\mathrm{t}) - \mathrm{y}_{\mathrm{estimated}}(\mathrm{t}) \tag{3.2}$$

The minimization of $e(t)$ is achieved by running the iterative minimization until the error becomes less than 0.01 or at most for 30 iterations. The resulting model is then saved in an array for each pole-zero combination. Once this process has been completed for all pole-zero combinations, it is required to select the most optimum model that describes the measured input-output dataset. For this, Akaike's Information Criterion (AIC) is calculated for all the models estimated and the model which has the least value for AIC is considered as the most optimum model for this data set.

After estimating all four transfer functions, $H_1(S)$, $H_2(S)$, $H_3(S)$, and $H_4(S)$, model suitability can be validated by developing a custom black-box generator model in PSCAD using estimated transfer functions. This black-box generator can be used to replace the generator which was used to obtain measurements. After applying the same disturbances to the black-box model as well, it can be validated by comparing the outputs measurements for the black-box model and actual generator model. For this comparison, Mean Square Error (MSE) has been utilized as the comparison metric.

The methodology proposed for estimating transfer function model orders and coefficients of the transfer functions $H_1(S)$, $H_2(S)$, $H_3(S)$ and $H_4(S)$ is illustrated below.

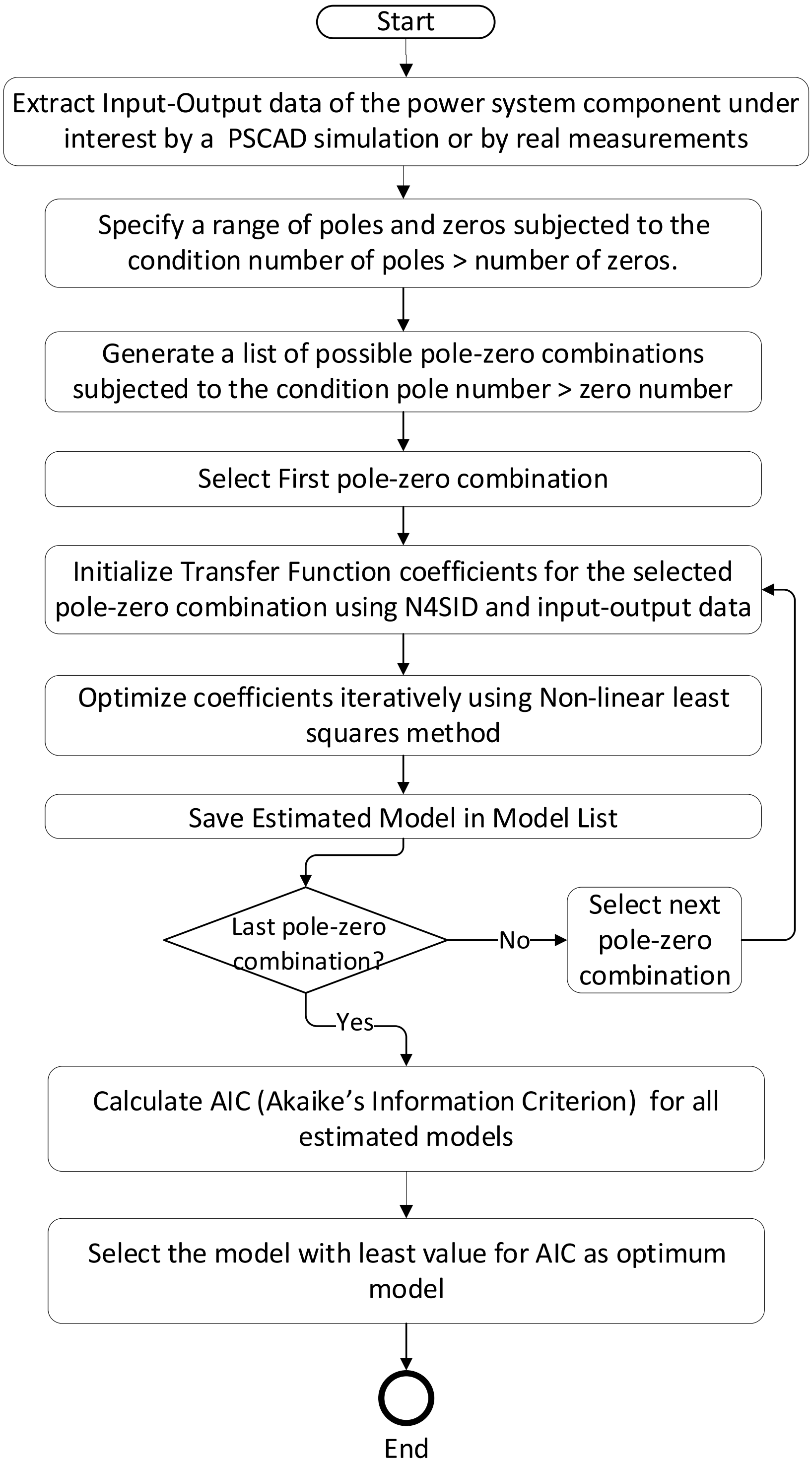

Figure 3.3: Proposed estimation methodology

3.5 Akaike's Information Criterion (AIC)

The Akaike information criterion (AIC) is a mathematical technique for assessing fit of a model to the data from which it was derived from. In practice AIC is used to compare several possible candidate models to determine the most optimum fit. This has been derived as an extension of the maximum likelihood principle by Hirotugu Akaike [44].

AIC is used to evaluate a model based on 2 parameters:

- Model Performance - Performance of a candidate model for the data set used for estimation. This is a measure of the models fit to data.
- Model Complexity – Number of parameters estimated model (In the case of the transfer function, number of poles and zeros)

Model performance improves when the model fit improves. But this in turn increases model complexity. To strike a balance between these 2 parameters, AIC is calculated.

AIC is calculated using below formula

$$AIC = 2k - 2\log(L) \tag{3.3}$$

Where:

k: Number of parameters

L: Maximum likelihood estimate of model

When comparing several models using AIC, the model with the lowest AIC is considered the best according to Akaike's theory. It gives a measurement of how much information is lost when compared to actual mode and hence model that has the least value for loss of information evidently shall best describe input-output data.

The maximum likelihood increases when more variables are added to the model which improves the model fit. The same time it increases complexity. Therefore, the "2k" term penalizes the AIC value and compensates for increased complexity.

3.6 Transfer function-based modelling of a generator

The dynamic behaviour of a generator is usually described by nonlinear equations which can be linearized around a particular operating point. These equations can be converted into a set of first-order differential or difference equations using state variables and can be represented in state-space form with *n* state variables, *i* inputs and *j* outputs as below:

$$\dot{x(t)} = Ax(t) + Bu(t) \tag{3.4}$$

$$y(t) = Cx(t) + Du(t) \tag{3.5}$$

Where:

$x(t)$= State vector, $\dot{x(t)} = \frac{dx(t)}{dt}$ (*n* x 1 dimension)

$u(t)$= Input vector (*i* x 1 dimension)

$y(t)$= Output vector (*j* x 1 dimension)

A= State matrix (*n* x *n* dimension)

B= Input matrix (*n* x *i* dimension)

C= Output matrix (*j* x *n* dimension)

D= Feedthrough matrix (*j* x *i* dimension) – This is zero when there is no feedthrough from input to output

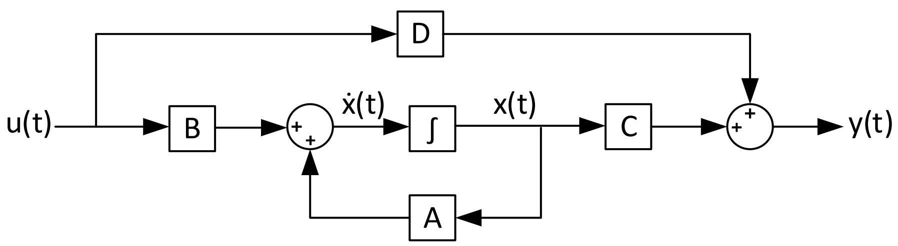

Figure 3.4: Block diagram representation of the state space form of a dynamic model of a system

This state space form can be converted to a transfer function format by converting state space equations 3.4 and 3.5 to Laplace Domain. Then Laplace transform of 3.4 becomes:

$$sX(s) = AX(s) + BU(s)$$
$$X(s) = (sI - A)^{-1}.B.U(s) \qquad (3.6)$$

When 3.6 is substituted to Laplace transform of 3.5 output becomes:

$$Y(s) = C.(sI - A)^{-1}.\ B.U(s) + D.U(s) \qquad (3.7)$$

Since D = 0, transfer function between input and output becomes

$$\frac{Y(s)}{U(s)} = C.(sI - A)^{-1}.\ B \qquad (3.8)$$

Since it was necessary to confirm the suitability of the proposed estimation method for estimating transfer functions of generators, several known transfer functions of generators were used to produce input-output data by simulating the transfer function model in Simulink. A known input was given to each transfer function model and output was recorded for back-estimation of the transfer function using the proposed method. For this purpose, generic synchronous generator dynamic models described in [7] were used along with the data for each parameter. All model details were provided in state space form.

In these simulations and estimations, input considered was deviation of mechanical torque ΔT_m and the output was deviation of rotor speed $\Delta\omega_r$. Other parameters were kept constant and hence the deviation of those parameters was considered zero.

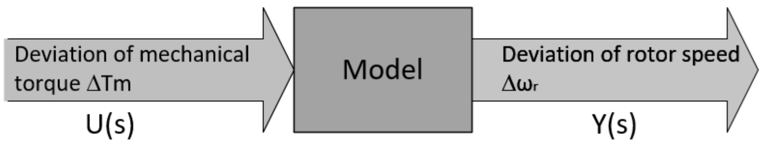

Figure 3.5: Inputs and outputs considered for synchronous generator modelling in Simulink

Results obtained for estimating 2nd order classical generator model are shown in this section.

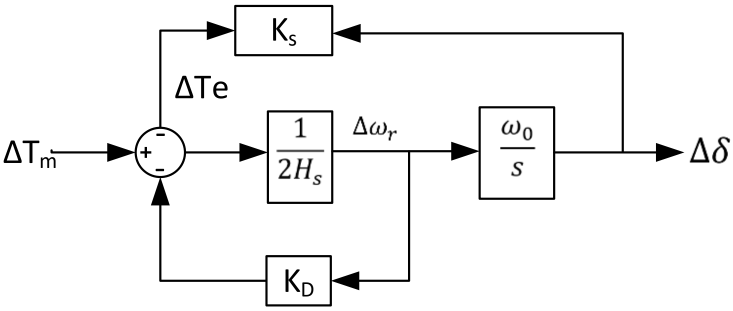

Figure 3.6: 2nd Order classical generator model block diagram

ΔT_m = Mechanical Toque deviation
ΔT_e = Electrical Toque deviation
K_D = Damping Torque Coefficient in pu
H = Inertia constant in MWs/MVA
$\Delta\omega_r$ = speed deviation in pu = $(\omega_r - \omega_r)/\omega_0$
$\Delta\delta$ = Rotor angle deviation in electrical rad
s= Laplace operator
$\Delta\omega_0$ = Rated speed in electrical rad/s

State space model of the 2nd order classical generator model are illustrated below where A, B, C and D matrices are separately identified as in the form of equations 3.4 and 3.5.

$$\underbrace{\begin{bmatrix}\Delta\dot{\omega}_r\\ \Delta\dot{\delta}\end{bmatrix}}_{} = \underbrace{\begin{bmatrix}-\frac{K_D}{2H} & -\frac{K_S}{2H}\\ \omega_0 & 0\end{bmatrix}}_{}\underbrace{\begin{bmatrix}\Delta\omega_r\\ \Delta\delta\end{bmatrix}}_{} + \underbrace{\begin{bmatrix}\frac{1}{2H}\\ 0\end{bmatrix}}_{}\underbrace{\Delta T_m}_{}$$

$$[\ \dot{X}\ ] = [\quad A \quad]\,[X(s)] + [\,B\,]\,[U(s)]$$

$$\underbrace{[\mathrm{Y(s)}]}_{} = \underbrace{[1 \quad 0]}_{}\underbrace{\begin{bmatrix}\Delta\omega_r\\ \Delta\delta\end{bmatrix}}_{} + \underbrace{[\ 0\ ]}_{}\underbrace{[\ 0\ ]}_{}$$

$$[Y(s)] = [\ C\ ]\,[X(s)] + [\,D\,]\,[U(s)]$$

Now, these matrices can be substituted in equation 3.8 to obtain the transfer function between ΔT_m and $\Delta\omega_r$ by using parameter details given below.

$$A = \begin{bmatrix} -1.4286 & -0.10814 \\ 377 & 0 \end{bmatrix}$$

$$B = \begin{bmatrix} 0.14286 \\ 0 \end{bmatrix}$$

H = 3.5
K_d = 10
ω_0 = 10
K_s = 0.757

$$\frac{\Delta\omega_r}{\Delta T_m} = \frac{0.1429\ s}{s^2 + 1.429\ s + 40.77}$$

This transfer function was then modelled in Simulink and inputs and outputs were recorded after providing a step input and running the simulation for 6 seconds.

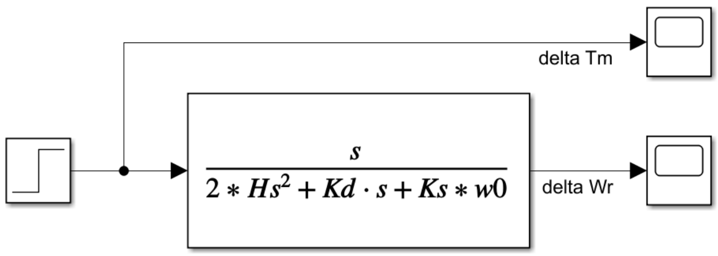

Figure 3.7: Simulink model for 2nd order synchronous generator

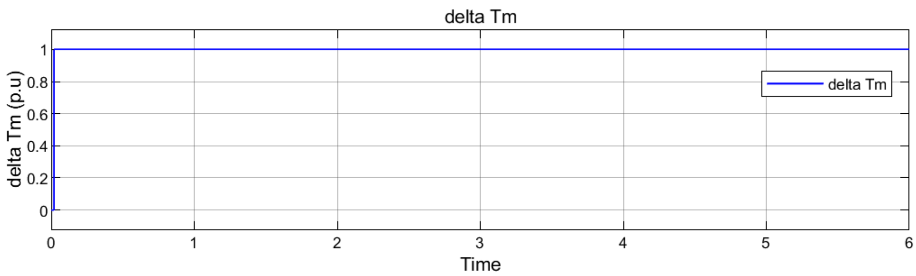

Figure 3.8: Step input given to Simulink transfer function model

These data recorded were then used to estimate the transfer function using the proposed estimation methodology using MATLAB. For estimation in MATLAB, the standard functions available for estimation in MATLAB System Identification Toolbox was utilized. The standard estimation function was run by initializing the estimate using N4SID and optimization using NLS method. Limits for number of zeros was selected as 9 and limit for number of poles was selected as 10. AIC values for all the estimated models for each viable pole-zero combination is shown in the below pivot table.

Table 3.1: AIC values of all models estimated for 2nd order synchronous generator model

Zeros / Poles	1	2	3	4	5	6	7	8	9
2	-45628.36								
3	-11985.13	-43922.13							
4	-10365.74	-12507.21	-21127.28						
5	-12320.35	-11434.75	-11432.75	-11532.44					
6	-12433.34	-12170.25	-11428.75	-12143.35	-12307.69				
7	-12437.84	-12396.16	-12446.27	-12444.27	-12248.07	-12399.08			
8	-12452.10	-12446.32	-12456.53	-12440.27	-12395.34	-12454.82	-12440.63		
9	-12464.55	-12462.19	-12462.26	-12455.17	-12453.17	-12465.27	-12435.57	-12451.40	
10	-12475.81	-12473.78	-12472.01	-12469.14	-12449.17	-12468.32	-12456.56	-12465.87	-12459.27

The lowest AIC value of -45628.36 resulted for 2 pole 1 zero model which is as same as the original transfer function. Estimate transfer function is as follows.

```
0.1429 s + 6.495e-16
---------------------
s^2 + 1.429 s + 40.77
```

The poles are same as that of the actual transfer function since the denominator coefficients are same. A constant has been added to the numerator coefficients which slightly changes the values of zeros. This however is not an issue since model behaviour is mainly dependant on the poles than zeros. To confirm that the estimated model behaviour is similar to the actual model, same input was provided for both the models using MATLAB and the outputs were plotted on top of each other and the curve fit percentages were compared.

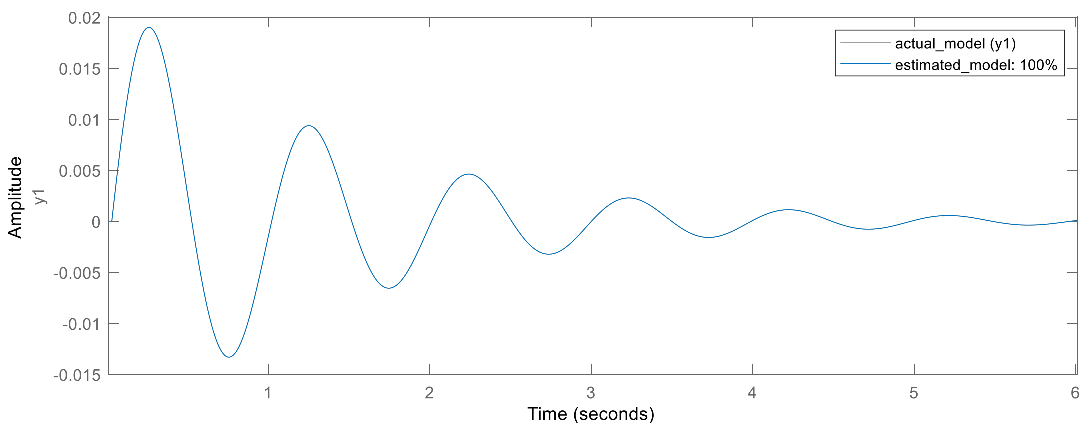

Figure 3.9: Comparison of outputs for actual and estimated models of 2nd order synchronous generator model

The same procedure was then carried on for estimating transfer functions of 3rd, 4th and 6th order models respectively. The estimated and actual transfer functions were compared for further verification. Detailed models, parameter values and results can be found in Appendix A .

Table 3.2: Transfer Functions estimated for each type of synchronous generator model

Model	Actual/ Estimated	Transfer function
2nd order classical model	Actual	$\frac{0.1429 s}{s^2 + 1.429 s + 40.77}$
	Estimated	$\frac{0.1429 s + 6.495e-16}{s^2 + 1.429 s + 40.77}$
3rd order model – Generator with field circuit	Actual	$\frac{0.1429 s^2 + 0.06041 s}{s^3 + 0.4229 s^2 + 41.17 s + 8.379}$
	Estimated	$\frac{0.1429 s^2 + 0.06041 s - 1.328e-15}{s^3 + 0.4229 s^2 + 41.17 s + 8.379}$
4th order model - Generator with Field circuit + AVR	Actual	$\frac{0.1429 s^3 + 7.203 s^2 + 84.34 s}{s^4 + 53.28 s^3 + 775.6 s^2 + 3754 s + 3.316e04}$
	Estimated	$\frac{0.1429 s^3 + 7.212 s^2 + 84.55 s - 4.936e-13}{s^4 + 53.34 s^3 + 777.1 s^2 + 3759 s + 3.323e04}$
6th order – Field circuit + AVR + PSS	Actual	$\frac{0.1667 s^5 + 13.57 s^4 + 387.6 s^3 + 4643 s^2 + 1.023e04 s}{s^6 + 81.44 s^5 + 2367 s^4 + 3.12e04 s^3 + 1.595e05 s^2 + 1.073e06 s + 7.175e05}$
	Estimated	$\frac{0.1666 s^5 + 13.58 s^4 + 386.8 s^3 + 4570 s^2 + 8679 s + 3.285e-09}{s^6 + 81.55 s^5 + 2371 s^4 + 3.129e04 s^3 + 1.599e05 s^2 + 1.076e06 s + 7.197e05}$

6th Order - Field Circuit + AVR + PSS (with Damper winding effect)	Actual	$\dfrac{s^5 + 65.45 s^4 + 1107 s^3 + 2410 s^2 + 818.5 s}{s^6 + 65.45 s^5 + 1152 s^4 + 5239 s^3 + 4.649e04 s^2 + 8.984e04 s + 1.613e04}$
	Estimated	$\dfrac{0.1667 s^5 + 10.93 s^4 + 185.2 s^3 + 404.3 s^2 + 135.4 s + 8.085e-09}{s^6 + 65.58 s^5 + 1156 s^4 + 5255 s^3 + 4.666e04 s^2 + 9.018e04 s + 1.619e04}$

3.7 Chapter summary

By comparing the transfer functions of all 5 synchronous generator models it was evident that the estimation methodology estimates transfer function models similar to actual transfer functions (similar number of poles and similar coefficient values of poles) when the system is a SISO type model. However, an actual power plant is a MIMO or SIMO type of a model which comprises of several transfer functions as described in 3.2 and 3.3.

The advantage of utilizing terminal measurements such as active power, reactive power, bus voltage and bus voltage phase angle as physical input measurements for estimation is that these are easily measurable in an actual power plant too and hence can practically be used for estimating transfer functions of those power plants.

For solar and wind power plants, this Simulink simulation was not done as building a state-space model white box transfer function model by referring WECC definitions is highly complicated. Therefore, for all 3 types of generators, input-output data was obtained by simulating already available standard PSCAD models in a IEEE 12-bus system as explained in Chapter 4.

4 VERIFICATION OF PROPOSED METHODOLOGY

4.1 Modelling test power system

4.1.1 IEEE 12-bus system

The approach tested in 3.6 was then extended to be tested using data obtained from a detailed power plant in a power system simulation using PSCAD for verification of the proposed methodology for an actual scenario where several parameters change simultaneously. For this, IEEE 12-bus system was utilized. Detailed data of the 12-bus system used is given in Appendix B .

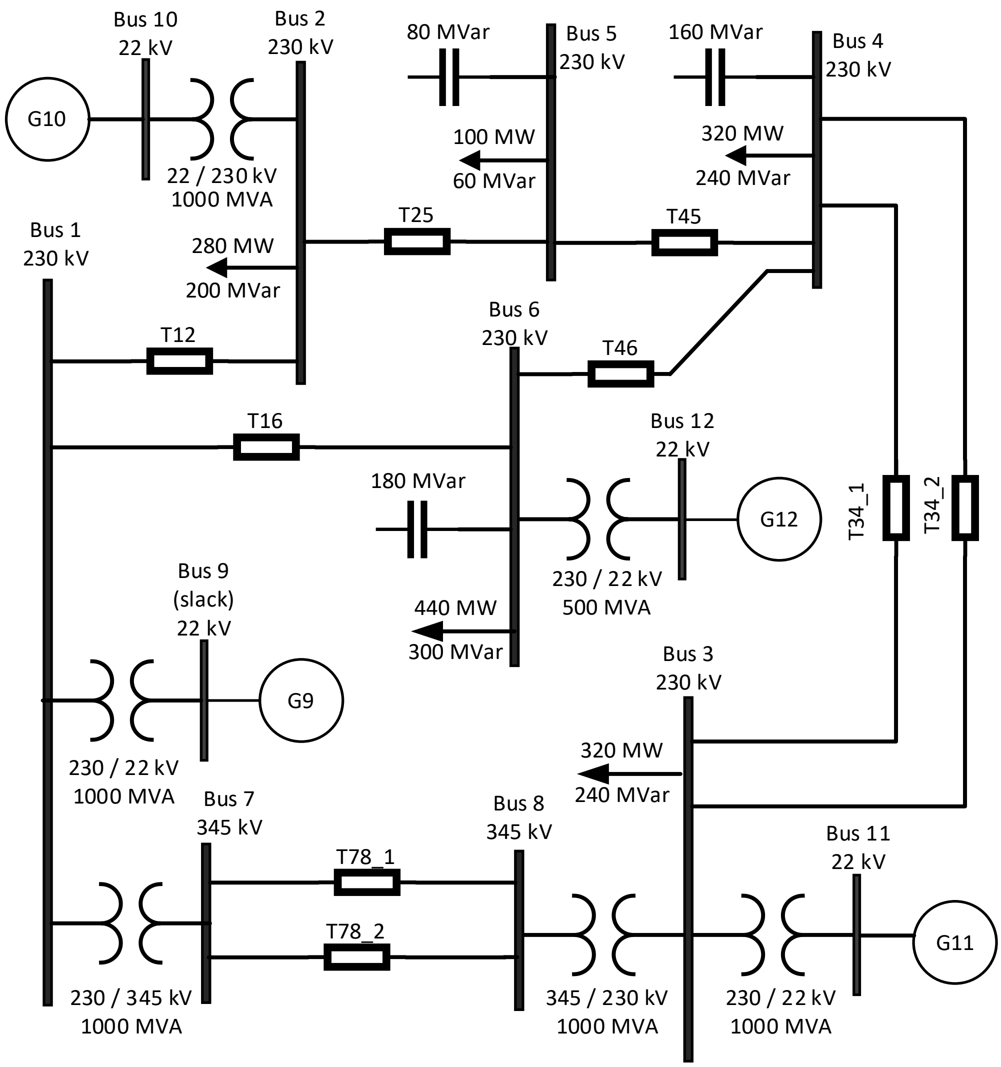

Figure 4.1: IEEE 12-bus system

Several software were utilized for obtaining data, estimation and method verification.

Table 4.1: Software utilized for the research

Software	Version	Purpose
PSS®E Xplore	34	Validation of IEEE 12 bus system
PSCAD	4.5.0	Modelling test power system, obtaining input-output data for estimation and simulation of estimated black box models
MATLAB	R2019a	Estimation of transfer functions using input-output data

4.1.2 Verification of IEEE 12-bus system PSCAD model load flow simulation

This IEEE 12-bus system was modelled in PSCAD environment using fixed three phase voltage sources as generators as shown in Figure B.1 using the data mentioned in Appendix B . To verify that the PSCAD model was correct, the same data was used to model the same system in PSS®E as in Figure B.2.

For comparison, measurements obtained at generator busses were compared for both models as indicated in Table 4.2 and it was observed that measurements to be close to one another in both simulations and hence it was concluded that PSCAD model steady state simulation was correct.

Table 4.2: Comparison of steady state load flow measurements at generator busses between IEEE 12-bus systems modelled in PSS®E and PSCAD

	Active Power (MW)		**Reactive Power (MVAr)**		**Voltage Phase Angle with reference to slack bus (degrees)**		**Voltage of bus (P.U)**	
Bus	**PSS/E**	**PSCAD**	**PSS/E**	**PSCAD**	**PSS/E**	**PSCAD**	**PSS/E**	**PSCAD**
9	483.50	478.40	-55.50	-67.84	0.00	0.02	1.05	1.05
10	500.00	500.30	109.10	104.60	4.47	4.46	1.02	1.02
11	200.00	214.30	67.20	60.51	-11.21	-10.16	1.01	1.01
12	300.00	291.50	93.70	90.80	-20.30	-20.25	1.02	1.02

Therefore, the voltage sources of the PSCAD simulation were replaced by detailed hydro power plant models with synchronous generators except the slack but which was kept as a voltage source to maintain the voltage phase angle reference and avoid phase angle wrapping in the simulation.

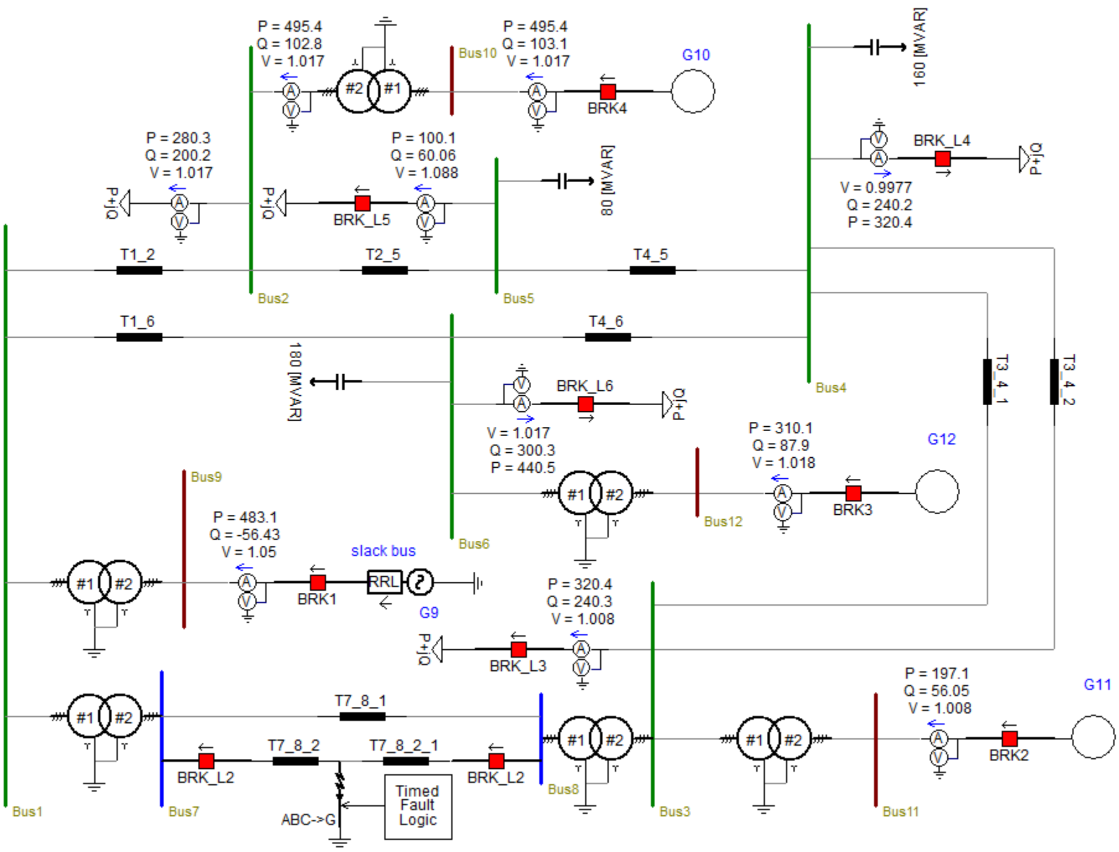

Figure 4.2: IEEE 12-bus system modelled in PSCAD with detailed generator models

G10 generator was used as the generator under test which was replaced sequentially with a wind power plant and solar power plant to obtain parameter measurements for internal as well as external disturbances.

4.1.3 Hydro Power Plant with synchronous generator PSCAD model

The hydro power plant used for this simulation was a 500 MW single machine power plant as shown in Figure 4.3 with a STA1 type excitor, PSS1A power system stabilizer and a TUR1 type hydro turbine. All the components used were standard PSCAD components. Active power reference was made controllable by manually controlling the turbine wicket gate position ‘z’. Detailed settings of this model can be found in Appendix C section C.1 .

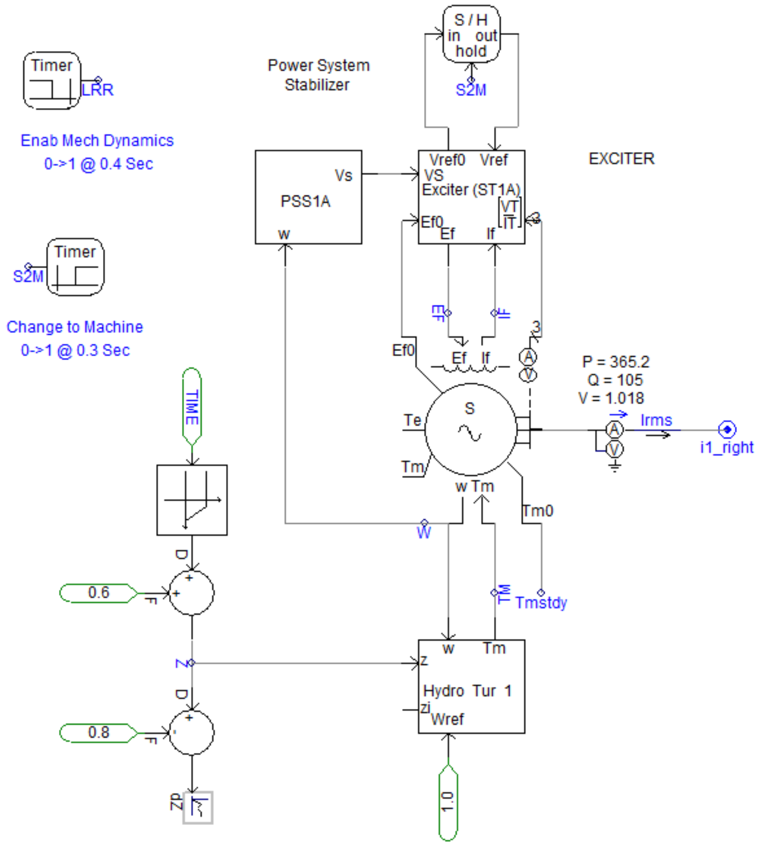

Figure 4.3: Hydro Power Plant with synchronous generator PSCAD model

4.1.4 Wind Power Plant PSCAD model

The 500 MW wind power plant shown in Figure 4.4 used consists of 100 type II wind generators of 5 MW. Wind speed (ms^{-1}) is controllable externally in this model. Detailed settings of the model can be found in Appendix C section C.2 .

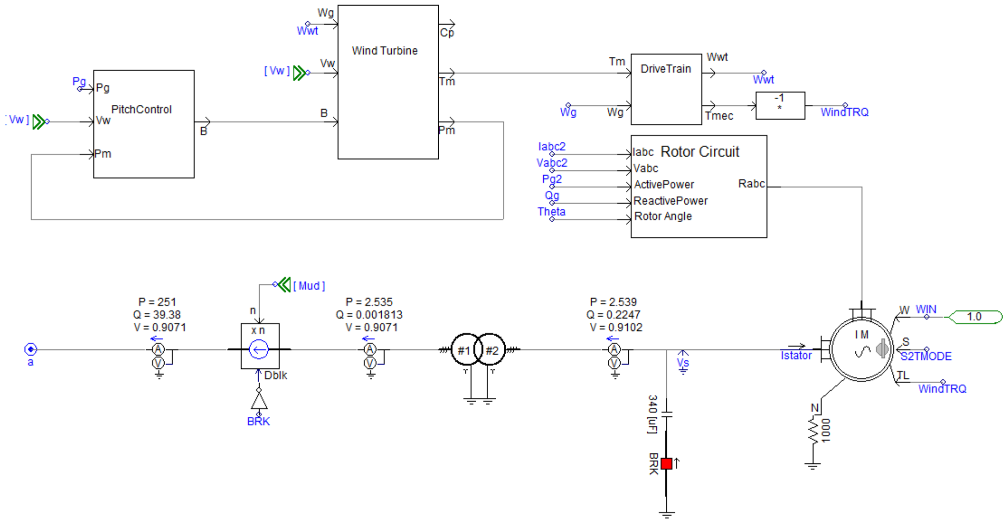

Figure 4.4: Type II Wind Turbine based power plant

4.1.5 Solar Power Plant PSCAD model

The 200 MW solar power plant Figure 4.5 used consists of 400 grid connected solar PV generator units rated 0.5 MW. (At 28^{0}C and 1200 Wm^{-2} each generator generates 0.29 MW) External temperature (^{0}C) and solar irradiance (Wm^{-2}) is controllable externally in this model.

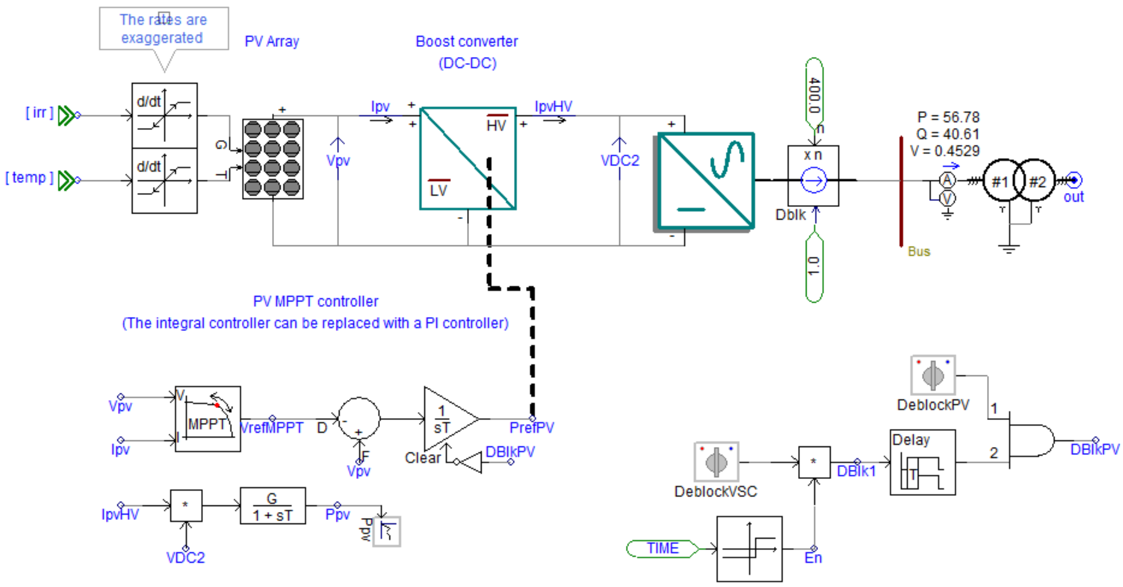

Figure 4.5: Solar Power Plant with MPPT and Boost Converter

4.2.6 Running PSCAD simulation

All simulations were run for 35 seconds and disturbances were applied at t=20. Solution step time used for HPP and WPP was 100 microseconds while for SPP solution step time of 20 microseconds was used due to high frequency switching requirements of the power electronic components of the generator.

A computer with an Intel® Core™ i7-8565U 8th Generation CPU having a base frequency of 1.80 GHz with a 16 GB DDR4 RAM and 500 GB PCIe M.2 SSD was used for estimation of transfer functions as well as running all the simulations.

4.2 Internal Disturbance

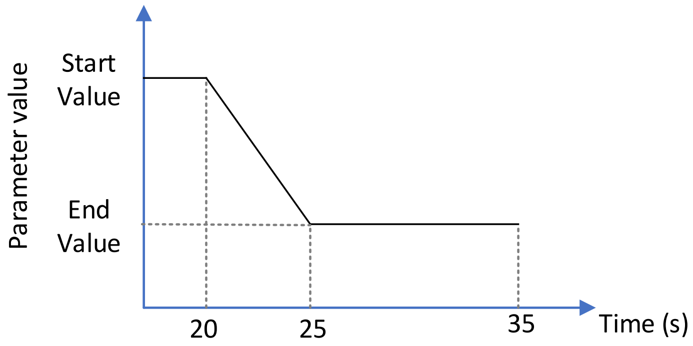

Figure 4.6: Internal disturbance input given to all 3 types of generators

A ramp input change of 5 seconds was given to the internally controllable parameters of each type of generator at t=20 seconds. For wind and solar, the change applied was considered to be applied uniformly for each generating unit. ΔPh, ΔV and ΔU_{int} were measured, and transfer functions were estimated.

Table 4.3: Types of internal disturbances given to each type of generator

Power Plant	**Controlled Parameter**	**Start value**	**End Value**
Hydro Power Plant	Active Power Reference	0.8	0.6
Wind Power Plant	Wind Speed (ms^{-1})	11.0	8.0
Solar Power Plant	Irradiance (Wm^{-2})	1200.0	600.0

After estimating each transfer function, the same input was given to the estimated model, and the resulting output measurements were compared with the output measurements obtained for the detailed model by calculating the Mean-Square Error (MSE) between the two measurements.

$$MSE = \frac{1}{n}\sum_{i=1}^{n}\left(Y_i - \hat{Y}_i\right)^2 \qquad (4.5)$$

MSE = mean squared error

n = number of data points

Y_i = observed values

$\hat{Y}_i$ = predicted values

Table 4.4 – Transfer functions estimated for all 3 types of power plants for internal disturbance

Power Plant	$H_1(s)$/ $H_2(s)$	Estimated Transfer Function
HPP	$H_1(s)$	$$\frac{-1568 s^3 - 6515 s^2 - 5.8e04 s + 4.072e04}{s^4 + 27.03 s^3 + 142.3 s^2 + 854.2 s + 1405}$$
	$H_2(s)$	$$\frac{-3.855 s^5 - 164.3 s^4 - 1295 s^3 + 1051 s^2 + 187.2 s - 63.35}{s^6 + 16.51 s^5 + 553.2 s^4 + 2860 s^3 + 1.734e04 s^2 + 3.346e04 s + 1.729e04}$$
WPP	$H_1(s)$	$$\frac{0.05492 s^3 + 3.589 s^2 + 31.02 s + 6.746}{s^4 + 1.184 s^3 + 51.25 s^2 + 20.36 s + 1.992}$$
	$H_2(s)$	$$\frac{-2.172 s^4 - 16.46 s^3 - 62.95 s^2 - 94.43 s + 21.57}{s^5 + 114.4 s^4 + 1647 s^3 + 1.251e04 s^2 + 2.061e04 s + 2878}$$
SPP	$H_1(s)$	$$\frac{-127.9 s^3 - 30.93 s^2 - 131.9 s + 547.5}{s^6 + 75.54 s^5 + 2839 s^4 + 3.25e04 s^3 + 8.61e04 s^2 + 1.383e05 s + 1.347e05}$$
	$H_2(s)$	$$\frac{0.1085 s^3 - 0.2705 s^2 - 0.2645 s + 0.2826}{s^5 + 364.7 s^4 + 2965 s^3 + 1.94e04 s^2 + 6.331e04 s + 4.971e04}$$

For comparison of results, measurements were obtained for model with detailed power plant and estimated black-box model at bus 10 (same source bus), bus 5 (load bus) and bus 11 (different source bus). Parameters measured were: Active Power

(MW), Reactive Power (MVAr), bus voltage phase angle with respect to slack bus (degrees) and RMS bus voltage (P.U).

4.2.1 Results for Hydro Power Plant Internal disturbance

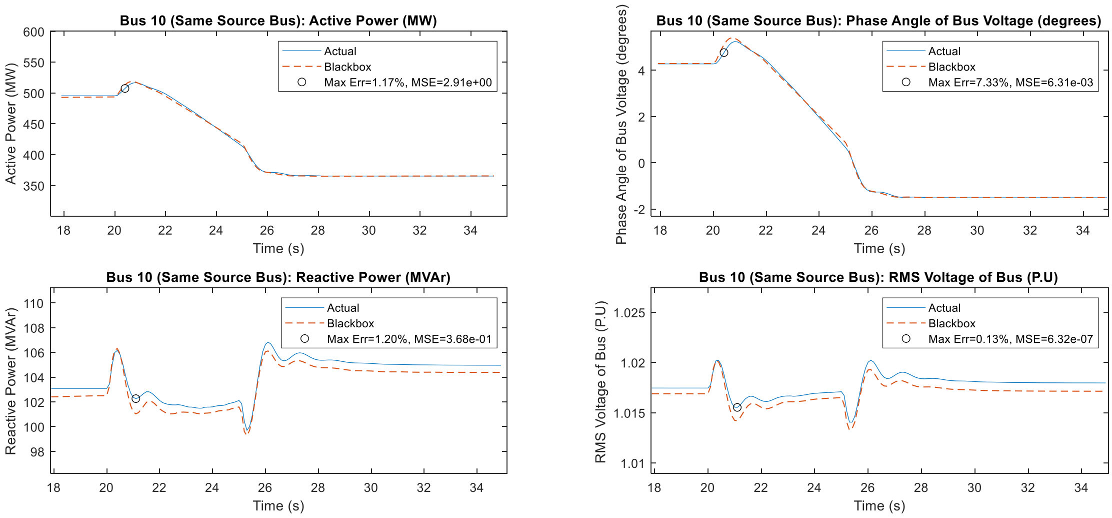

Figure 4.7: Measurements obtained at bus 10 for actual and black box models of HPP for internal disturbance

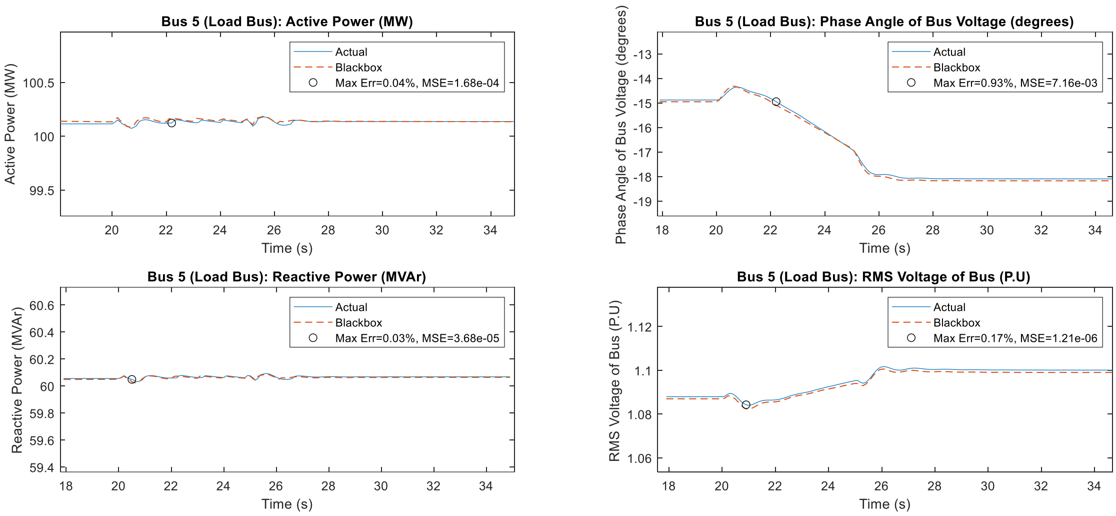

Figure 4.8: Measurements obtained at bus 5 for actual and black box models of HPP for internal disturbance

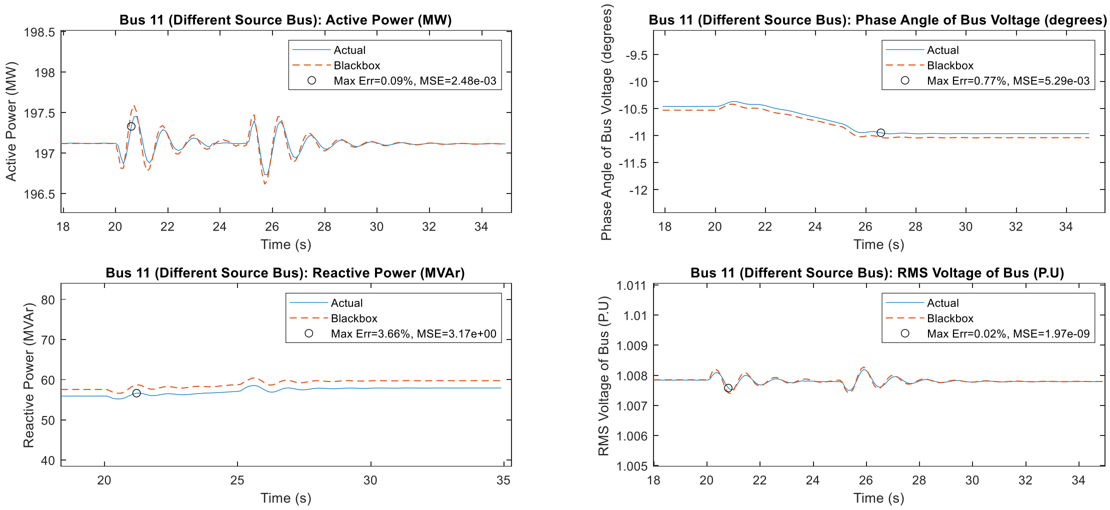

Figure 4.9: Measurements obtained at bus 11 for actual and black box models of HPP for internal disturbance

4.2.2 Results for Wind Power Plant Internal disturbance

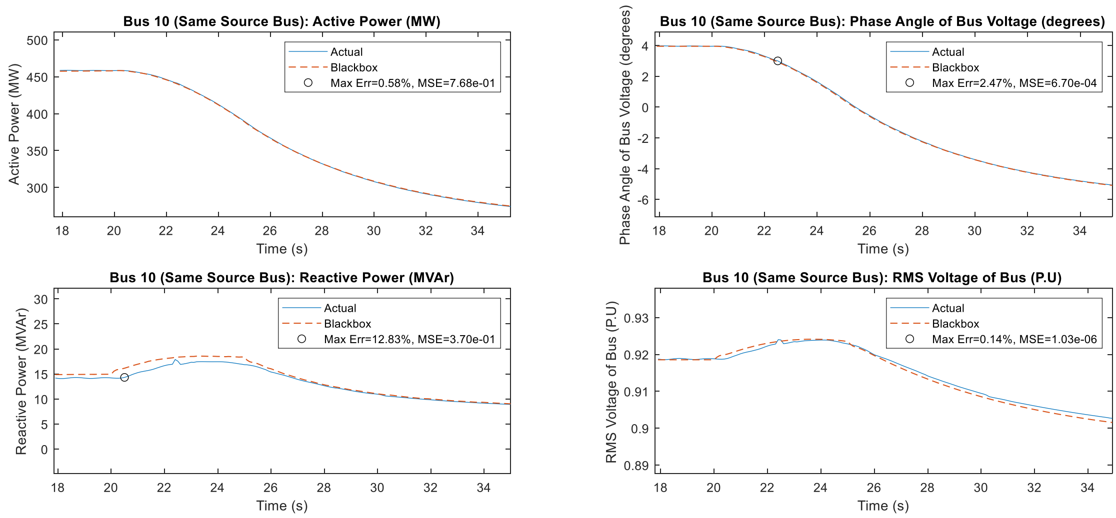

Figure 4.10: Measurements obtained at bus 10 for actual and black box models of WPP for internal disturbance

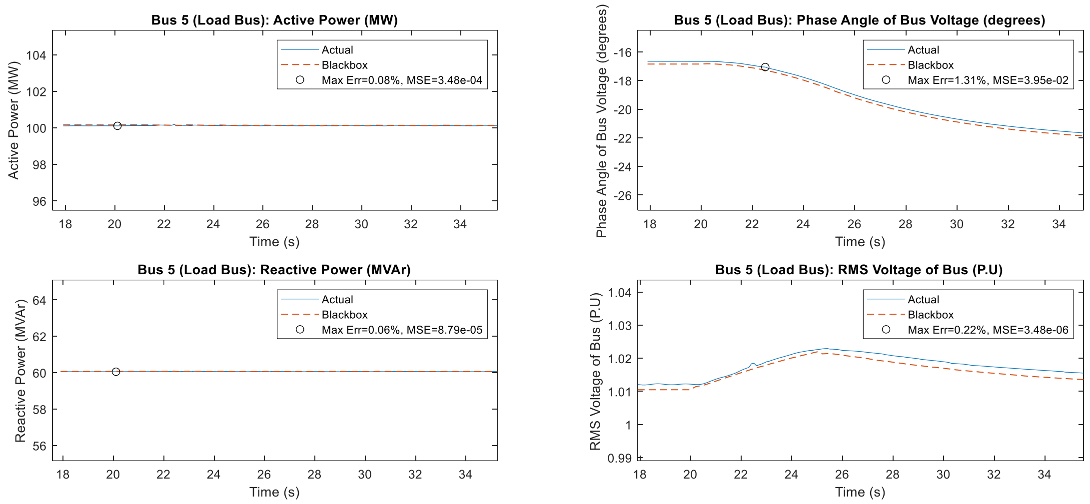

Figure 4.11: Measurements obtained at bus 5 for actual and black box models of WPP for internal disturbance

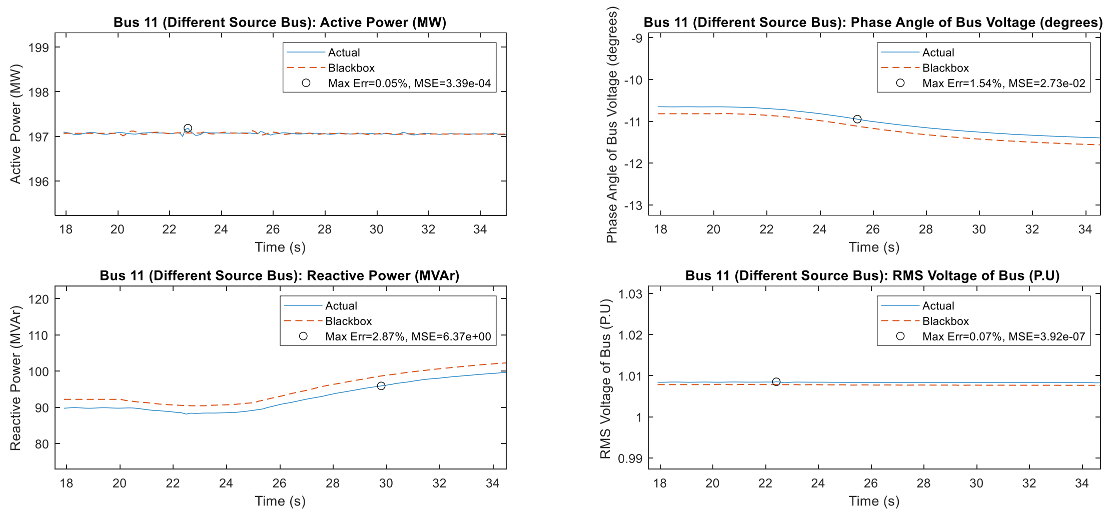

Figure 4.12: Measurements obtained at bus 11 for actual and black box models of WPP for internal disturbance

4.2.3 Results for Solar Power Plant Internal disturbance

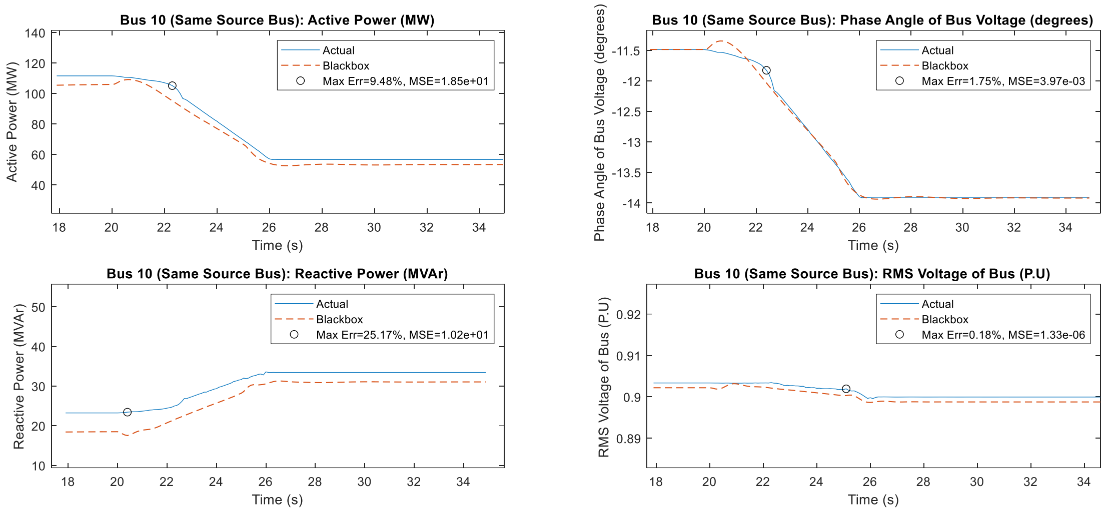

Figure 4.13: Measurements obtained at bus 10 for actual and black box models of SPP for internal disturbance

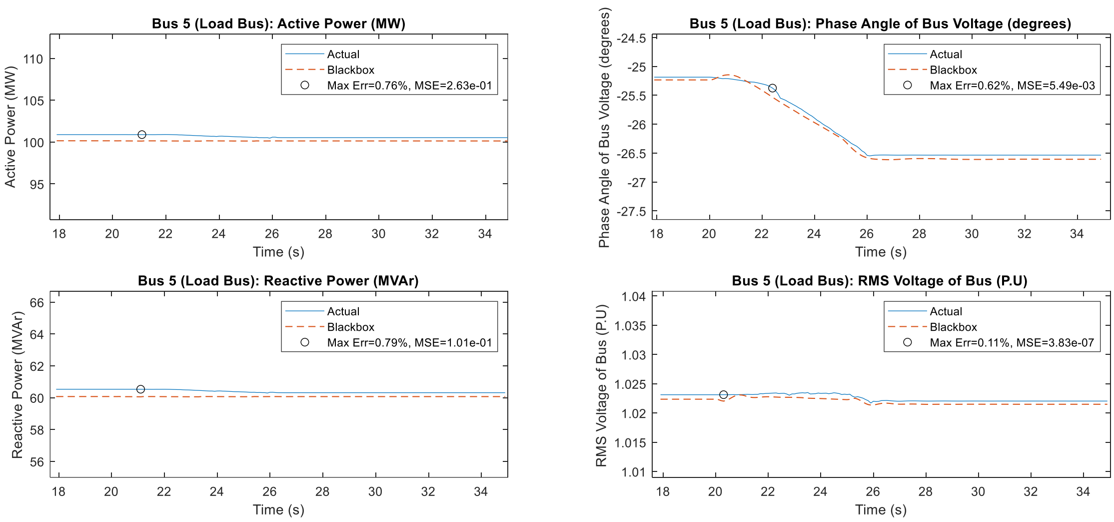

Figure 4.14: Measurements obtained at bus 5 for actual and black box models of SPP for internal disturbance

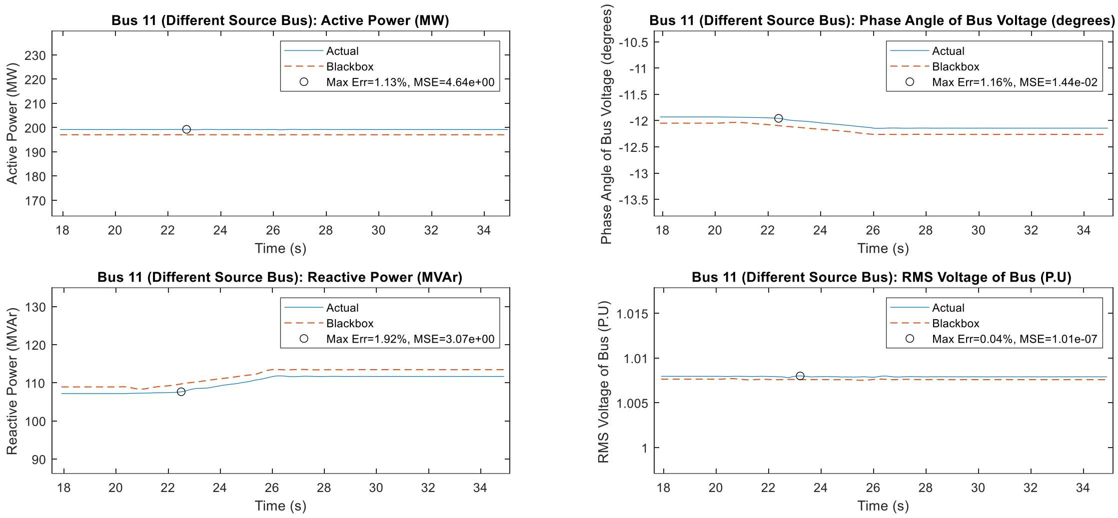

Figure 4.15: Measurements obtained at bus 11 for actual and black box models of SPP for internal disturbance

4.3 External Disturbance 1

A disturbance was applied to the power system while keeping the internal parameters of the power plant under test and measurements at the point of interconnection of the power plant to the power system were measured for estimating the transfer function.

A solid three phase to ground fault at the middle of one of transmission lines between bus 7 and bus 8.

- Fault applied at t=20 s.
- Fault duration = 100 ms
- Fault was cleared and line was tripped after 100 ms.

ΔPh, ΔV, ΔP and ΔQ were measured at bus 10 to estimate the transfer functions of the DEM for all 3 types of power plants.

ΔP and ΔPh measurements were used to estimate $H_3(s)$. ΔQ and ΔV measurements were used to estimate $H_4(s)$.

Table 4.5: Transfer functions estimated for all 3 types of power plants for external disturbance 1

Power Plant	**$H_3(s)$/ $H_4(s)$**	**Estimated Transfer Function**
HPP	$H_3(s)$	299.5 s^6 - 4042 s^5 - 2.155e05 s^4 - 2.598e06 s^3 - 3.367e07 s^2 - 7.917e07 s - 4.599e07 -- s^9 + 531.8 s^8 + 7.715e04 s^7 + 3.839e06 s^6 + 8.999e07 s^5 + 1.212e09 s^4 + 1.36e10 s^3 + 6.647e10 s^2 + 1.258e11 s + 7.551e10
	$H_4(s)$	-991.4 s^3 - 5578 s^2 - 2.419e04 s - 3.679e04 -- s^7 + 13.88 s^6 + 450.7 s^5 + 4791 s^4 + 2.635e04 s^3 + 1.456e05 s^2 + 3.534e05 s + 5.502e05
WPP	$H_3(s)$	1.864 s^5 + 83.86 s^4 + 1474 s^3 + 1.451e04 s^2 + 3.501e04 s + 6992 -- s^6 + 65.27 s^5 + 1443 s^4 + 3.485e04 s^3 + 1.579e05 s^2 + 3.194e05 s + 4.829e04
	$H_4(s)$	0.2453 s^9 + 8.744 s^8 + 223.8 s^7 + 3715 s^6 + 4.041e04 s^5 + 2.888e05 s^4 + 1.532e06 s^3 + 5.805e06 s^2 + 1.349e07 s + 7.256e06 -- s^10 + 19.14 s^9 + 1190 s^8 + 1.539e04 s^7 + 3.619e05 s^6 + 2.95e06 s^5 + 2.745e07 s^4 + 1.129e08 s^3 + 5.286e08 s^2 + 8.683e08 s + 1.256e08
SPP	$H_3(s)$	17.83 s^8 + 607.5 s^7 + 1.411e04 s^6 + 1.881e05 s^5 + 1.846e06 s^4 + 1.259e07 s^3 + 5.842e07 s^2 + 1.903e08 s + 4.246e08 -- s^9 + 42.81 s^8 + 1493 s^7 + 2.731e04 s^6 + 3.426e05 s^5 + 2.805e06 s^4 + 1.421e07 s^3 + 5.136e07 s^2 + 1.2e08 s + 9.746e07

	$H_4(s)$	$\dfrac{0.6704\ s^3 + 18.36\ s^2 + 292.5\ s + 1794}{s^4 + 9.745\ s^3 + 747.2\ s^2 + 4077\ s + 4.34e04}$

4.3.1 Results for Hydro Power Plant External disturbance 1

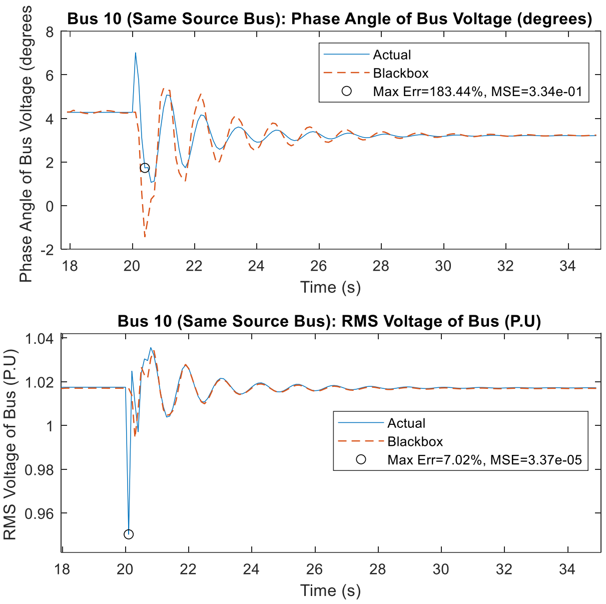

Figure 4.16: Measurements obtained at bus 10 for actual and black box models of HPP for external disturbance 1

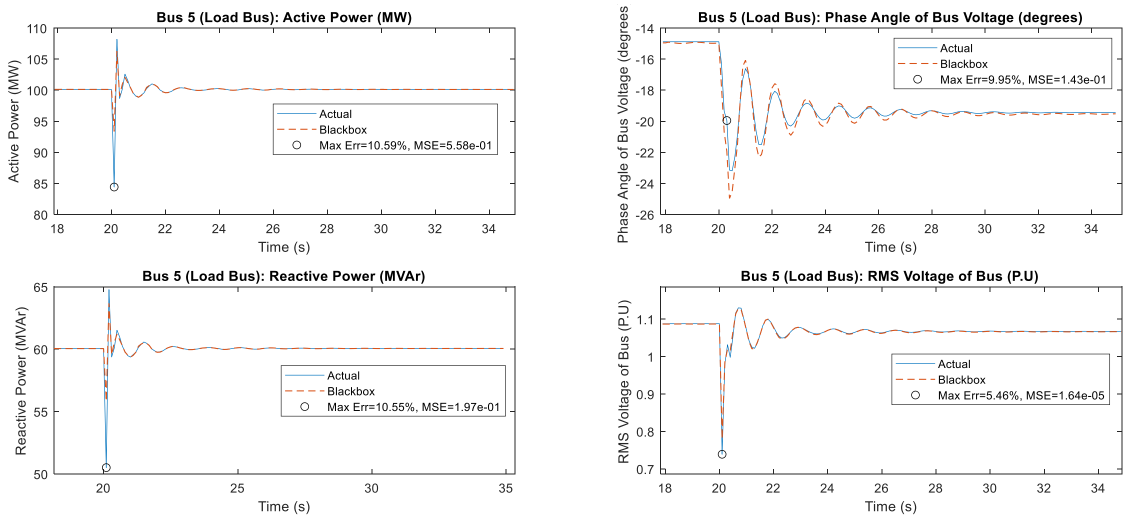

Figure 4.17: Measurements obtained at bus 5 for actual and black box models of HPP for external disturbance 1

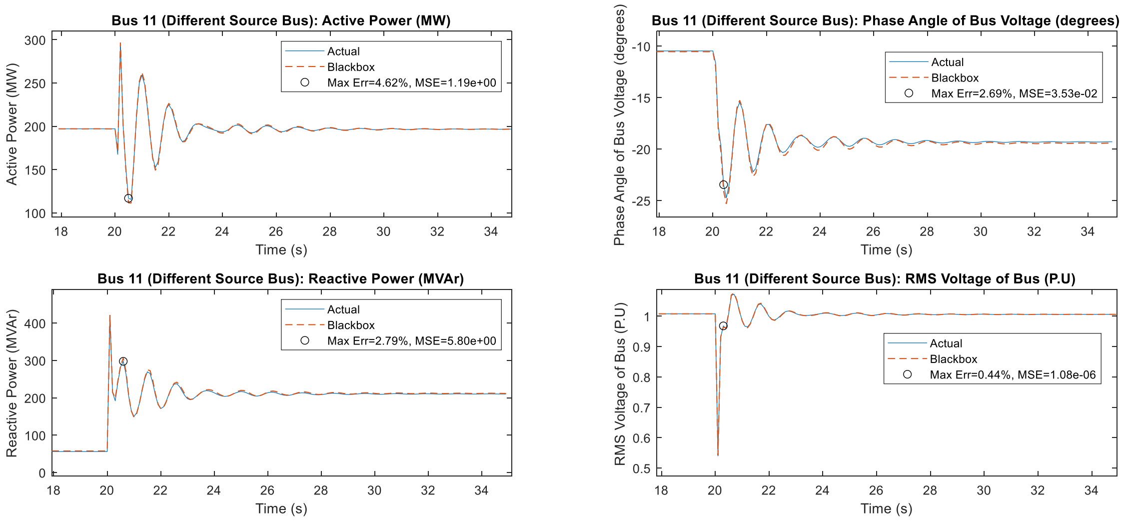

Figure 4.18: Measurements obtained at bus 11 for actual and black box models of HPP for external disturbance 1

4.3.2 Results for Wind Power Plant External disturbance 1

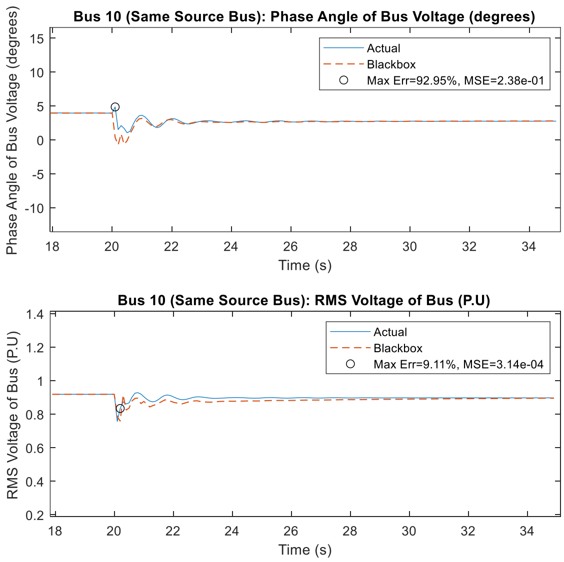

Figure 4.19: Measurements obtained at bus 10 for actual and black box models of WPP for external disturbance 1

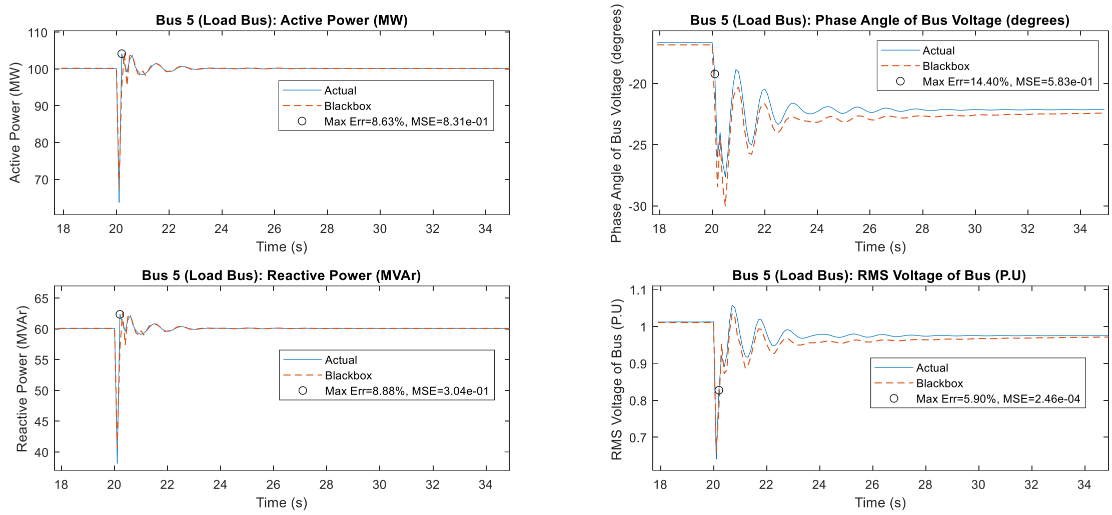

Figure 4.20: Measurements obtained at bus 5 for actual and black box models of WPP for external disturbance 1

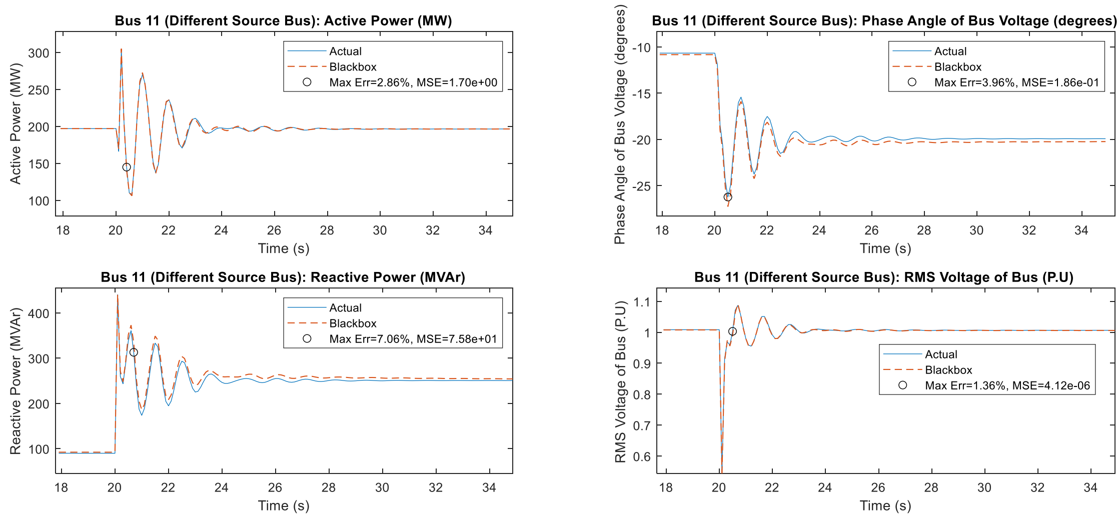

Figure 4.21: Measurements obtained at bus 11 for actual and black box models of WPP for external disturbance

4.3.3 Results for Solar Power Plant External disturbance 1

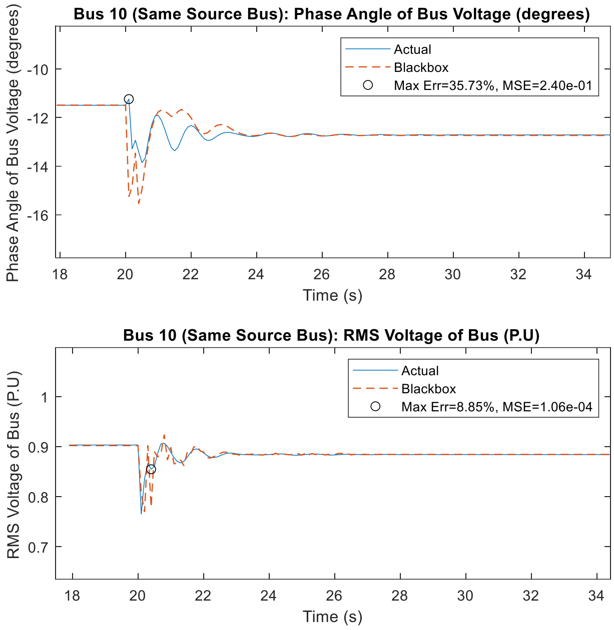

Figure 4.22: Measurements obtained at bus 10 for actual and black box models of SPP for external disturbance 1

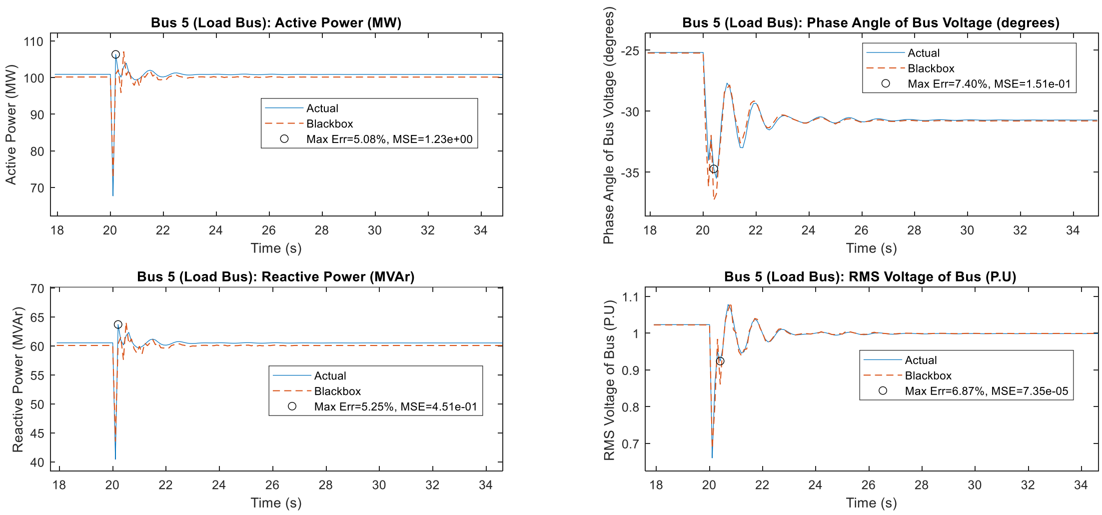

Figure 4.23: Measurements obtained at bus 5 for actual and black box models of SPP for external disturbance 1

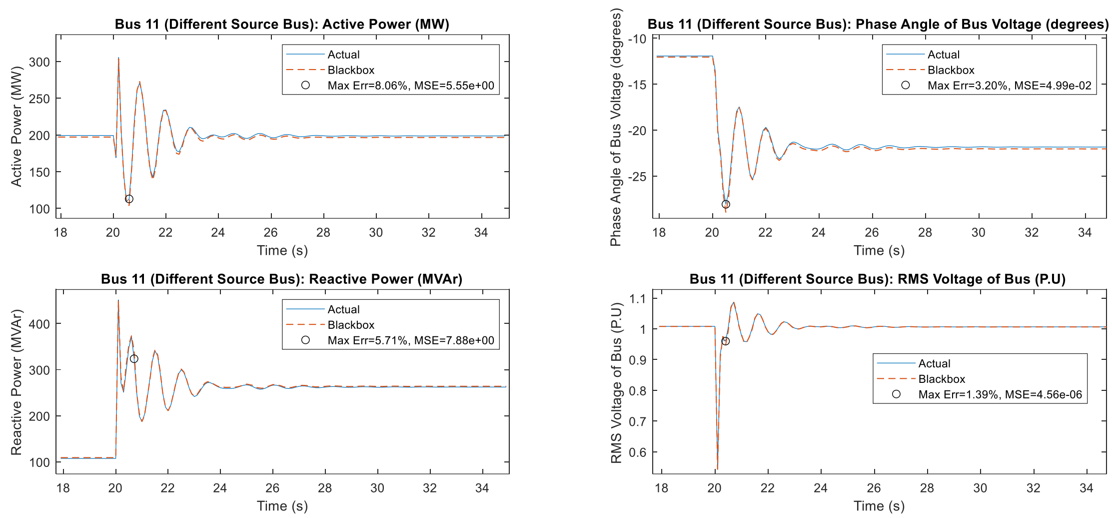

Figure 4.24: Measurements obtained at bus 11 for actual and black box models of SPP for external disturbance 1

4.4 External Disturbance 2

For the same black box models estimated in 4.3, a different external disturbance was provided to examine the accuracy of the behaviour of each type of power plant models. The provided external disturbance was cutting off load L4 (320 MW, 240 MVAr) connected to bus 4 at t=20 seconds. The same measurements taken in 4.3 were used to compare the model performance. In PSCAD simulation BRK_L4 was tripped to simulate this disturbance.

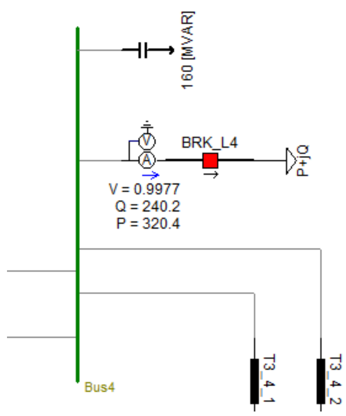

Figure 4.25: PSCAD Simulation of External Disturbance 2

4.4.1 Results for Hydro Power Plant External disturbance 2

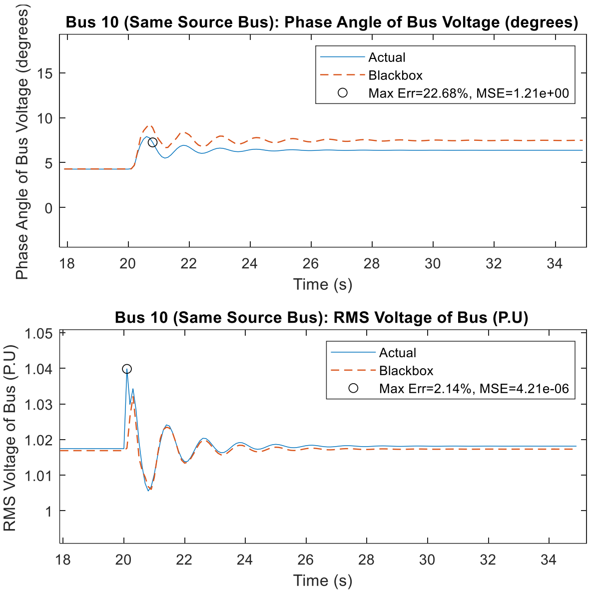

Figure 4.26: Measurements obtained at bus 10 for actual and black box models of HPP for external disturbance 2

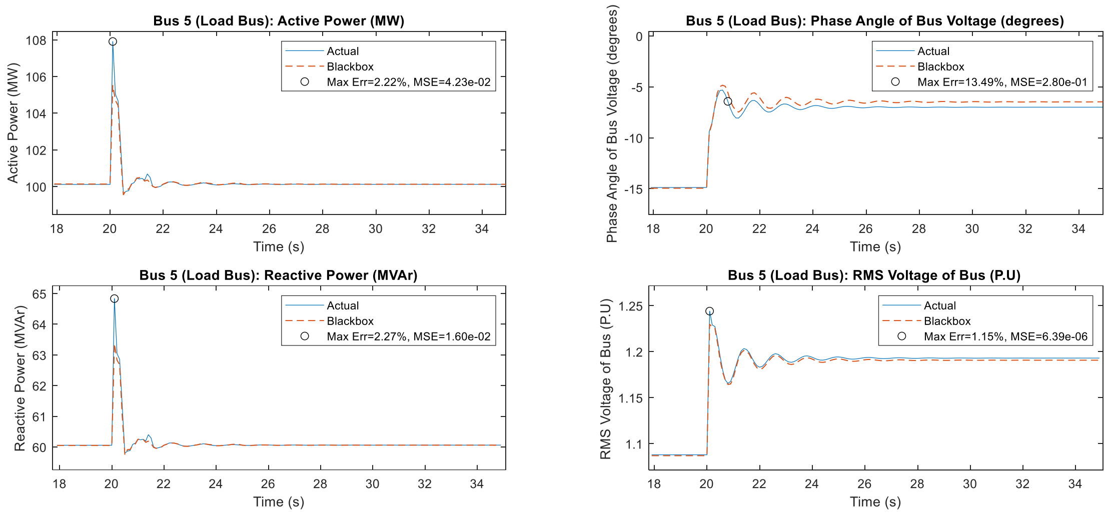

Figure 4.27: Measurements obtained at bus 5 for actual and black box models of HPP for external disturbance 2

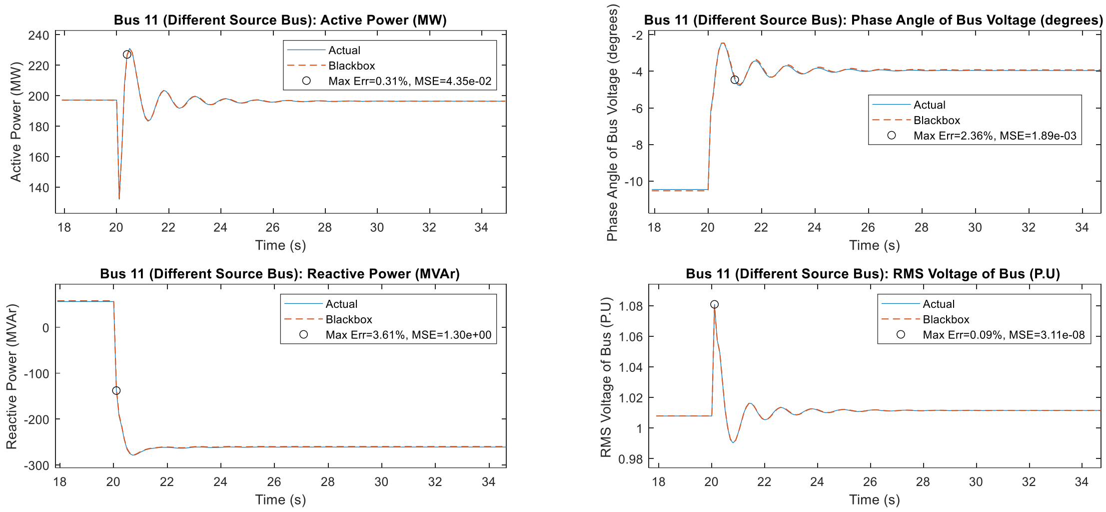

Figure 4.28: Measurements obtained at bus 11 for actual and black box models of HPP for external disturbance 2

4.4.2 Results for Wind Power Plant External disturbance 2

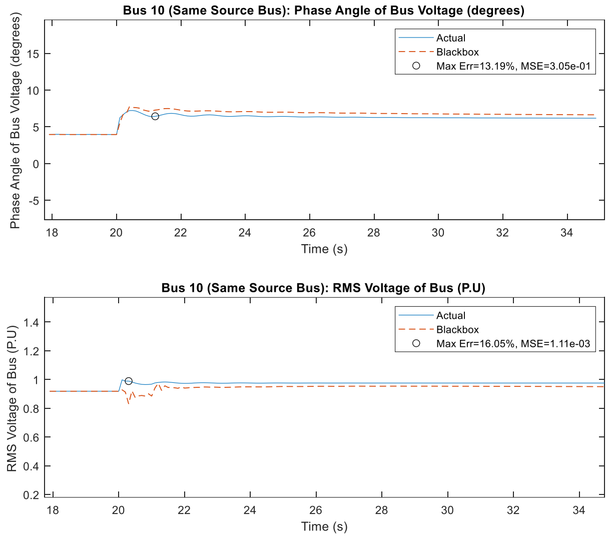

Figure 4.29: Measurements obtained at bus 10 for actual and black box models of WPP for external disturbance 2

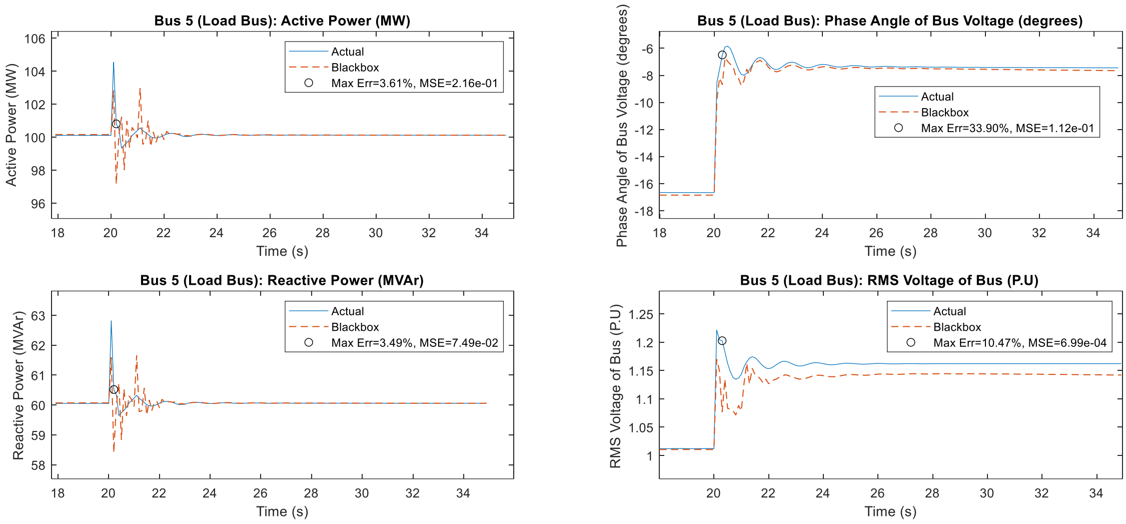

Figure 4.30: Measurements obtained at bus 5 for actual and black box models of WPP for external disturbance 2

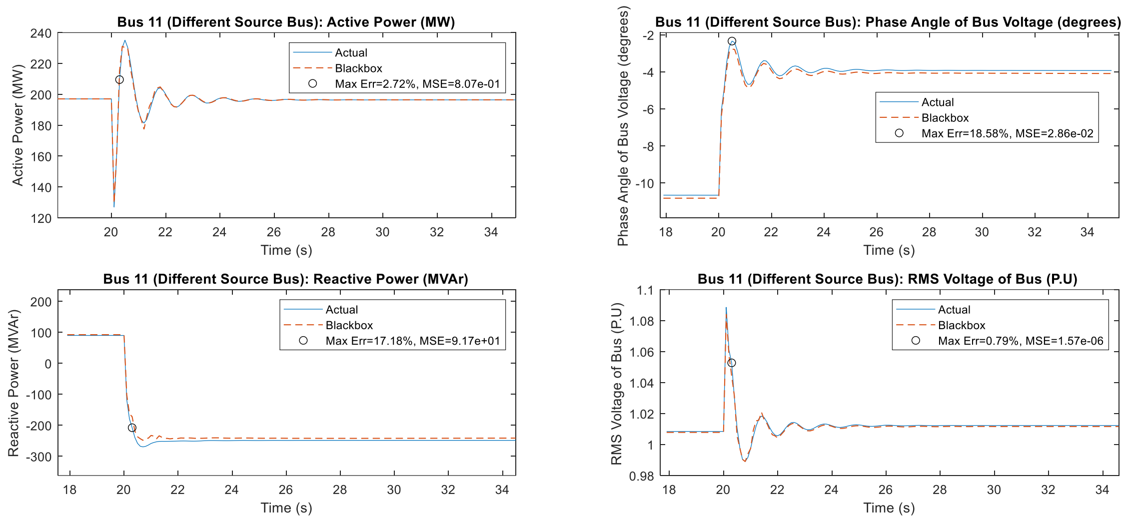

Figure 4.31: Measurements obtained at bus 11 for actual and black box models of WPP for external disturbance 2

4.4.3 Results for Solar Power Plant External disturbance 2

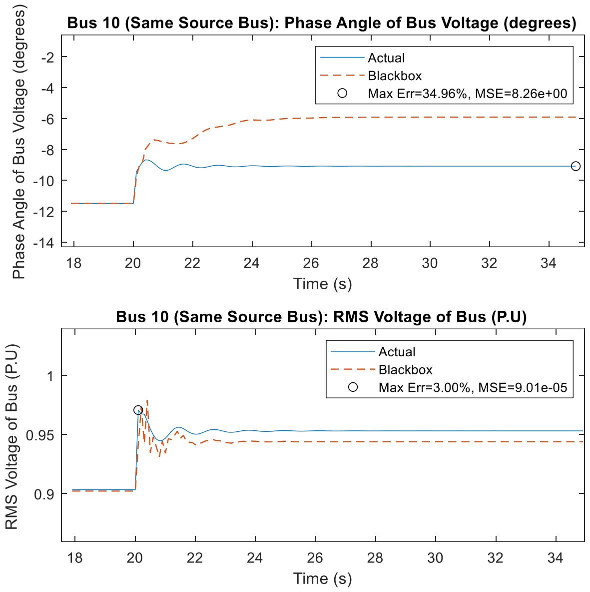

Figure 4.32: Measurements obtained at bus 10 for actual and black box models of SPP for external disturbance 2

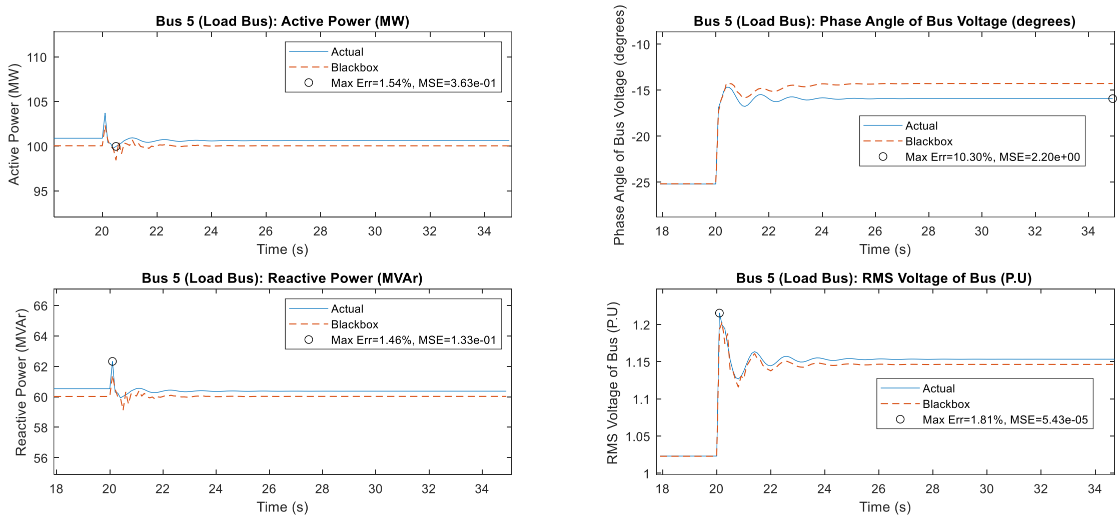

Figure 4.33: Measurements obtained at bus 5 for actual and black box models of SPP for external disturbance 2

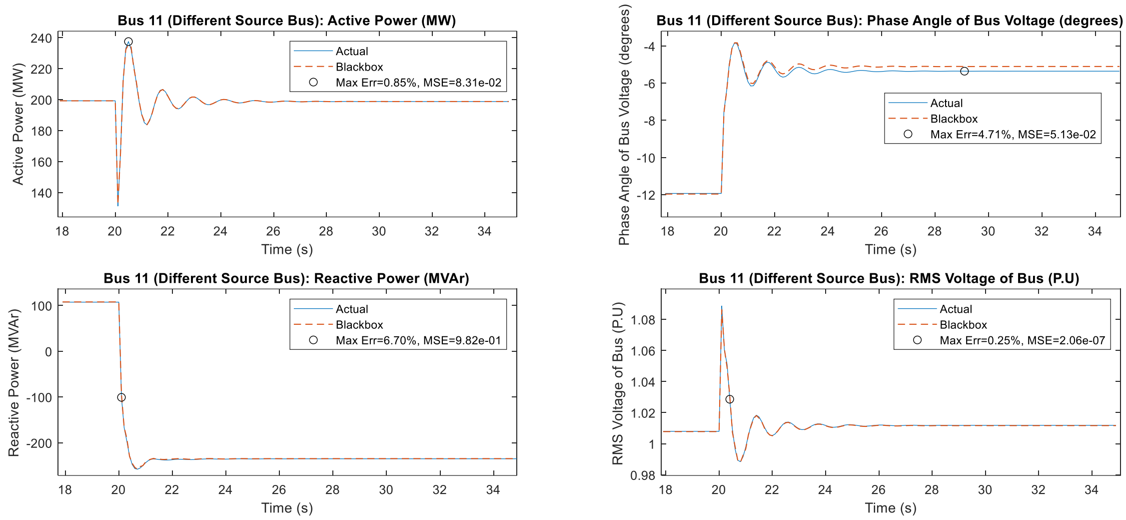

Figure 4.34: Measurements obtained at bus 11 for actual and black box models of SPP for external disturbance 2

4.5 Comparison of MSE of simulation results

MSE was calculated for each of the measurement comparison to mathematically determine how close the estimated model results are to that of actual model measurements.

4.5.1. Internal disturbance model

Table 4.6: MSE of measurements between simulation with detailed model and black-box model for internal disturbance

Power Plant	**Bus**	**MSE values**			
		Active Power	**Reactive Power**	**Bus voltage phase angle**	**Bus voltage**
HPP	10	2.91×10^{0}	3.68×10^{-1}	6.31×10^{-3}	6.32×10^{-7}
	5	1.68×10^{-4}	3.68×10^{-5}	7.16×10^{-3}	1.21×10^{-6}
	11	2.48×10^{-3}	3.17×10^{0}	5.29×10^{-3}	1.97×10^{-9}
WPP	10	7.68×10^{-1}	3.70×10^{-1}	6.70×10^{-4}	1.03×10^{-6}
	5	3.48×10^{-4}	8.79×10^{-5}	3.95×10^{-2}	3.48×10^{-6}
	11	3.39×10^{-4}	6.37×10^{0}	2.73×10^{-2}	3.92×10^{-7}
SPP	10	1.85×10^{1}	1.02×10^{-1}	5.84×10^{-3}	1.29×10^{-6}
	5	2.63×10^{-1}	1.01×10^{-1}	5.49×10^{-3}	3.83×10^{-7}
	11	4.64×10^{0}	3.07×10^{0}	1.44×10^{-2}	1.01×10^{-7}

The MSE of the measured results were satisfactorily low which mathematically indicates the estimated models adequately represent the detailed model.

4.5.2. External disturbance models

Table 4.7: MSE of measurements between simulation with detailed model and black-box model for external disturbance 1

Power Plant	Bus	MSE values			
		Active Power	**Reactive Power**	**Bus voltage phase angle**	**Bus voltage**
HPP	10	-	-	3.34×10^{-1}	3.37×10^{-5}
	5	5.58×10^{-1}	1.97×10^{-1}	1.43×10^{-1}	1.64×10^{-1}
	11	1.19×10^{0}	5.8×10^{0}	3.53×10^{-2}	1.08×10^{-6}
WPP	10	-	-	2.38×10^{-1}	3.14×10^{-4}
	5	8.31×10^{-1}	3.04×10^{-1}	5.83×10^{-1}	2.46×10^{-4}
	11	1.70×10^{0}	7.58×10^{1}	1.86×10^{-1}	4.12×10^{-6}
SPP	10	-	-	2.04×10^{-1}	1.06×10^{-4}
	5	1.23×10^{0}	4.51×10^{-1}	1.51×10^{-1}	7.35×10^{-5}
	11	5.55×10^{0}	7.88×10^{0}	4.99×10^{-2}	4.56×10^{-6}

Table 4.8: MSE of measurements between simulation with detailed model and black-box model for external disturbance 2

Power Plant	Bus	MSE values			
		Active Power	**Reactive Power**	**Bus voltage phase angle**	**Bus voltage**
HPP	10	-	-	1.21×10^{0}	4.21×10^{-6}
	5	4.23×10^{-2}	1.60×10^{-2}	2.80×10^{-1}	6.39×10^{-6}
	11	4.35×10^{-2}	1.30×10^{0}	1.89×10^{-3}	3.11×10^{-8}
WPP	10	-	-	3.05×10^{-1}	1.11×10^{-3}
	5	2.16×10^{-1}	7.49×10^{-2}	1.12×10^{-1}	6.99×10^{-4}
	11	8.07×10^{-1}	9.17×10^{1}	2.86×10^{-2}	1.57×10^{-6}
SPP	10	-	-	8.26×10^{0}	9.01×10^{-5}
	5	3.63×10^{-1}	1.33×10^{-1}	2.20×10^{0}	5.43×10^{-5}
	11	8.31×10^{-2}	9.82×10^{-1}	5.13×10^{-2}	2.06×10^{-7}

For both the types of internal and external disturbance models, The MSE of the measured results were satisfactorily low and closer to 0. This mathematically indicates the estimated models adequately represent the detailed model.

4.6 Discussion of results

It was evident that for internal disturbances the actual and estimated model measurements had almost identical behaviour. However, for external disturbances where extreme events such as tripping a large load and a 3-phase to ground fault on a transmission line was being simulated, there were some initial spikes in the measurements of simulation with actual model, which were not represented in the simulation with estimated model. This is due to the non-linearities in the actual model that are not captured when linearizing the dynamic model into a transfer function-based model.

Another noteworthy observation of the simulations was that the estimated linear models improved the simulation runtimes especially of those power plants with complex controls. Simulation runtimes for external disturbance 1 of PSCAD models for all 3 types of power plants by using both detailed and estimated models were compared for performance evaluation.

Table 4.9: Comparison of simulation runtimes between detailed models and estimated models for all 3 types of power plants estimated for external disturbance 1

Power plant	**Simulation with actual generator model**		**Simulation with black-box generator model**		**% drop in run time**
	Solution step time (μs)	**Simulation run time (s)**	**Solution step time (μs)**	**Simulation run time (s)**	
HPP	100	30.1	100	29.9	0.7
WPP	100	57.1	100	33.1	42.0
SPP	20	1025.0	20	230.0	77.6

For SPP and WPP, a drastic reduction in simulation time was observed due to reduction in model complexity as the detailed models involved many complicated subsystems. For HPP the change in simulation run time was negligible as the synchronous machine detailed model itself does not have complex components as the other two types.

In SPP, the solution step time had to be kept at 20 μs due to high switching frequency power electronic components in detailed model, which in turn resulted in a long simulation time of 1025 seconds for a full 35 second run. However, when the model was replaced by an estimated DEM due to absence of power electronic components, for the same solution step time it resulted in a 77.6% drop in simulation run time. This can further be improved by increasing the step time further since there are no high frequency switching elements in DEM.

4.7 Chapter summary

The plotted results obtained at measurement points for simulation with detailed model and estimated black-box model showed similar trends to one-another which indicated that the DEMs estimated closely mimicked the behaviour of the power plants for both internal as well as external disturbances. However, due to non-linearities of the actual model, there seemed to be certain spikes in the measurements especially at the very beginning of the disturbances which were not observed exactly in the estimated model.

This visual confirmation was further validated by comparing the Mean Square Error between the actual and estimated measurements. The MSE calculated in 4.5 further illustrates that the MSE between measured parameters of actual and estimated models are satisfactorily small enough and mostly close to zero to conclude that the estimated DEM simulates a behaviour similar to that of the actual detailed model.

5 CONCLUSIONS

5.1 General conclusions

Due to increased absorption of non-conventional energy sources to the electrical power grids, usage of wind and solar power plants has increased. Hence their impact on the stability of the power system is increasing gradually. Therefore, due to complexities of the power system, detailed models of these power plants for analysing the behaviour during disturbances in the power system is a key requirement. However, the control systems of these power plants can change from manufacturer to manufacturer and due to certain technologies being proprietary. Moreover, these detailed models may not be exposed to the utilities by manufacturer.

This indicated the importance of estimating DEMs of power plants using input and output measurements as proposed in this research. It has been shown that a N4SID and NLS based estimation method can be used to estimate a transfer function based DEM of a hydro, wind and a solar power plant. Estimation method has been validated by implementing the estimated black-box models in PSCAD simulations and comparing measurements with that of the measurements obtained in simulations with detailed model.

However, there are certain limitations of the estimated black-box DEM which cannot be achieved by this estimation methodology. An equivalent model does not replicate the exact non-linearities present in the detailed model. Moreover, operational limits of control components and operation of protection systems will not be captured correctly by this estimation methodology and these will not be replicated in the DEM. In addition, protection schemes, unless specially modelled, would not come into play when simulating a DEM.

5.2 Practical applications of the proposed methodology

The results obtained in Chapter 4 indicates that the proposed estimation methodology can be used to model dynamic equivalent models in PSCAD for simulating the behaviour of power plants during disturbances that occur either in the power system or due to disturbances that occur to control parameters of the power plant itself.

For all 3 types of hydro, wind and solar power plants it was evident that this method can be used to replace complicated detailed power plants in PSCAD simulations. The key applications of this methodology for Small Signal Stability analysis are identified as follows:

a) Design DEMs of power plants in PSCAD using actual measurements – Electrical measurements such as voltage, voltage phase angle, active power, reactive power can be obtained through measurements using measurement devices at power plants as well as PMUs (Phasor Measurement Units), while other physical parameter data such as wind speed, solar irradiance can be obtained by sensor measurements. These actual data can be used to model power plant black-box models of actual power plants and use those models in SSSA simulations.

b) Maintain up to date DEMs of power plants – Due to ageing, the control parameters of power plants may be subjected to changes. However, since the proposed input and output data can be obtained easily for any type of power plant, it is possible to use this estimation and modelling methodology to have up to date dynamic models of power plants for more accurate SSSA simulations.

c) Reduce simulation and design time – As the proposed black-box models are based on two transfer functions, there are no complex controls that involve fast switching power electronics which require the simulation step time to be extremely small which in turn increases the simulation time excessively. As demonstrated in 4.6 for SPP and WPP, simulation speed increased massively due to reduction in complexity. Moreover, designing complex power plant controls in a software like PSCAD can be overwhelming even if the detailed model is available as it is essential to know the behaviour and operational procedures of internal controls. However, a simple transfer function model, becomes easier to be modelled and simulated.

d) Transfer function-based DEM can be used as a representative model – Manufacturers could provide this transfer function based black-box DEM details to the utility for performing studies instead of providing their proprietary detailed model which is beneficial for both manufacturer as well as utility. This way, manufacturers can protect their proprietary technologies while utilities could use the black-box models easily to integrate to their power system simulations for SSSA. These models therefore, can easily be made open source data without compromising any proprietary technologies.

5.3 Suggestions for future works

There are several areas that can be explored on the basis of this study as future works.

The wind power plant used in this study is a Type II wind power plant whereas nowadays, Type III and Type IV power plants are being used more commonly. The reason for this was that PSCAD 4.5 only supports the standard Type I and Type II wind power plants provided by PSCAD. Meanwhile Type III and Type IV is supported by PSCAD higher versions which are not freely available. Once PSCAD makes a higher version available for free use, black-box DEMs can be estimated for these power plants too and estimation methodology can be verified the same way.

This can also be extended to replace other types of unconventional power generating sources that involve complex control systems such as battery banks.

For external disturbances, the model estimated using one disturbance may not fully describe the behaviour for another totally different type of extreme external disturbance. It is worthwhile to research on the possibility of using several input output measurements for different types of disturbances to further optimize transfer function that could satisfy the behaviour of many types of external disturbances. Artificial Neural Networks or other types of machine learning techniques maybe utilized to find the optimum transfer function that satisfies these many input-output combinations.

References

[1] P. Kundur et al., “Definition and classification of power system stability IEEE/CIGRE joint task force on stability terms and definitions,” *IEEE Transactions on Power Systems,* vol. 14, no. 3, pp. 1387-1401, 2004.

[2] IEA, “Renewables 2020,” IEA, Paris, 2020.

[3] M. Eremia and M. Shahidehpour, Handbook of Electrical Power System Dynamics: Modeling, Stability, and Control, Wiley-IEEE Press, 2013.

[4] S. Avdakovic, A. Nuhanovic, M. Kusljugic, W. Becirovic and M. Music, “Identification of low frequency oscillations in power system,” in *2009 International Conference on Electrical and Electronics Engineering - ELECO 2009,* 2009.

[5] K.-S. Shim, S.-J. Ahn and J.-H. Choi, “Synchronization of Low-Frequency Oscillation in Power Systems,” *Energies,* vol. 10, no. 4, p. 558, April 2017.

[6] P. Sauer and M. A. Pai, Power System Dynamics and Stability, Prentice Hall, 1998.

[7] P. Kundur, Power System Stability and Control, New York: McGraw Hill, 2004.

[8] IEEE Power Engineering Society, “IEEE Guide for Synchronous Generator Modeling Practices and Applications in Power System Stability Analysis,” IEEE, New York, 2019.

[9] IEEE Power Engineering Society, “IEEE Recommended Practice for Excitation System Models for Power System Stability Studies,” IEEE, New York, 2006.

[10] IEEE Power and Energy Society, “Dynamic Models for Turbine-Governors in Power System Studies,” IEEE, 2013.

[11] A. Ellis, Y. Kazachkov, E. Muljadi, P. Pourbeik and J. Sanchez-Gasca, “Description and technical specifications for generic WTG models — A status report,” in *IEEE/PES Power Systems Conference and Exposition*, 2011.

[12] M. Singh and S. Santoso, “Dynamic Models for Wind Turbines and Wind Power Plants,” National Renewable Energy Laboratory, Colorado, 2011.

[13] E. Muljadi, M. Singh and V. Gevorgian, “User Guide for PV Dynamic Model Simulation Written on PSCAD Platform,” National Renewable Energy Laboratory, Colorado, 2014.

[14] WECC, “Solar Photovoltaic Power Plant Modeling and Validation Guideline,” 2019.

[15] P. Ju, L. Ni and F. Wu, “Dynamic equivalents of power systems with online measurements. Part 1: theory,” *IEE Proceedings - Generation, Transmission and Distribution,* vol. 151, no. 2, p. 175 – 178, 2004.

[16] P. Ju, F. Li, N. N.G. Yang, X. Wu and N. He, “Dynamic equivalents of power systems with online measurements Part 2: applications,” *IEE Proceedings - Generation, Transmission and Distribution,* vol. 151, no. 2, p. 179 – 182, 2004.

[17] A. Stankovic and A. Saric, “Transient power system analysis with measurement-based gray box and hybrid dynamic equivalents,” *IEEE Transactions on Power Systems,* vol. 19, no. 1, pp. 455-462, 2004.

[18] K. Burnham and D. Anderson, Model Selection and Multimodel Inference: A Practical Information-Theoretic Approach, Springer, 1998.

[19] L. Ljung, System Identification: Theory for the User, New Jersy: Prentice Hall, 1998.

[20] L. Chen, S. JunWei and L. JingYin, “Self-Coupling Black Box Model of a Dynamic System Based on ANN and Its Application,” *Mathematical Problems in Engineering,* pp. 1-12, 2020.

[21] L. Ljung, “Black-box Models from Input-output Measurements,” in *Instrumentation and Measurement Technology Conference,* 2001.

[22] K. Sadeghi, A. Razminia and E. Roshandel, “Comparison of iterative and recursive algorithms for identifying a solar power plant system,” in *2017 5th International Conference on Control, Instrumentation, and Automation (ICCIA)*, 2017.

[23] Y.-L. Hu and Y.-K. Wu, “A Review on the model validation and estimation approaches of wind

power generators," *The Journal of Engineering,* vol. 2017, no. 13, pp. 2407-2411, 2017.

[24] M. Karrari and O. P. Malik, "Identification of physical parameters of a synchronous Generator from online measurements," *IEEE Transactions on Energy Conversion,* vol. 19, no. 2, pp. 407-415, 2004.

[25] L. Sun, A. P. S. Meliopoulos, Y. Liu and &. X. B. , "Dynamic state estimation based synchronous generator model calibration using PMU data," in *IEEE Power & Energy Society General Meeting*, 2017.

[26] K. Pelckmans, "Lecture Notes for a course on System Identification," 2011.

[27] A. Mohammadi, H. Khaloozadeh and R. Amjadifard, "Small Signal Monitoring of Power System using Subspace System Identification," *International Journal of Computers Communications & Control*, vol. 7, no. 2, pp. 325-340, 2012.

[28] M. Rahimpour, M. A. Talebi, H. A. Shayanfar and M. R. Azad Hosseini, "On line synchronous generator parameters estimation based on applying small disturbance on excitation system using ANN," in *2009 IEEE/PES Power Systems Conference and Exposition.* , 2009.

[29] M. E. Jahromi, B. Firouzi and A. M. & Ranjbar, "Possibility of large synchronous generator parameters estimation via on-line field tests using genetic algorithm," in *IEEE Power India Conference,* 2006.

[30] T. Sun, X. Mou and Z. Li, "A practical clustering method of DFIG wind farms based on dynamic current error," in *IEEE Power & Energy Society General Meeting,* 2015.

[31] F. Wu et al., "Transfer function based equivalent modeling method for wind farm," *Journal of Modern Power Systems and Clean Energy,* vol. 7, no. 3, pp. 549-557, 2019.

[32] D.-E. Kim and M. A. El-Sharkawi, "Dynamic Equivalent Model of Wind Power Plant Using Parameter Identification," *IEEE Transactions on Energy Conversion,* vol. 31, no. 1, pp. 37-45, 2016.

[33] M. A. El-Sharkawi, "Dynamic equivalent models for wind power plants," in *IEEE Power and Energy Society General Meeting,* 2011.

[34] I. Houtzager, B. Kulcsár, J.-W. v. Wingerden and M. Verhaegen, "System identification for the control of wind turbine systems," in *TORQUE 2010: The Science of Making Torque from Wind,* 2010.

[35] D. Remon, A. M. Cantarellas, M. A. A. Elsaharty, C. Koch-Ciobotaru and P. Rodrigue, "Equivalent model of a synchronous PV power plant," in *2015 IEEE Energy Conversion Congress and Exposition (ECCE),* 2015.

[36] D. Remon, A. Cantarellas and P. Rodriguez, "Equivalent Model of Large-Scale Synchronous Photovoltaic Power Plants," *IEEE Transactions on Industry Applications,* vol. 52, no. 6, pp. 5029-5040, 2016.

[37] F. R. Lemes, E. P. T. Cari and V. A. Correa, "Parameter Estimation of Photovoltaic System Using Real Condition Data.," in *IEEE Canadian Conference of Electrical and Computer Engineering (CCECE),* 2019 .

[38] S. J. Plathottam, S. Abhyankar and P. Hazra, "Dynamic Modeling of Solar PV Systems for Distribution System Stability Analysis," in *IEEE Power & Energy Society Innovative Smart Grid Technologies Conference,* 2019.

[39] S. Soni, "Solar PV Plant Model Validation for Grid Integration Studies," Arizona, 2014.

[40] Q. Wang et al., "Dynamic modeling and small signal stability analysis of distributed photovoltaic grid-connected system with large scale of panel level DC optimizers.," *Applied Energy,* 2019.

[41] U. D. Annakkage et al., "Dynamic System Equivalents: A Survey of Available Techniques," *IEEE Transactions on Power Delivery,* vol. 27, no. 1, pp. 411-420, 2012.

[42] H. Liu, "Wide-Area Measurement-Driven Approaches for Power System Modeling and Analytics," 2017.

[43] M. Mansouri, D. Westwick and A. Knight, "A N4SID-Based Strategy to Estimate the Parameters of Disturbances in Power Systems," in *2018 IEEE PES Innovative Smart Grid Technologies Conference Europe (ISGT-Europe),* 2018.

[44] H. Akaike, “A new look at the statistical model identification,” *IEEE Transactions on Automatic Control*, vol. 19, no. 6, pp. 716-723, 1974.

Appendix A Synchronous generator dynamic models modelled in Simulink and estimated in MATLAB

A.1 - 3^{rd} order model - Generator with Field circuit

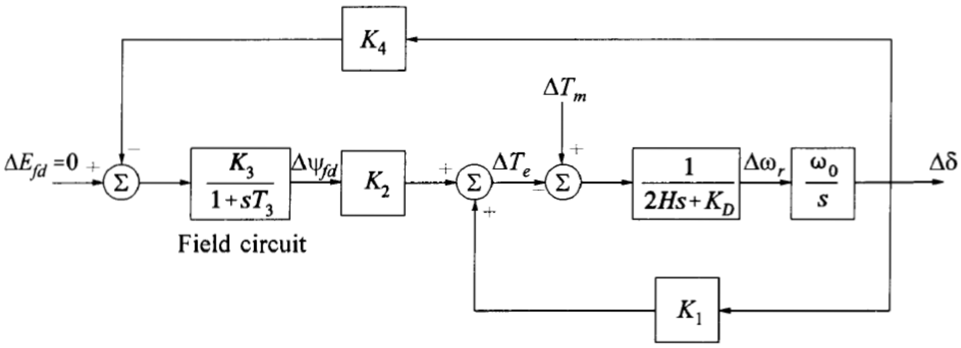

Figure A.1: 3^{rd} Order synchronous generator model block diagram

$$\begin{bmatrix} \Delta\dot{\omega}_r \\ \Delta\dot{\delta} \\ \Delta\dot{\psi}_{fd} \end{bmatrix} = \begin{bmatrix} a_{11} & a_{12} & a_{13} \\ a_{21} & 0 & 0 \\ 0 & a_{32} & a_{33} \end{bmatrix} \begin{bmatrix} \Delta\omega_r \\ \Delta\delta \\ \Delta\psi_{fd} \end{bmatrix} + \begin{bmatrix} b_{11} & 0 \\ 0 & 0 \\ 0 & b_{32} \end{bmatrix} \begin{bmatrix} \Delta T_m \\ \Delta E_{fd} \end{bmatrix}$$

$$A = \begin{bmatrix} -2.8571 & -0.1236 & 0 & 0 \\ 376.99 & 0 & 0 & 0 \\ 0 & -0.1938 & -0.4229 & -27.317 \\ 0 & -7.3125 & 20.839 & -50 \end{bmatrix} \quad B = \begin{bmatrix} 0.14286 \\ 0 \\ 0 \\ 0 \end{bmatrix} \quad \Delta E_{fd} = 0$$

Figure A.2: 3^{rd} Order synchronous generator model data of block diagram

Source: P. Kundur, Power System Stability and Control, New York: McGraw Hill, 2004

Min of AIC	Zeros									
Poles	1	2	3	4	5	6	7	8	9	Min of AIC
2	-6350.01									-6350.01
3	-9040.76	-44344.83								-44344.83
4	-9893.33	-10103.22	-44063.06							-44063.06
5	-11777.14	-10345.71	-10259.20	-20866.93						-20866.93
6	-10339.03	-10356.29	-10241.80	-10239.42	-10262.35					-10356.29
7	-10357.14	-10358.02	-10331.52	-10235.30	-10354.46	-10349.47				-10358.02
8	-10361.04	-10359.48	-10353.47	-10359.42	-10357.44	-10336.26	-10346.75			-10361.04
9	-10366.82	-10364.86	-10362.38	-10362.19	-10353.47	-10352.08	-10358.81	-10352.94		-10366.82
10	-10371.89	-10369.90	-10367.85	-10366.13	-10363.47	-10361.46	-10361.85	-10355.98	-10356.01	-10371.89
Min of AIC	**-11777.14**	**-44344.83**	**-44063.06**	**-20866.93**	**-10363.47**	**-10361.46**	**-10361.85**	**-10355.98**	**-10356.01**	**-44344.83**

Figure A.3: AIC values of all models estimated for 3^{rd} order synchronous generator model

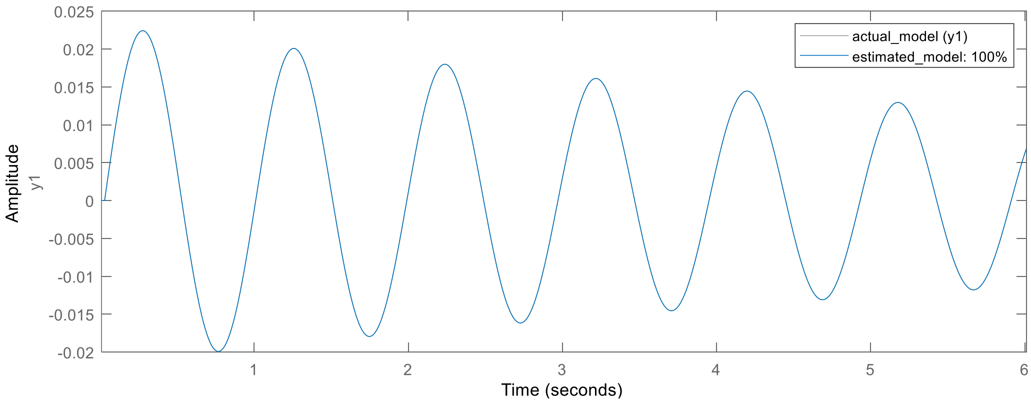

Figure A.4: Comparison of outputs for actual and estimated models of 3rd order synchronous generator model

A.2 - 4th order model - Generator with Field circuit + AVR

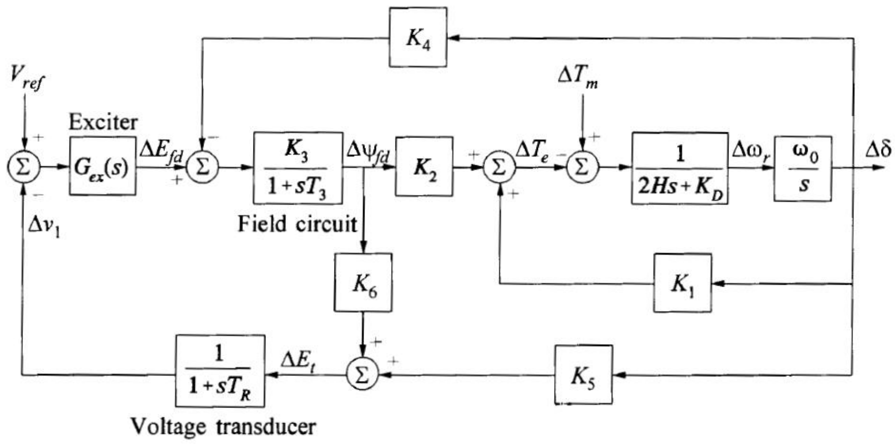

Figure A.5: 4th Order synchronous generator model block diagram

Source: P. Kundur, Power System Stability and Control, New York: McGraw Hill, 2004

$$\begin{bmatrix} \Delta\dot{\omega}_r \\ \Delta\dot{\delta} \\ \Delta\dot{\psi}_{fd} \\ \Delta\dot{v}_1 \end{bmatrix} = \begin{bmatrix} a_{11} & a_{12} & a_{13} & 0 \\ a_{21} & 0 & 0 & 0 \\ 0 & a_{32} & a_{33} & a_{34} \\ 0 & a_{42} & a_{43} & a_{44} \end{bmatrix} \begin{bmatrix} \Delta\omega_r \\ \Delta\delta \\ \Delta\psi_{fd} \\ \Delta v_1 \end{bmatrix} + \begin{bmatrix} b_1 \\ 0 \\ 0 \\ 0 \end{bmatrix} \Delta T_m$$

$$A = \begin{bmatrix} -2.8571 & -0.1236 & 0 & 0 \\ 376.99 & 0 & 0 & 0 \\ 0 & -0.1938 & -0.4229 & -27.317 \\ 0 & -7.3125 & 20.839 & -50 \end{bmatrix} \quad B = \begin{bmatrix} 0.14286 \\ 0 \\ 0 \\ 0 \end{bmatrix} \quad \Delta E_{fd} = 0$$

Figure A.6: 4th Order synchronous generator model data of block diagram

Min of AIC	Zeros									
Poles	1	2	3	4	5	6	7	8	9	Min of AIC
2	-10786.57									-10786.57
3	-9331.44	-13084.56								-13084.56
4	-10486.44	-9594.53	-46143.59							-46143.59
5	-10853.09	-10309.11	-11566.46	-12154.91						-12154.91
6	-12002.03	-12427.55	-10750.40	-11297.47	-11209.36					-12427.55
7	-12558.32	-12505.92	-12320.74	-12042.37	-11780.95	-11863.59				-12558.32
8	-12596.42	-12595.52	-12555.54	-12470.92	-12589.85	-12258.60	-12463.91			-12596.42
9	-12594.84	-12592.88	-12589.79	-12582.16	-12571.53	-12541.14	-12509.10	-12576.55		-12594.84
10	-12591.23	-12589.24	-12587.07	-12586.07	-12579.00	-12581.19	-12571.21	-12551.82	-12575.17	-12591.23
Min of AIC	**-12596.42**	**-13084.56**	**-46143.59**	**-12586.07**	**-12589.85**	**-12581.19**	**-12571.21**	**-12576.55**	**-12575.17**	**-46143.59**

Figure A.7: AIC values of all models estimated for 4th order synchronous generator model

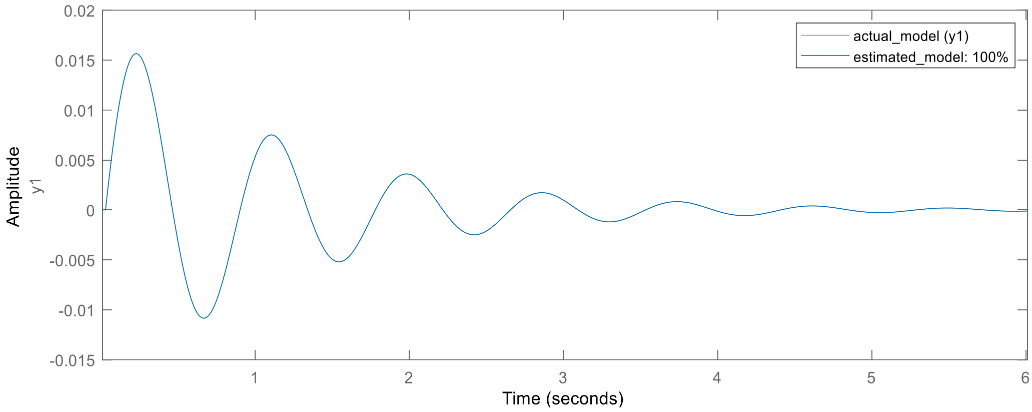

Figure A.8: Comparison of outputs for actual and estimated models of 4th order synchronous generator model

A.3 - 6th order model - Generator with Field circuit + AVR + PSS

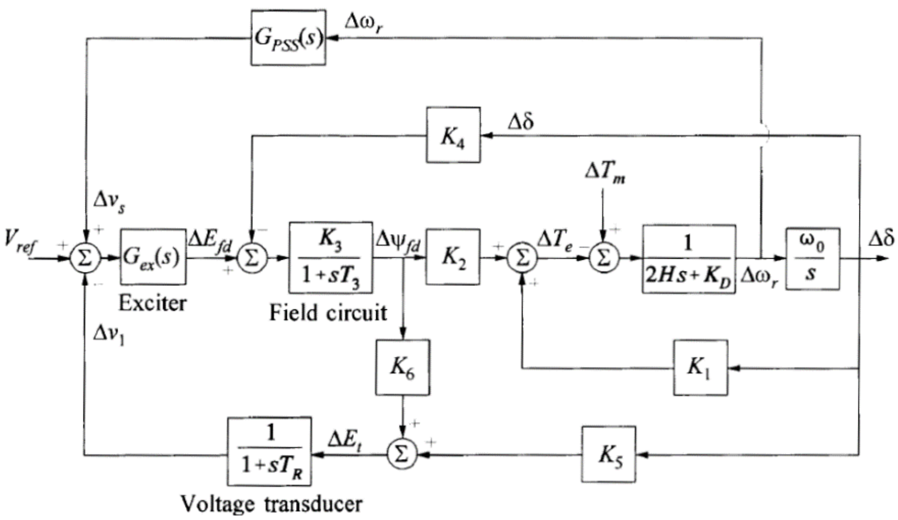

Figure A.9: 6th Order synchronous generator model block diagram

Source: P. Kundur, Power System Stability and Control, New York: McGraw Hill, 2004

$$
\begin{bmatrix} \Delta\dot{\omega}_r \\ \Delta\dot{\delta} \\ \Delta\dot{\psi}_{fd} \\ \Delta\dot{v}_1 \\ \Delta\dot{v}_2 \\ \Delta\dot{v}_s \end{bmatrix} = \begin{bmatrix} a_{11} & a_{12} & a_{13} & 0 & 0 & 0 \\ a_{21} & 0 & 0 & 0 & 0 & 0 \\ 0 & a_{32} & a_{33} & a_{34} & 0 & a_{36} \\ 0 & a_{42} & a_{43} & a_{44} & 0 & 0 \\ a_{51} & a_{52} & a_{53} & 0 & a_{55} & 0 \\ a_{61} & a_{62} & a_{63} & 0 & a_{65} & a_{66} \end{bmatrix} \begin{bmatrix} \Delta\omega_r \\ \Delta\delta \\ \Delta\psi_{fd} \\ \Delta v_1 \\ \Delta v_2 \\ \Delta v_s \end{bmatrix} + \begin{bmatrix} b_{11} \\ 0 \\ 0 \\ 0 \\ 0 \\ 0 \end{bmatrix} [\Delta T_m]
$$

$$
\mathbf{A} = \begin{bmatrix} 0 & -0.1092 & -0.1236 & 0 & 0 & 0 \\ 376.99 & 0 & 0 & 0 & 0 & 0 \\ 0 & -0.1938 & -0.4229 & -27.3172 & 0 & 27.3172 \\ 0 & -7.3125 & 20.8391 & -50.0 & 0 & 0 \\ 0 & -1.0372 & -1.1738 & 0 & -0.7143 & 0 \\ 0 & -4.8404 & -5.4777 & 0 & 26.9697 & -30.3030 \end{bmatrix} \quad B = \begin{bmatrix} 0.14286 \\ 0 \\ 0 \\ 0 \\ 0 \\ 0 \end{bmatrix} \quad \Delta E_{fd} = 0
$$

Figure A.10: 6th Order synchronous generator model data of block diagram

Min of AIC	Zeros									
Poles	1	2	3	4	5	6	7	8	9	Min of AIC
2	-5708.73									-5708.73
3	-7774.63	-7928.54								-7928.54
4	-8889.25	-8412.65	-13102.91							-13102.91
5	-9885.68	-9789.92	-9579.13	-16686.05						-16686.05
6	-10765.94	-10754.96	-10862.08	-9893.45	-36513.75					-36513.75
7	-10845.18	-10837.15	-10984.09	-10156.22	-11517.76	-11198.81				-11517.76
8	-12149.53	-12149.94	-12071.73	-12950.89	-10815.01	-11213.28	-11105.61			-12950.89
9	-12939.53	-12937.37	-12941.39	-12805.01	-12380.81	-12415.10	-11873.52	-11973.92		-12941.39
10	-12969.58	-12967.58	-12965.26	-12968.68	-12862.23	-12797.20	-12950.15	-12406.10	-12737.32	-12969.58
Min of AIC	**-12969.58**	**-12967.58**	**-13102.91**	**-16686.05**	**-36513.75**	**-12797.20**	**-12950.15**	**-12406.10**	**-12737.32**	**-36513.75**

Figure A.11: AIC values of all models estimated for 6th order synchronous generator model

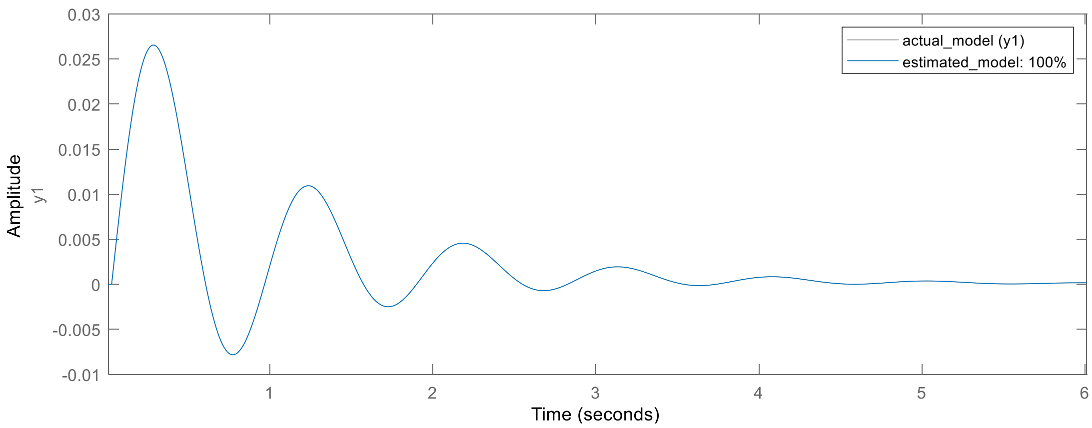

Figure A.12: Comparison of outputs for actual and estimated models of 6th order synchronous generator model

A.4 - 6^{th} order model - Generator with Field circuit + AVR + PSS + damper winding

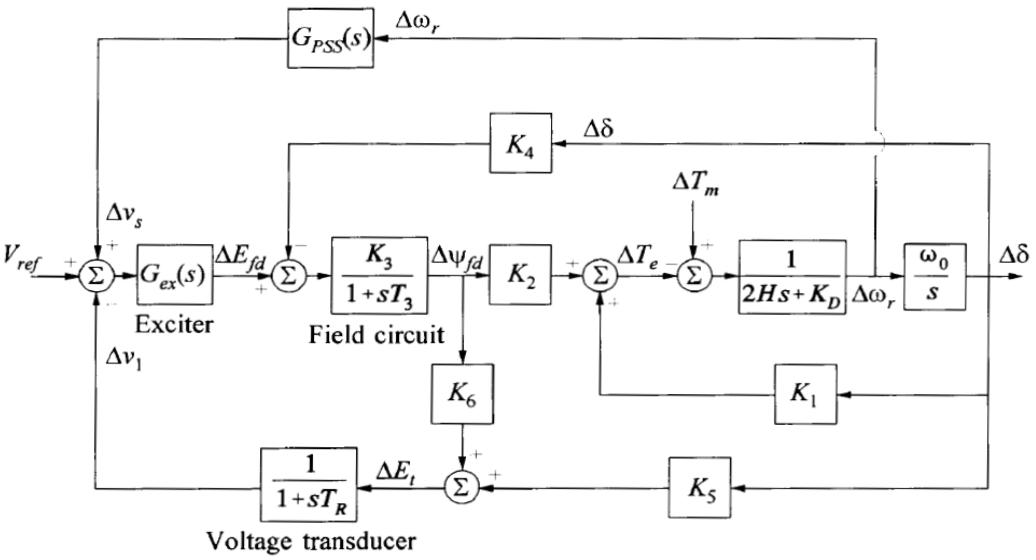

Figure A.13: 6^{th} Order synchronous generator model (with Damper winding effect) block diagram

Source: P. Kundur, Power System Stability and Control, New York: McGraw Hill, 2004

$$\begin{bmatrix} \Delta\dot{\omega}_r \\ \Delta\dot{\delta} \\ \Delta\dot{\psi}_{fd} \\ \Delta\dot{\psi}_{1d} \\ \Delta\dot{\psi}_{1q} \\ \Delta\dot{\psi}_{2q} \end{bmatrix} = \begin{bmatrix} a_{11} & a_{12} & a_{13} & a_{14} & a_{15} & a_{16} \\ a_{21} & 0 & 0 & 0 & 0 & 0 \\ 0 & a_{32} & a_{33} & a_{34} & a_{35} & a_{36} \\ 0 & a_{42} & a_{43} & a_{44} & a_{45} & a_{46} \\ 0 & a_{52} & a_{53} & a_{54} & a_{55} & a_{56} \\ 0 & a_{62} & a_{63} & a_{64} & a_{65} & a_{66} \end{bmatrix} \begin{bmatrix} \Delta\omega_r \\ \Delta\delta \\ \Delta\psi_{fd} \\ \Delta\psi_{1d} \\ \Delta\psi_{1q} \\ \Delta\psi_{2q} \end{bmatrix} + \begin{bmatrix} b_{11} & 0 \\ 0 & 0 \\ 0 & b_{32} \\ 0 & 0 \\ 0 & 0 \\ 0 & 0 \end{bmatrix} \begin{bmatrix} \Delta T_m \\ \Delta E_{fd} \end{bmatrix}$$

$$\mathbf{A} = \begin{bmatrix} 0 & -0.121 & -0.069 & -0.076 & -0.003 & -0.023 \\ 377 & 0 & 0 & 0 & 0 & 0 \\ 0 & -0.109 & -0.883 & 0.645 & 0 & 0.0003 \\ 0 & -4.928 & 26.72 & -37.47 & 0.002 & 0.013 \\ 0 & -0.058 & -0.0005 & -0.0005 & -2.914 & 2.250 \\ 0 & -1.39 & -0.011 & -0.012 & 8.367 & -24.18 \end{bmatrix} \qquad B = \begin{bmatrix} 0.14286 \\ 0 \\ 0 \\ 0 \\ 0 \\ 0 \end{bmatrix} \quad \Delta E_{fd} = 0$$

Figure A.14: 6^{th} Order synchronous generator model (with Damper winding effect) data of block diagram

Min of AIC	Zeros									
Poles	**1**	**2**	**3**	**4**	**5**	**6**	**7**	**8**	**9**	**Min of AIC**
2	-6308.77									-6308.77
3	-6933.50	-7159.28								-7159.28
4	-9641.51	-9201.96	-12988.24							-12988.24
5	-9761.49	-9749.84	-9232.75	-15633.18						-15633.18
6	-10396.71	-10437.26	-10505.08	-9599.67	-35873.92					-35873.92
7	-10214.07	-10718.10	-10790.23	-10102.11	-11522.12	-10364.88				-11522.12
8	-10462.88	-10460.88	-10457.51	-10463.13	-10218.03	-10359.36	-10310.40			-10463.13
9	-10464.63	-10462.63	-10460.88	-10451.85	-10471.15	-10410.20	-10362.07	-10385.67		-10471.15
10	-10478.85	-10476.85	-10474.87	-10472.31	-10474.79	-10451.16	-10463.13	-10470.80	-10465.83	-10478.85
Min of AIC	**-10478.85**	**-10718.10**	**-12988.24**	**-15633.18**	**-35873.92**	**-10451.16**	**-10463.13**	**-10470.80**	**-10465.83**	**-35873.92**

Figure A.15: AIC values of all models estimated for 6th order synchronous generator model (with Damper winding effect)

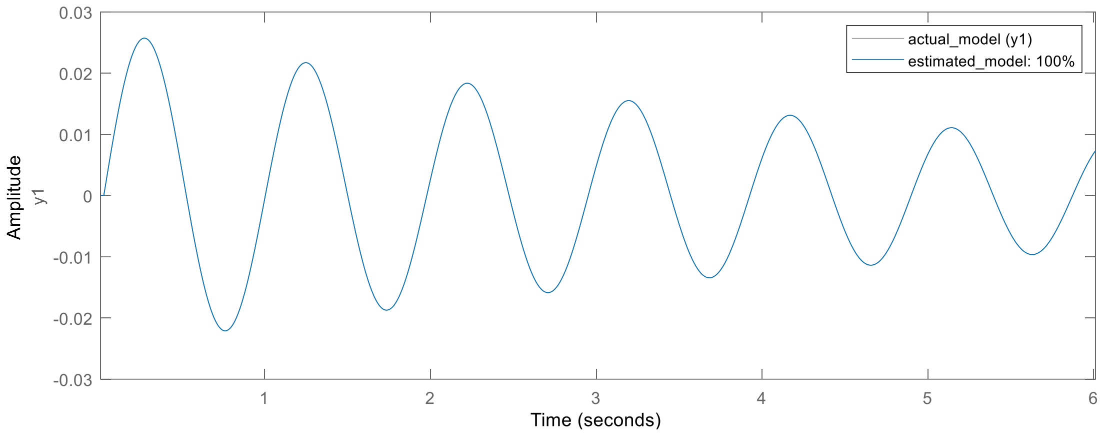

Figure A.16: Comparison of outputs for actual and estimated models of 6th order synchronous generator model (with Damper winding effect)

Appendix B IEEE 12 bus system model

B.1 Data used for PSCAD and PSS®E IEEE 12-bus models

Table B.1: IEEE 12-bus system Bus data

Bus #	Area #	Bus type	Nominal voltage (kV)	Specified voltage (pu)	Shunt capacitance (MVar)	Generation (MW)	Load	
							(MW)	(MVar)
1	1	PQ	230					
2	1	PQ	230				280	200
3	2	PQ	230				320	240
4	2	PQ	230		160		320	240
5	2	PQ	230		80		100	60
6	3	PQ	230		180		440	300
7	1	PQ	345					
8	2	PQ	345					
9	1	Slack	22	1.05				
10	1	PV	22	1.02		500		
11	2	PV	22	1.01		200		
12	3	PV	22	1.02		300		

Table B.2: IEEE 12-bus system Transformer data

From Bus	To Bus	Circuit	R (pu)	X (pu)	B (pu)	Rating (MVA)
1	7	1	0.00000	0.0010	0.000	1000
1	9	1	0.00000	0.0010	0.000	1000
2	10	1	0.00000	0.0010	0.000	1000
3	8	1	0.00000	0.0010	0.000	1000
3	11	1	0.00000	0.0010	0.000	1000
6	12	1	0.00000	0.0020	0.000	500

Table B.3: IEEE 12-bus system Generation capacities and type

Bus #	Unit #	Area	Generation Type	Installed Capacity (MW)	Pmin (MW)	Qmax (MVar)	Qmin (MVar)
9	1	1	Hydro	550	0.0	330.0	-150.0
10	1	1	Hydro	500	0.0	300.0	-100.0
11	1	2	Hydro	400	0.0	240.0	-80.0
12	1	3	Thermal	300	100.0	180.0	-60.0

Table B.4: IEEE 12-bus system Shunt compensation

Bus #	Shunt capacitance (MVar)	Shunt reactance (MVar)
4	5×40	1×40
5	4×20	1×20
6	6×30	0

B.2 PSCAD IEEE 12-bus models developed for verification

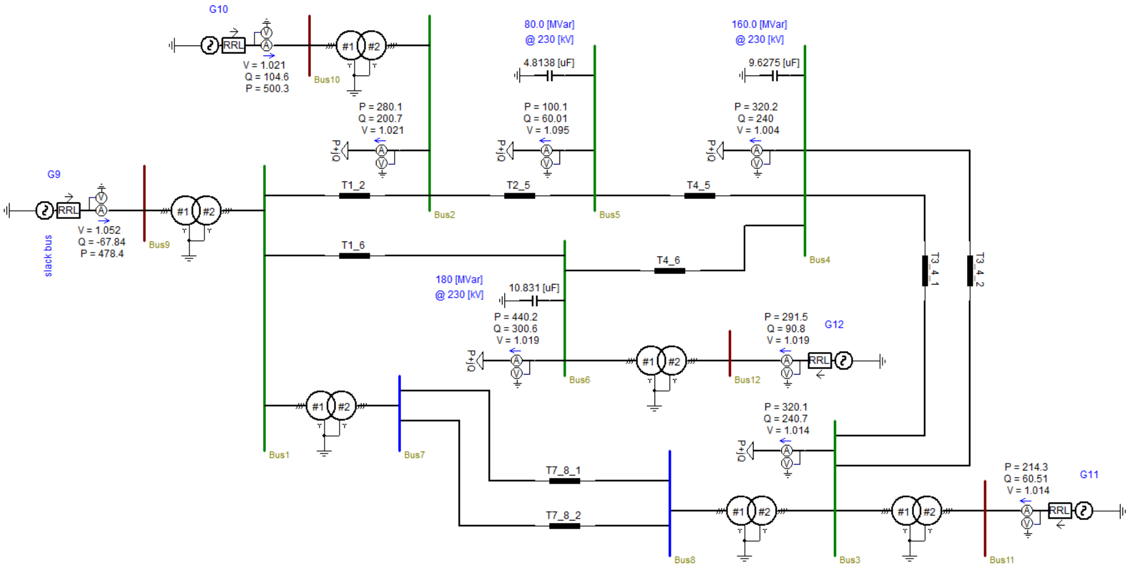

Figure B.1: IEEE 12-bus PSCAD model using fixed voltage sources

B.3 PSS®E IEEE 12-bus model

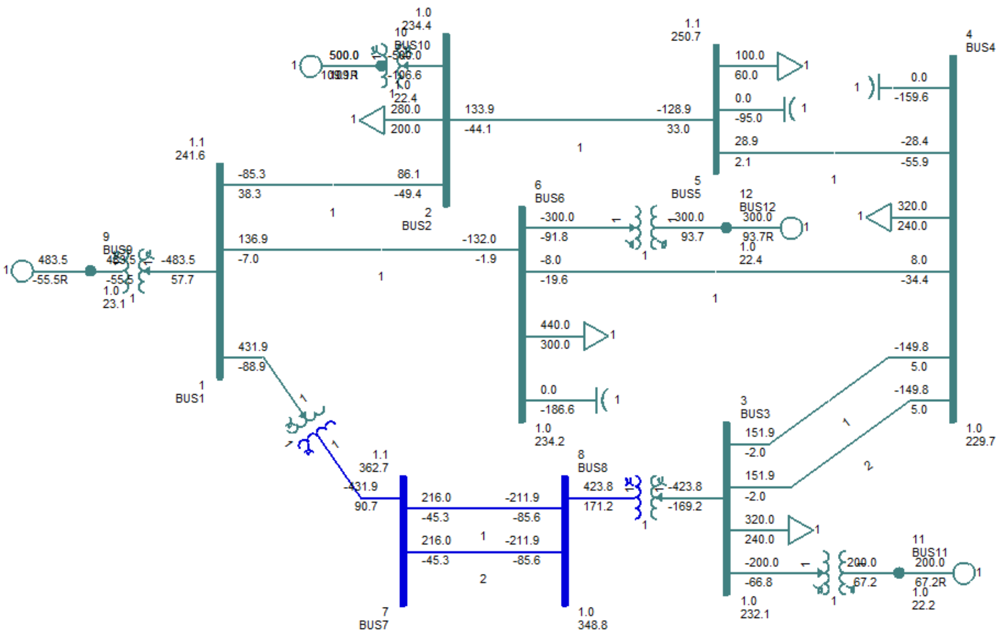

Figure B.2: IEEE 12-bus system modelled in PSS®E

Bus

Network data ✕

	Bus Name	Base kV	Area Num	Area Name	Zone Num	Zone Name	Owner Num	Owner Name	Code	Voltage (pu)	Angle (deg)
	BUS1	230.0	1		1		1		1	1.0505	-0.25
	BUS2	230.0	1		1		1		1	1.0189	4.19
	BUS3	230.0	2		1		1		1	1.0093	-11.32
	BUS4	230.0	2		1		1		1	0.9986	-19.25
	BUS5	230.0	2		1		1		1	1.0900	-15.54
	BUS6	230.0	3		1		1		1	1.0182	-20.63
	BUS7	345.0	1		1		1		1	1.0514	-0.48
	BUS8	345.0	2		1		1		1	1.0110	-11.08
	BUS9	22.0	1		1		1		3	1.0500	0.00
	BUS10	22.0	1		1		1		2	1.0200	4.47
	BUS11	22.0	2		1		1		2	1.0100	-11.21
	BUS12	22.0	3		1		1		2	1.0200	-20.30

Plant

	Bus Number	Bus Name	Area Num	Area Name	Code	PGen (MW)	QGen (Mvar)	QMax (Mvar)	QMin (Mvar)	VSched (pu)
	9	BUS9 22.000	1		3	483.5	-55.5	330.0	-150.0	1.0500
	10	BUS10 22.000	1		2	500.0	109.1	300.0	-100.0	1.0200
▸	11	BUS11 22.000	2		2	200.0	67.2	240.0	-80.0	1.0100
	12	BUS12 22.000	3		2	300.0	93.7	180.0	-60.0	1.0200
*										

Machine

	Bus Number	Bus Name	Id	Term Node	Term Node	Area Num	Area Name	Zone	Zone Name	Code	VSched	Remote Bus	In Service	PGen (MW)	PMax (MW)	PMin (MW)	QGen (Mvar)	QMax (Mvar)	QMin (Mvar)	Mbase (MVA)	R Source (pu)
	9	BUS9 22.000	1			1		1		3	1.0500	0	☑	483.54	550.000	0.0000	-55.513	330.00	-150.0	641.00	0.000000
	10	BUS10 22.000	1			1		1		2	1.0200	0	☑	500.00	500.000	0.0000	109.113	300.00	-100.0	583.00	0.000000
	11	BUS11 22.000	1			2		1		2	1.0100	0	☑	200.00	400.000	0.0000	67.1899	240.00	-80.00	466.00	0.000000
	12	BUS12 22.000	1			3		1		2	1.0200	0	☑	300.00	300.000	100.00	93.7439	180.00	-60.00	350.00	0

Load

	Bus Number	Bus Name	Id	Term Node	Term Node	Code	Area Num	Area Name	Zone Num	Zone Name	Owner	Owner Name	In Service	Scalable	Interruptible	Pload (MW)	Qload (Mvar)
	2	BUS2 230.00	1			1	1		1		1		☑	☑ Yes	☐ Yes	280.000	200.000
	3	BUS3 230.00	1			1	2		1		1		☑	☑ Yes	☐ Yes	320.000	240.000
	4	BUS4 230.00	1			1	2		1		1		☑	☑ Yes	☐ Yes	320.000	240.000
	5	BUS5 230.00	1			1	2		1		1		☑	☑ Yes	☐ Yes	100.000	60.0000
▸	6	BUS6 230.00	1			1	3		1		1		☑	☑ Yes	☐ Yes	440.000	300.000

Fixed Shunt

	Bus Number	Bus Name	Id	Term Node	Term Node	Area Num	Area Name	Zone Num	Zone Name	Code	In Service	G-Shunt (MW)	B-Shunt (Mvar)
	4	BUS4 230.00	1			2		1		1	☑	0.00	160.00
	5	BUS5 230.00	1			2		1		1	☑	0.00	80.00
	6	BUS6 230.00	1			3		1		1	☑	0.00	180.00

Branch

	From Bus	From Bus Name	To Bus Number	To Bus Name	Id	Name	Term Node	Term Node	Term Node	Term Node	Line R (pu)	Line X (pu)	Charging B (pu)
	1	BUS1 230.00	2	BUS2 230.00	1	T1_2					0.009200	0.092000	0.178000
	1	BUS1 230.00	6	BUS6 230.00	1	T1_6					0.028300	0.276700	0.535000
	2	BUS2 230.00	5	BUS5 230.00	1	T2_5					0.028300	0.276700	0.535000
	3	BUS3 230.00	4	BUS4 230.00	1	T3_4_1					0.009200	0.092000	0.178000
▸	3	BUS3 230.00	4	BUS4 230.00	2	T3_4_2					0.009200	0.092000	0.178000
	4	BUS4 230.00	5	BUS5 230.00	1	T4_5					0.028300	0.276700	0.535000
	4	BUS4 230.00	6	BUS6 230.00	1	T4_6					0.028300	0.276700	0.535000
	7	BUS7 345.00	8	BUS8 345.00	1	T7_8_1					0.009300	0.092500	1.613000
	7	BUS7 345.00	8	BUS8 345.00	2	T7_8_2					0.009300	0.092500	1.613000

Figure B.3: PSSE settings for IEEE 12-bus model

Appendix C PSCAD Detailed Power Plant models

C.1 Hydro Power Plant with Synchronous Generator details

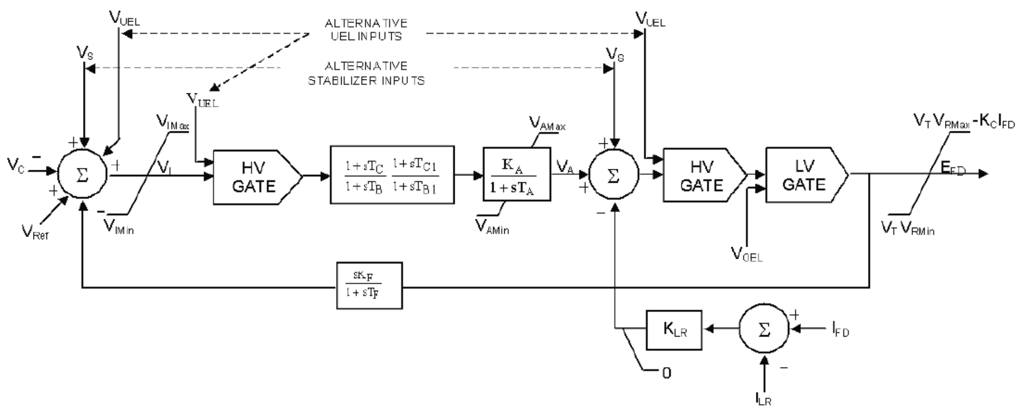

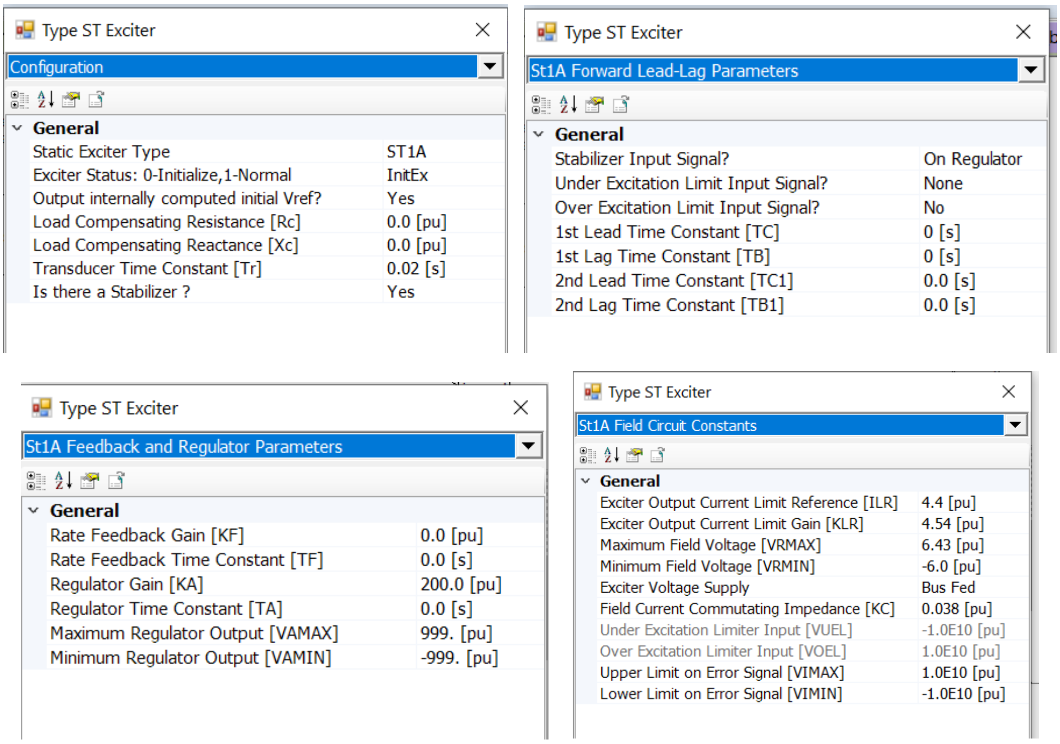

Type ST Exciter — Configuration

General	
Static Exciter Type	ST1A
Exciter Status: 0-Initialize,1-Normal	InitEx
Output internally computed initial Vref?	Yes
Load Compensating Resistance [Rc]	0.0 [pu]
Load Compensating Reactance [Xc]	0.0 [pu]
Transducer Time Constant [Tr]	0.02 [s]
Is there a Stabilizer ?	Yes

Type ST Exciter — St1A Forward Lead-Lag Parameters

General	
Stabilizer Input Signal?	On Regulator
Under Excitation Limit Input Signal?	None
Over Excitation Limit Input Signal?	No
1st Lead Time Constant [TC]	0 [s]
1st Lag Time Constant [TB]	0 [s]
2nd Lead Time Constant [TC1]	0.0 [s]
2nd Lag Time Constant [TB1]	0.0 [s]

Type ST Exciter — St1A Feedback and Regulator Parameters

General	
Rate Feedback Gain [KF]	0.0 [pu]
Rate Feedback Time Constant [TF]	0.0 [s]
Regulator Gain [KA]	200.0 [pu]
Regulator Time Constant [TA]	0.0 [s]
Maximum Regulator Output [VAMAX]	999. [pu]
Minimum Regulator Output [VAMIN]	-999. [pu]

Type ST Exciter — St1A Field Circuit Constants

General	
Exciter Output Current Limit Reference [ILR]	4.4 [pu]
Exciter Output Current Limit Gain [KLR]	4.54 [pu]
Maximum Field Voltage [VRMAX]	6.43 [pu]
Minimum Field Voltage [VRMIN]	-6.0 [pu]
Exciter Voltage Supply	Bus Fed
Field Current Commutating Impedance [KC]	0.038 [pu]
Under Excitation Limiter Input [VUEL]	-1.0E10 [pu]
Over Excitation Limiter Input [VOEL]	1.0E10 [pu]
Upper Limit on Error Signal [VIMAX]	1.0E10 [pu]
Lower Limit on Error Signal [VIMIN]	-1.0E10 [pu]

Figure C.1: ST1A exciter settings of HPP

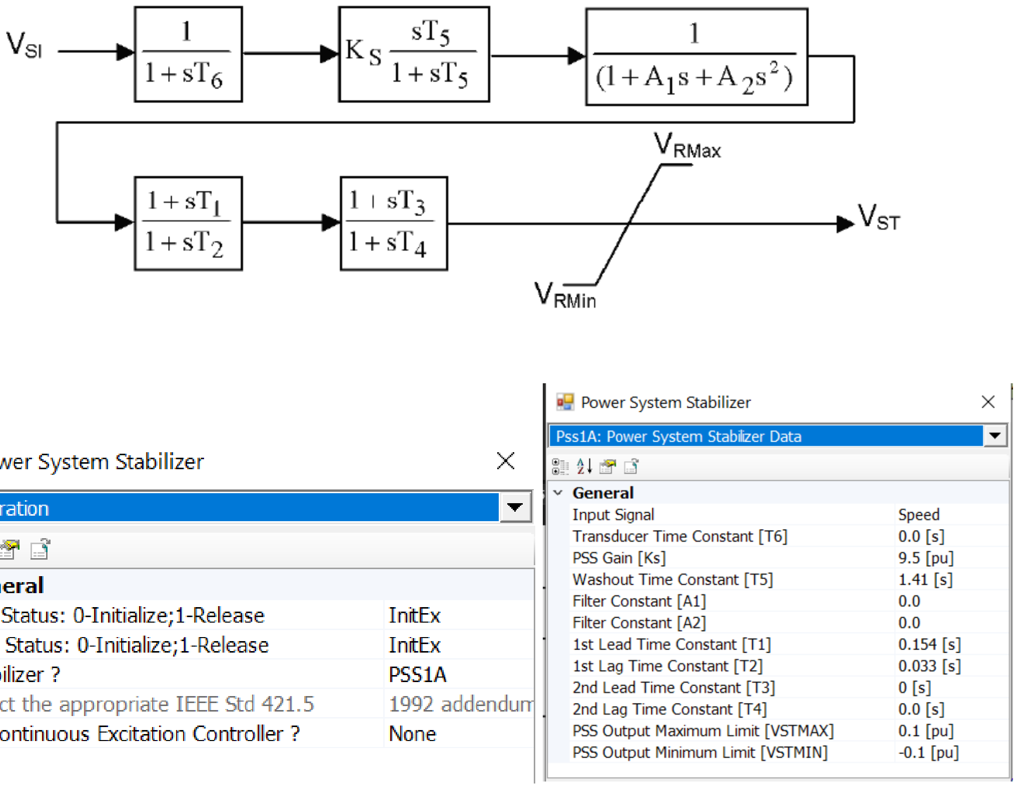

Figure C.2: PSS1A Power system stabilizer settings of HPP

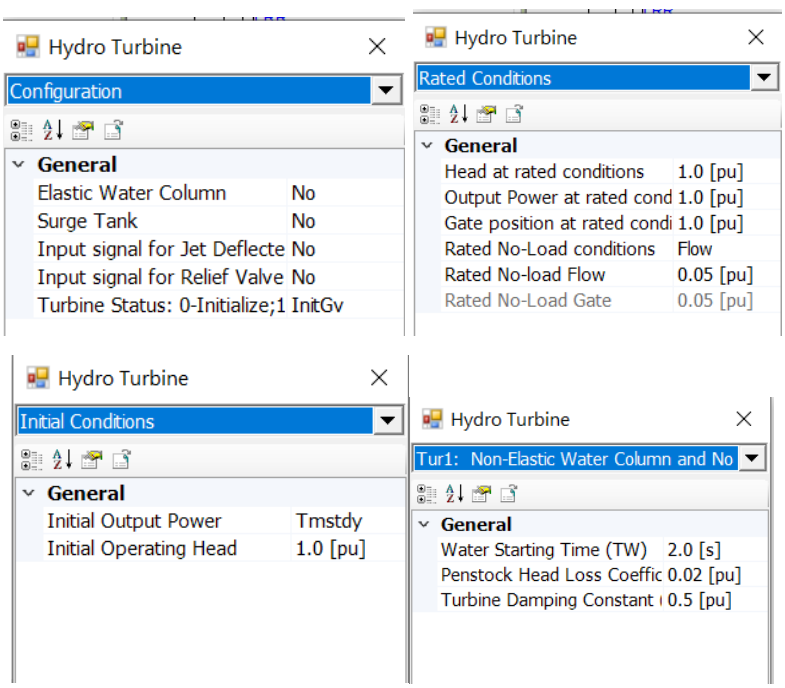

Figure C.3: TUR1 Hydro turbine settings of HPP

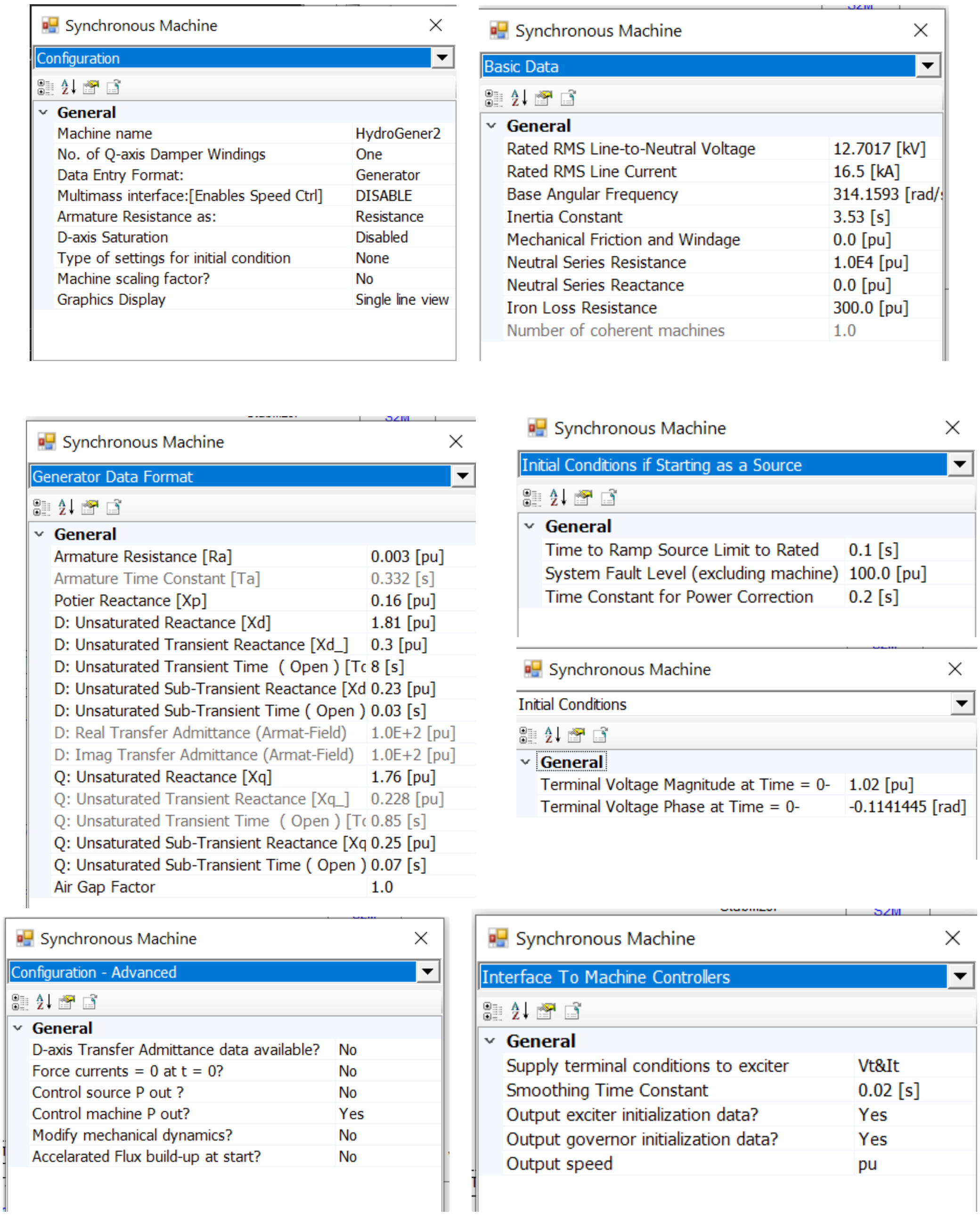

Figure C.4: Synchronous machine settings for HPP

C.2 Wind Power Plant (Type II) details

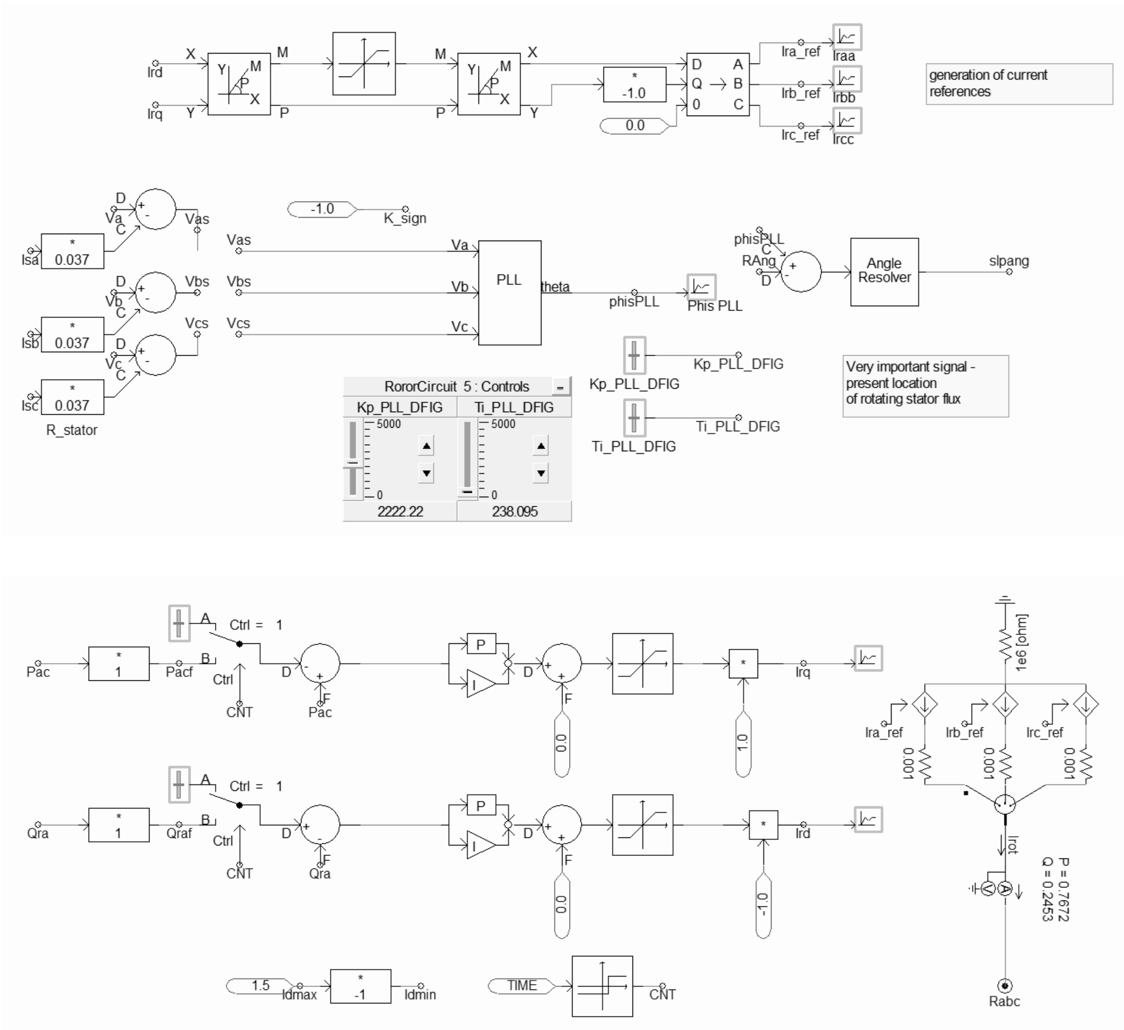

Figure C.5 – Rotor circuit system of WPP

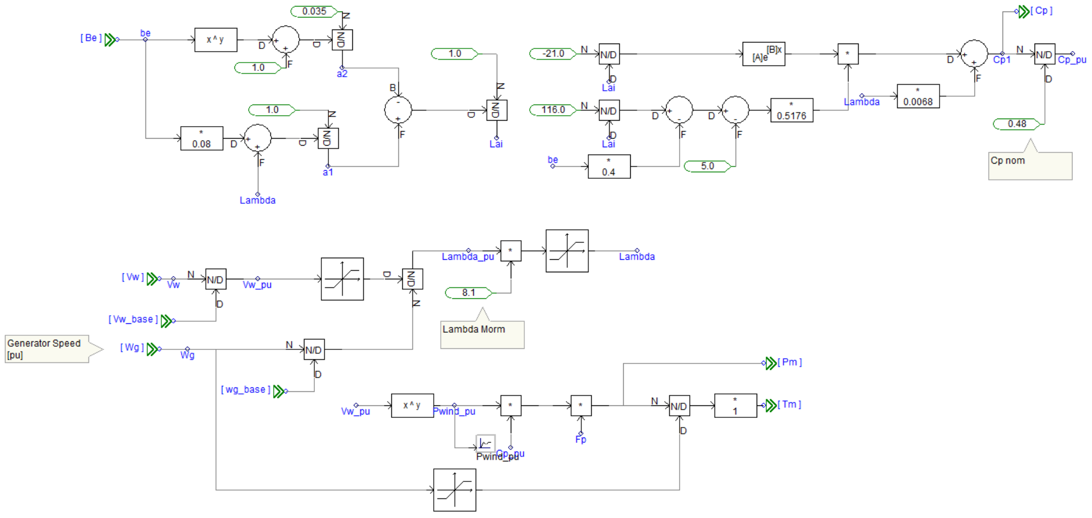

Figure C.6: Turbine model of WPP

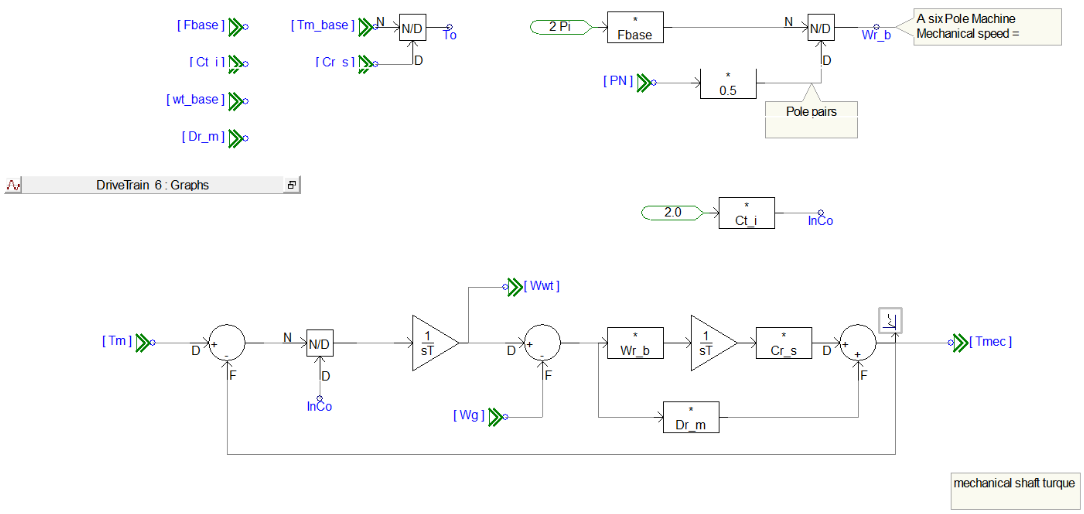

Figure C.7: Drive train model of WPP

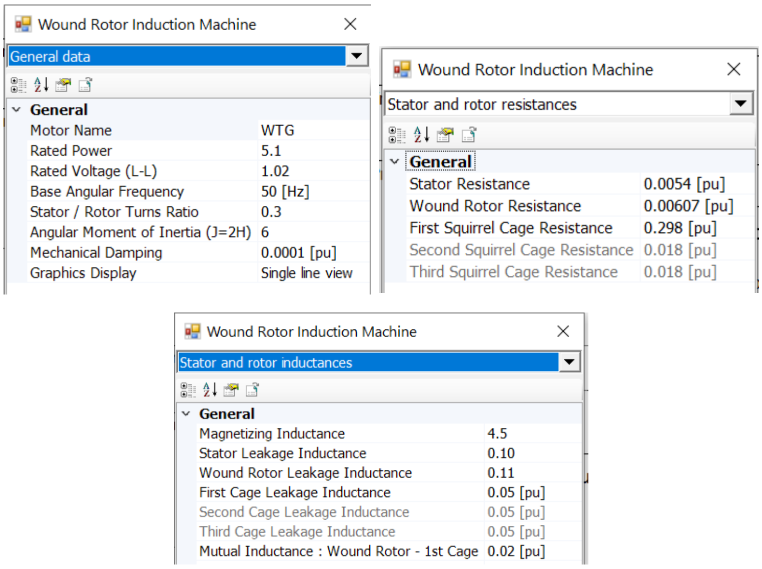

Figure C.8: Wound Rotor Induction machine settings of WPP

C.3 Solar Power Plant details

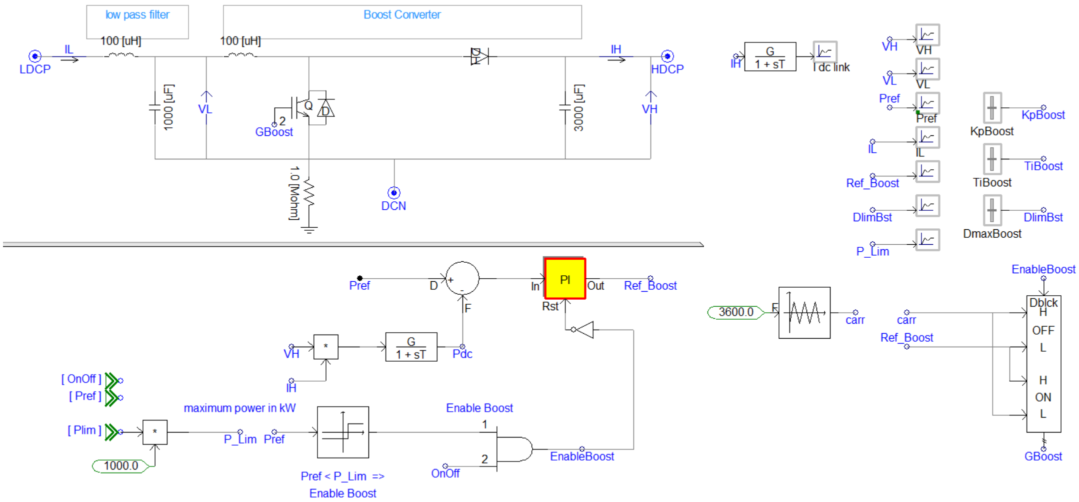

Figure C.9: DC-DC Bidirectional converter of SPP

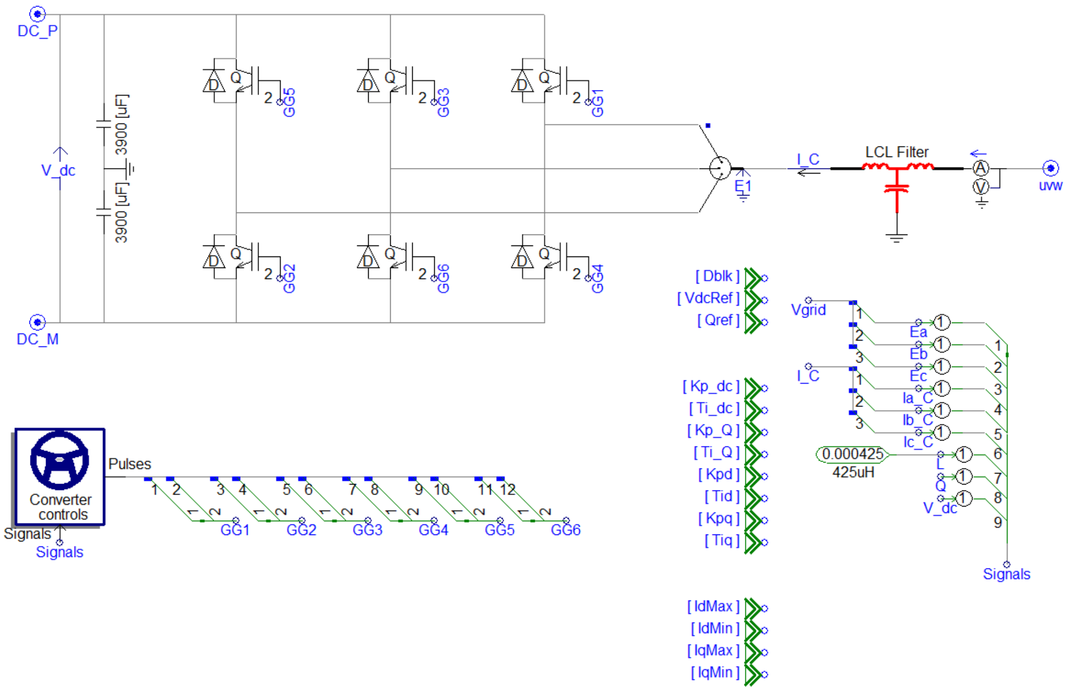

Figure C.10: Voltage Source Converter control system of SPP

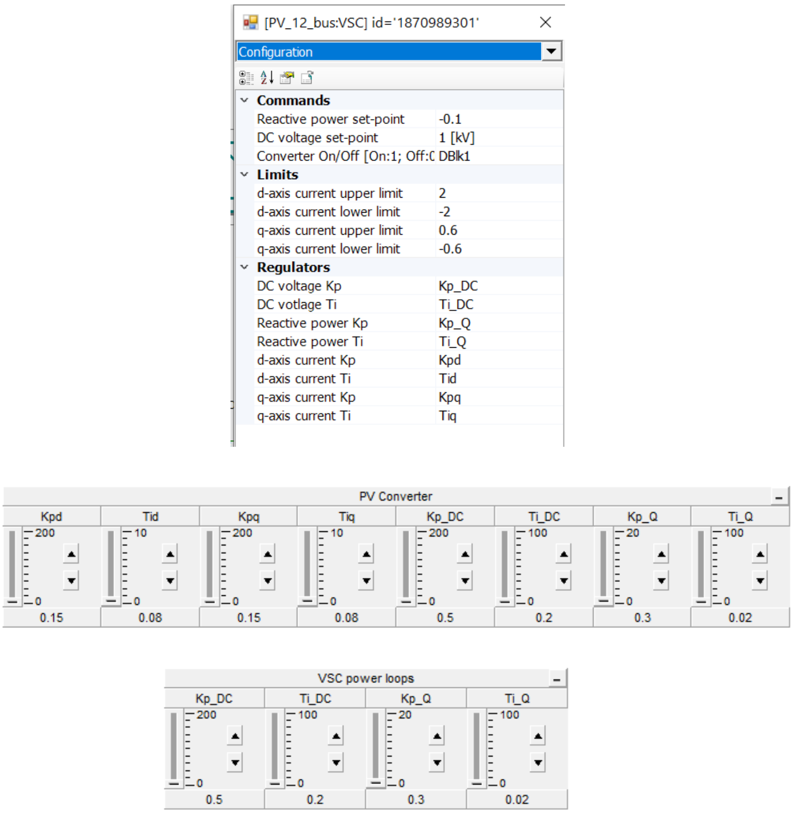

Figure C.11: Voltage Source Converter settings of SPP

Appendix D MATLAB programmes for estimation and comparison

D.1 MATLAB programmes for obtaining results in Appendix A

i) 2nd order model

```
% Based on Power Systems by Kundur Example 12.2
H = 3.5;
Kd = 10;
w0 = 377;
Ks = 0.757;

%transfer function
tf_x = tf([1/(2*H) 0],[1 Kd/(2*H) Ks*w0/(2*H)])

%generate data by running the step input simulation
SimOut = sim('synchronous_gen_order_2.slx');

u1 = SimOut.u1(:,2);
y1 = SimOut.y1(:,2);
```

ii) 3rd order model - Generator with Field circuit

```
% Based on Power Systems by Kundur Example 12.3
H = 3.5;
Kd = 20;
w0 = 376.991;
Ks = 0.757;
Rfd = 0.0006;
Ladu = 1.65;

syms s

a11 = 0;                    %-Kd/(2*H);
a12 = -0.1092;              %-K1/(2*H);
a13 = -0.1236;              %-K2/(2*H);
a21 = 376.991;              %w0;
a32 = -0.1938;              %-w0*Rfd*m1*L_ads;
a33 = -0.4229;              %-w0*Rfd/Lfd*(1-L_ads/Lfd+m2*L_ads);
b11 = 1/(2*H);
b32 = w0*Rfd/Ladu;

A_3=[0 -0.1092 -0.1236;376.991 0 0;0 -0.1938 -0.4229];
B_3=[b11;0;0];
Phi=inv(s*eye(3)-A_3)*B_3;
pretty(simplify(Phi(1)));    % delta(Omega)r
[nf3, df3] = numden(Phi(1));
tfn3 = sym2poly(nf3);
tfd3 = sym2poly(df3);
tf3 = tf(tfn3/tfd3(1), tfd3/tfd3(1))


%transfer function
tf_3 = tf([b11 -b11*a33 0],[1 -(a11+a33) (a11*a33-a12*w0) (a12*a33-
a13*a32)*w0])
```

```
%generate data by running the step input simulation
SimOut = sim('synchronous_gen_order_3.slx');

u1 = SimOut.u1(:,2);
y1 = SimOut.y1(:,2);
```

iii) 4th order model - Generator with Field circuit + AVR

```
I_t = 0.9-0.3i;
E_ = 1.09+0.27i;
d0 = 79.13; % degrees
Eb = 0.995;
Xt = 0.95;
w0 = 376.991;
Ks = 0.757;

Ka = 10;   % vary from 0 - 200
K5 = -0.12; K6 = 0.3; Tr = 0.02;  Gex = Ka; H = 3.5; Kd=20;

a11 = -Kd/(2*H);
b11 = 1/(2*H);


%Example 12.4 with AVR without PSS
A_4 = [a11 -0.1092 -0.1236 0;
     376.99 0 0 0;
     0 -0.1938 -0.4229 -27.3172;
     0 -7.3125 20.8391 -50 ]
B_4=[1/(2*H);0;0;0];
C_4 = [1 0 0 0];
Phi_4=inv(s*eye(4)-A_4)*B_4;
Y_4 = C_4*Phi_4;

[nf4, df4] = numden(Y_4);
tfn4 = sym2poly(nf4)
tfd4 = sym2poly(df4)
tf4 = tf(tfn4/tfd4(1), tfd4/tfd4(1))

%generate data by running the step input simulation
SimOut = sim('synchronous_gen_order_4.slx');

u1 = SimOut.u1(:,2);
y1 = SimOut.y1(:,2);
```

iv) 6th order models - Generator with Field circuit + AVR + PSS and with field winding

```
w0 = 376.991;
Ks = 0.757;
Rfd = 0.0006;
d0 = 0;

 %page 762
 Ka = 10;   % vary from 0 - 200
```

```
 K1 = 1.591; K2 = 1.5; K3 = 0.333; K4 = 1.8; T3 = 1.91;
 K5 = -0.12; K6 = 0.3; Tr = 0.02;  Gex = Ka; H = 3; Kd=0;

b11 = 1/(2*H);

% %Example 12.4 with AVR+PSS
% A_6 = [0 -0.1092 -0.1236 0 0 0;
%       376.99 0 0 0 0 0;
%       0 -0.1938 -0.4229 -27.3172 0 27.3172;
%       0 -7.3125 20.8391 -50 0 0;
%       0 -1.0372 -1.1738 0 -0.7143 0;
%       0 -4.8404 -5.4777 0 26.9697 -30.303]
%
%Example 12.5 with AVR+PSS + amotissures
A_6 = [0 -0.121 -0.069 -0.076 -0.003 -0.023;
     377 0 0 0 0 0;
     0 -0.109 -0.883 0.645 0 0.0003;
     0 -4.928 26.72 -37.47 0.002 0.013;
     0 -0.058 -0.0005 -0.0005 -2.914 2.250;
     0 -1.39 -0.011 -0.012 8.367 -24.18]

B_6=[b11;0;0;0;0;0];
C_6 = [1 0 0 0 0 0];
Phi_6=inv(s*eye(6)-A_6)*B_6;
Y_6 = C_6*Phi_6
[nf6, df6] = numden(Y_6);
tfn6 = sym2poly(nf6);
tfd6 = sym2poly(df6);

tf_6 = tf(tfn6/tfd6(1), tfd6/tfd6(1))

P6 = poly(pole(tf_6));
Z6 = poly(zero(tf_6));
tf6 = tf(Z6,P6)

pole(tf6)

%generate data by running the step input simulation
SimOut = sim('synchronous_gen_order_6.slx');

u1 = SimOut.u1(:,2);
y1 = SimOut.y1(:,2);
```

D.2 MATLAB programmes for estimating models using PSCAD data

i) Code for loading data from PSCAD for estimation for internal disturbance model

```
% This example shows data for solar power plant internal disturbance
Test1_01 = load('C:\Users\Lahiru\OneDrive\Documents\MSC Project\Estimating
results\transfer function test\PSCAD_simulations\solar
estimation\PV_12_bus.gf42\Test1_01.out');
Test1_02 = load('C:\Users\Lahiru\OneDrive\Documents\MSC Project\Estimating
results\transfer function test\PSCAD_simulations\solar
estimation\PV_12_bus.gf42\Test1_02.out');
Test1_03 = load('C:\Users\Lahiru\OneDrive\Documents\MSC Project\Estimating
results\transfer function test\PSCAD_simulations\solar
estimation\PV_12_bus.gf42\Test1_03.out');

%Input output data set for H1(s) and H2(s)
```

```
u1=Test1_01(200*1:300*1,2);  %dIrradiation
y1=Test1_03(200*1:300*1,2);  %dPh10 comment when estimating H2(s)
%y1=Test1_02(200*1:300*1,10); %dV10 Uncomment when estimating H2(s)

tx =Test1_01(200*1:300*1,1); %t
```

ii) Code for loading data from PSCAD for estimation for external disturbance model

```
%This example shows data for solar power plant external disturbance
Test1_03 = load('C:\Users\Lahiru\OneDrive\Documents\MSC Project\Estimating
results\transfer function test\PSCAD_simulations\solar
estimation\PV_12_bus_ext4.gf42\Test1_03.out');

%For estimating H3(s) P - Ph
u1=Test1_03(200*1:400*1,5);%dP10
y1=Test1_03(200*1:400*1,4); %dPh10

% For estimating H4(s) Q - V
% u1=Test1_03(200*1:400*1,3);%dQ10
% y1=Test1_03(200*1:400*1,2); %dV10

tx =Test1_03(200*1:400*1,1); %t
```

iii) Code for estimating transfer function from loaded PSCAD data

```
format short g

%estimation options
opt = tfestOptions;
opt.InitializeMethod = 'n4sid';   %Initialization N4SID
opt.Display = 'on';
opt.InitialCondition = 'auto';

%Data object for estimation. Data sampling rate is 0.1 seconds
dat = iddata(y1,u1,0.1);

tf_p = 3:10;     %poles
tf_z = 3:10;     %zeros

%All possible combinations of model orders.
orders = zeros(size(tf_p,2)*size(tf_z,2),2);
pz_count=1;

for w1= size(tf_p,2):-1:1

    zero_count = size(tf_z,2);
    %Poles should be > number of zeros
    if(size(tf_z,2)>=w1)
        zero_count = w1-1;   % Always number of poles > number of zeros
    end

    for w2 = zero_count:-1:1
```

```
            orders(pz_count,1) = tf_p(1,w1);
            orders(pz_count,2) = tf_z(1,w2);
            pz_count=pz_count+1;
      end
end

lastn = size(tf_p,2)*size(tf_z,2) - pz_count+1;

orders = orders(1:end-lastn,:);

models = cell(size(orders,1),1);            % All combinations of models

%Assign all possible model details to variable 'models'
for ct = 1:size(orders,1)
   models{ct} = tfest(dat, orders(ct,1),orders(ct,2),opt);
end

V = aic(models{:});                         % AIC of all models
[Vmin, I] = min(V);                         % Model with minimum AIC


%Fit to estimate of all models
AIC = cell(size(orders,1),1);

for q=1:size(orders,1)
        AIC{q} = models{q}.Report.Fit.AIC;
end

%Estimated model transfer function
tf_est = tf(models{I}.Numerator,models{I}.Denominator);


%Comparison between actual and estimated models
actual_model = dat;
estimated_model = models{I};
opt_comp = compareOptions('InitialCondition','auto');
compare(actual_model,estimated_model,opt_comp)
```

iv) Code for plotting and comparing results measured in PSCAD for actual model and estimated black-box model for internal disturbance

```
%Load data for actual model measurements for solar power plant internal
disturbance
Solar1 = load('C:\Users\Lahiru\OneDrive\Documents\MSC Project\Estimating
results\transfer function test\PSCAD_simulations\solar
estimation\PV_12_bus.gf42\Test1_01.out');
Solar2 = load('C:\Users\Lahiru\OneDrive\Documents\MSC Project\Estimating
results\transfer function test\PSCAD_simulations\solar
estimation\PV_12_bus.gf42\Test1_02.out');
Solar3 = load('C:\Users\Lahiru\OneDrive\Documents\MSC Project\Estimating
results\transfer function test\PSCAD_simulations\solar
estimation\PV_12_bus.gf42\Test1_03.out');

%Load data for estimated model measurements for solar power plant internal
disturbance
Est1 = load('C:\Users\Lahiru\OneDrive\Documents\MSC Project\Estimating
results\transfer function test\PSCAD_simulations\solar
estimation\PV_blackbox1.gf42\Test1_01.out');
```

```
Est2 = load('C:\Users\Lahiru\OneDrive\Documents\MSC Project\Estimating
results\transfer function test\PSCAD_simulations\solar
estimation\PV_blackbox1.gf42\Test1_02.out');
Est3 = load('C:\Users\Lahiru\OneDrive\Documents\MSC Project\Estimating
results\transfer function test\PSCAD_simulations\solar
estimation\PV_blackbox1.gf42\Test1_03.out');


%Irradiance Input
Irr =Solar1(1:350,3);
tx =Solar1(1:350,1); %time

%Data for each parameter from each measurement point for actual model

%Bus 10 actual model data
P10_A =Solar1(180:350,4);
Ph10_A=Solar1(180:350,5);
Q10_A =Solar1(180:350,6);
V10_A =Solar1(180:350,7);

%Bus 11 actual model data
P11_A =Solar2(180:350,2);
Ph11_A=Solar2(180:350,3);
Q11_A =Solar2(180:350,4);
V11_A =Solar2(180:350,5);


%Bus 5 actual model data
P5_A =Solar2(180:350,10);
Ph5_A =Solar2(180:350,11);
Q5_A =Solar3(180:350,2);
V5_A =Solar3(180:350,3);

%Data for each parameter from each measurement point for estimated model

%Bus 10 estimated model data
P10_E =Est1(180:350,4);
Ph10_E=Est1(180:350,5);
Q10_E =Est1(180:350,6);
V10_E =Est1(180:350,7);

%Bus 11 estimated model data
P11_E =Est2(180:350,2);
Ph11_E=Est2(180:350,3);
Q11_E =Est2(180:350,4);
V11_E =Est2(180:350,5);

%Bus 5 estimated model data
P5_E =Est2(180:350,10);
Ph5_E =Est2(180:350,11);
Q5_E =Est3(180:350,2);
V5_E =Est3(180:350,3);

%Plot Input
plot(tx,Irr);
title('Change in Solar Irradiance with time');
ylabel('Solar Irradiance (W/m2)')
xlabel('Time (s)')

%===========================================================%
%plot result comparison for bus 10

%Bus 10 Active Power
subplot(2,2,1);
```

```
plot(tx,P10_A);
hold on
plot(tx,P10_E,'--','LineWidth',0.8);

[P10_maxerr,P10_mse,P10_index] = errors(P10_A,P10_E);
P10_maxpt = tx(P10_index);
plot(P10_maxpt, P10_A(P10_index,1), 'ko');
P10_str = sprintf('Max Err=%.2f%%, MSE=%.2e%', P10_maxerr,P10_mse);

hold off
legend('Actual','Blackbox',P10_str);
title('Bus 10 (Same Source Bus): Active Power (MW)');
ylabel('Active Power (MW)')
xlabel('Time (s)')

%Bus 10 Phase Angle
subplot(2,2,2);
plot(tx,Ph10_A);
hold on
plot(tx,Ph10_E,'--','LineWidth',0.8);

[Ph10_maxerr,Ph10_mse,Ph10_index] = errors(Ph10_A,Ph10_E);
Ph10_maxpt = tx(Ph10_index);
plot(Ph10_maxpt, Ph10_A(Ph10_index,1), 'ko');
Ph10_str = sprintf('Max Err=%.2f%%, MSE=%.2e%', Ph10_maxerr,Ph10_mse);

hold off
legend('Actual','Blackbox',Ph10_str);
title('Bus 10 (Same Source Bus): Phase Angle of Bus Voltage (degrees)');
ylabel('Phase Angle of Bus Voltage (degrees)')
xlabel('Time (s)')
%Bus 10 Reactive Power
subplot(2,2,3);
plot(tx,Q10_A);
hold on
plot(tx,Q10_E,'--','LineWidth',0.8);

[Q10_maxerr,Q10_mse,Q10_index] = errors(Q10_A,Q10_E);
Q10_maxpt = tx(Q10_index);
plot(Q10_maxpt, Q10_A(Q10_index,1), 'ko');
Q10_str = sprintf('Max Err=%.2f%%, MSE=%.2e%', Q10_maxerr,Q10_mse);

hold off
legend('Actual','Blackbox',Q10_str);

title('Bus 10 (Same Source Bus): Reactive Power (MVAr)');
ylabel('Reactive Power (MVAr)')
xlabel('Time (s)')

%Bus 10 Voltage
subplot(2,2,4);
plot(tx,V10_A) ;
hold on
plot(tx,V10_E,'--','LineWidth',0.8);

[V10_maxerr,V10_mse,V10_index] = errors(V10_A,V10_E);
V10_maxpt = tx(V10_index);
plot(V10_maxpt, V10_A(V10_index,1), 'ko');
V10_str = sprintf('Max Err=%.2f%%, MSE=%.2e%', V10_maxerr,V10_mse);

hold off
legend('Actual','Blackbox',V10_str);

title('Bus 10 (Same Source Bus): RMS Voltage of Bus (P.U)');
```

```
ylabel('RMS Voltage of Bus (P.U)') ;
xlabel('Time (s)');



%=============================================================%
%plot result comparison for bus 5

%Bus 5 Active Power
subplot(2,2,1);
plot(tx,P5_A);
hold on
plot(tx,P5_E,'--','LineWidth',0.8);
[P5_maxerr,P5_mse,P5_index] = errors(P5_A,P5_E);
P5_maxpt = tx(P5_index);
plot(P5_maxpt, P5_A(P5_index,1), 'ko');
P5_str = sprintf('Max Err=%.2f%%, MSE=%.2e%', P5_maxerr,P5_mse);

hold off
legend('Actual','Blackbox',P5_str);
title('Bus 5 (Load Bus): Active Power (MW)');
ylabel('Active Power (MW)')
xlabel('Time (s)')

%Bus 5 Phase angle
subplot(2,2,2);
plot(tx,Ph5_A);
hold on
plot(tx,Ph5_E,'--','LineWidth',0.8);
[Ph5_maxerr,Ph5_mse,Ph5_index] = errors(Ph5_A,Ph5_E);
Ph5_maxpt = tx(Ph5_index);
plot(Ph5_maxpt, Ph5_A(Ph5_index,1), 'ko');
Ph5_str = sprintf('Max Err=%.2f%%, MSE=%.2e%', Ph5_maxerr,Ph5_mse);

hold off
legend('Actual','Blackbox',Ph5_str);title('Bus 5 (Load Bus): Phase Angle of
Bus Voltage (degrees)');
ylabel('Phase Angle of Bus Voltage (degrees)')
xlabel('Time (s)')

%Bus 5 Reactive Power
subplot(2,2,3);
plot(tx,Q5_A);
hold on
plot(tx,Q5_E,'--','LineWidth',0.8);
[Q5_maxerr,Q5_mse,Q5_index] = errors(Q5_A,Q5_E);
Q5_maxpt = tx(Q5_index);
plot(Q5_maxpt, Q5_A(Q5_index,1), 'ko');
Q5_str = sprintf('Max Err=%.2f%%, MSE=%.2e%', Q5_maxerr,Q5_mse);

hold off
legend('Actual','Blackbox',Q5_str);
title('Bus 5 (Load Bus): Reactive Power (MVAr)');
ylabel('Reactive Power (MVAr)')
xlabel('Time (s)')

%Bus 5 Voltage
subplot(2,2,4);
plot(tx,V5_A) ;
hold on
plot(tx,V5_E,'--','LineWidth',0.8);
[V5_maxerr,V5_mse,V5_index] = errors(V5_A,V5_E);
V5_maxpt = tx(V5_index);
plot(V5_maxpt, V5_A(V5_index,1), 'ko');
```

```
V5_str = sprintf('Max Err=%.2f%%, MSE=%.2e%', V5_maxerr,V5_mse);

hold off
legend('Actual','Blackbox',V5_str);
title('Bus 5 (Load Bus): RMS Voltage of Bus (P.U)');
ylabel('RMS Voltage of Bus (P.U)')
xlabel('Time (s)')

%==========================================================%
%plot result comparison for bus 11

%Bus 11 Active Power
subplot(2,2,1);
plot(tx,P11_A);
hold on
plot(tx,P11_E,'--','LineWidth',0.8);
[P11_maxerr,P11_mse,P11_index] = errors(P11_A,P11_E);
P11_maxpt = tx(P11_index);
plot(P11_maxpt, P11_A(P11_index,1), 'ko');
P11_str = sprintf('Max Err=%.2f%%, MSE=%.2e%', P11_maxerr,P11_mse);

hold off
legend('Actual','Blackbox',P11_str);
title('Bus 11 (Different Source Bus): Active Power (MW)');
ylabel('Active Power (MW)')
xlabel('Time (s)')

%Bus 11 Phase angle
subplot(2,2,2);
plot(tx,Ph11_A);
hold on
plot(tx,Ph11_E,'--','LineWidth',0.8);
[Ph11_maxerr,Ph11_mse,Ph11_index] = errors(Ph11_A,Ph11_E);
Ph11_maxpt = tx(Ph11_index);
plot(Ph11_maxpt, Ph11_A(Ph11_index,1), 'ko');
Ph11_str = sprintf('Max Err=%.2f%%, MSE=%.2e%', Ph11_maxerr,Ph11_mse);

hold off
legend('Actual','Blackbox',Ph11_str);
title('Bus 11 (Different Source Bus): Phase Angle of Bus Voltage
(degrees)');
ylabel('Phase Angle of Bus Voltage (degrees)')
xlabel('Time (s)')

%Bus 11 Reactive Power
subplot(2,2,3);
plot(tx,Q11_A);
hold on
plot(tx,Q11_E,'--','LineWidth',0.8);
[Q11_maxerr,Q11_mse,Q11_index] = errors(Q11_A,Q11_E);
Q11_maxpt = tx(Q11_index);
plot(Q11_maxpt, Q11_A(Q11_index,1), 'ko');
Q11_str = sprintf('Max Err=%.2f%%, MSE=%.2e%', Q11_maxerr,Q11_mse);

hold off
legend('Actual','Blackbox',Q11_str);
title('Bus 11 (Different Source Bus): Reactive Power (MVAr)');
ylabel('Reactive Power (MVAr)')
xlabel('Time (s)')

%Bus 11 Voltage
subplot(2,2,4);
plot(tx,V11_A) ;
hold on
```

```
plot(tx,V11_E,'--','LineWidth',0.8);
[V11_maxerr,V11_mse,V11_index] = errors(V11_A,V11_E);
V11_maxpt = tx(V11_index);
plot(V11_maxpt, V11_A(V11_index,1), 'ko');
V11_str = sprintf('Max Err=%.2f%%, MSE=%.2e%', V11_maxerr,V11_mse);

hold off
legend('Actual','Blackbox',V11_str);
title('Bus 11 (Different Source Bus): RMS Voltage of Bus (P.U)');
ylabel('RMS Voltage of Bus (P.U)')
xlabel('Time (s)')
```

v) Function for calculating MSE, maximum error and maximum error index for two given datasets

```
function [maxerr,mse,maxerr_index] = errors(act,est)
    n = length(act);

    [max_err_val, maxerr_index] = max(abs(act-est));

    mse_cum = 0;  %Cumulative square error

    %Calculate MSE from 20th sample onwards as that is when disturbance is
applied
    for c = 20:n
        mse_cum=mse_cum+(act(c,1)-est(c,1))^2;
    end

    %Max error %
    maxerr = round(abs(max_err_val/act(maxerr_index,1))*100,2);

    %MSE
    mse=mse_cum/(n-19);
end
```